AD-A036 384 YANG STEVENS FABIAN ENGINEERS NEW YORK F/G 13/2
NONDESTRUCTIVE EVALUATION OF CIVIL AIRPORT PAVEMENTS.(U)
SEP 76 N C YANG DACW39-76-C-0010
UNCLASSIFIED FAA-RD-76-83 NL

1 OF 2
AD A036384

REPORT NO. FAA-RD-76-83

NONDESTRUCTIVE EVALUATION of CIVIL AIRPORT PAVEMENTS

BY

NAI C. YANG

YANG, STEVENS, FABIAN, ENGINEERS

UNDER CONTRACT WITH
U.S. ARMY ENGINEER WATERWAYS EXPERIMENT STATION
SOILS AND PAVEMENTS LABORATORY
VICKSBURG, MISSISSIPPI 39180

SEPTEMBER 1976

FINAL REPORT

Prepared for

U.S. DEPARTMENT OF TRANSPORTATION
FEDERAL AVIATION ADMINISTRATION
Systems Research & Development Service
Washington, D.C. 20590

NOTICE

Technical Report Documentation Page

1. Report No.	2. Government Accession No.	3. Recipient's Catalog No.
FAA-RD-76-83		

4. Title and Subtitle	5. Report Date
Nondestructive Evaluation of Civil Airport Pavements	Sept. 1976
	6. Performing Organization Code
	8. Performing Organization Report No.
7. Author(s) Nai C. Yang	
9. Performing Organization Name and Address Yang, Stevens, Fabian, Engineers, P.C. 60 East 42 Street New York, N.Y. 10017	10. Work Unit No. (TRAIS) 11. Contract or Grant No. DACW-39-76-C-0010
12. Sponsoring Agency Name and Address U.S. Department of Transportation Federal Aviation Administration Systems Research and Development Service Washington, D.C. 20590	13. Type of Report and Period Covered Final Report 14. Sponsoring Agency Code ARD-430

15. Supplementary Notes

Under Contract with
U.S. Army Engineer Waterways Experiment Station
Soils and Pavement Laboratory,
Vicksburg, Mississippi 39180

16. Abstract

The nondestructive test(NDT) is used to define the physical conditions of an existing pavement system without destroying it. The frequency sweep NDT was introduced to replace conventional plate bearing tests. A 16 kip vibrator operated by the Waterways Experiment Station (WES) has conducted such tests at 15 civil airports. The results from these tests confirmed the frequency sweep theory and the reliability of the data acquired under it.

The NDT test procedures have now been standardized and the results can automatically be included in the functional pavement design and evaluation program. The computer program consists of three subsystems. The first subsystem relates aircraft response to pavement smoothness. The pavement structure's capacity to withstand repeated aircraft loadings is related to the user's requirements, the demand forecast and the need for maintenance. The second subsystem determines the pavement thickness and composition required to meet the tolerances defined in the first subsystem. The third subsystem evaluates the cost/benefit aspects of design alternatives. The end products of this program will provide the pavement designer a definite criteria in planning airport pavements.

17. Key Words		18. Distribution Statement
Pavement Design	Aircraft Movement	Document is available to the public through the National Technical Information Service, Springfield, Va.22151
Airport Pavement	Cost Benefit	
Nondestructive Test		
Functional Pavement		

19. Security Classif. (of this report)	20. Security Classif. (of this page)	21. No. of Pages	22. Price
Unclassified	Unclassified	140	

Form DOT F 1700.7 (8-72) Reproduction of completed page authorized

METRIC CONVERSION FACTORS

Approximate Conversions to Metric Measures

Symbol	When You Know	Multiply by	To Find	Symbol
		LENGTH		
in	inches	*2.5	centimeters	cm
ft	feet	30	centimeters	cm
yd	yards	0.9	meters	m
mi	miles	1.6	kilometers	km
		AREA		
in^2	square inches	6.5	square centimeters	cm^2
ft^2	square feet	0.09	square meters	m^2
yd^2	square yards	0.8	square meters	m^2
mi^2	square miles	2.6	square kilometers	km^2
	acres	0.4	hectares	ha
		MASS (weight)		
oz	ounces	28	grams	g
lb	pounds	0.45	kilograms	kg
	short tons (2000 lb)	0.9	tonnes	t
		VOLUME		
tsp	teaspoons	5	milliliters	ml
Tbsp	tablespoons	15	milliliters	ml
fl oz	fluid ounces	30	milliliters	ml
c	cups	0.24	liters	l
pt	pints	0.47	liters	l
qt	quarts	0.95	liters	l
gal	gallons	3.8	liters	l
ft^3	cubic feet	0.03	cubic meters	m^3
yd^3	cubic yards	0.76	cubic meters	m^3
		TEMPERATURE (exact)		
°F	Fahrenheit temperature	5/9 (after subtracting 32)	Celsius temperature	°C

*1 in = 2.54 (exactly). For other exact conversions and more detailed tables, see NBS Misc. Publ. 286, Units of Weights and Measures, Price $2.25, SD Catalog No. C13.10:286.

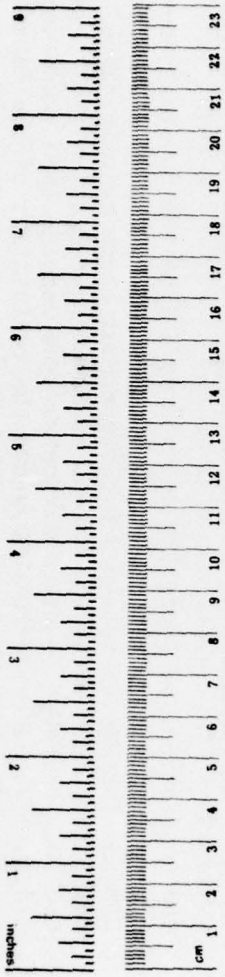

Approximate Conversions from Metric Measures

Symbol	When You Know	Multiply by	To Find	Symbol
		LENGTH		
mm	millimeters	0.04	inches	in
cm	centimeters	0.4	inches	in
m	meters	3.3	feet	ft
m	meters	1.1	yards	yd
km	kilometers	0.6	miles	mi
		AREA		
cm^2	square centimeters	0.16	square inches	in^2
m^2	square meters	1.2	square yards	yd^2
km^2	square kilometers	0.4	square miles	mi^2
ha	hectares (10,000 m^2)	2.5	acres	
		MASS (weight)		
g	grams	0.035	ounces	oz
kg	kilograms	2.2	pounds	lb
t	tonnes (1000 kg)	1.1	short tons	
		VOLUME		
ml	milliliters	0.03	fluid ounces	fl oz
l	liters	2.1	pints	pt
l	liters	1.06	quarts	qt
l	liters	0.26	gallons	gal
m^3	cubic meters	35	cubic feet	ft^3
m^3	cubic meters	1.3	cubic yards	yd^3
		TEMPERATURE (exact)		
°C	Celsius temperature	9/5 (then add 32)	Fahrenheit temperature	°F

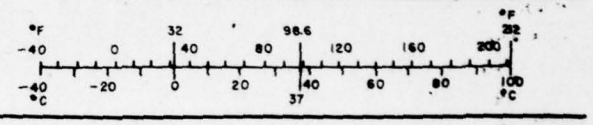

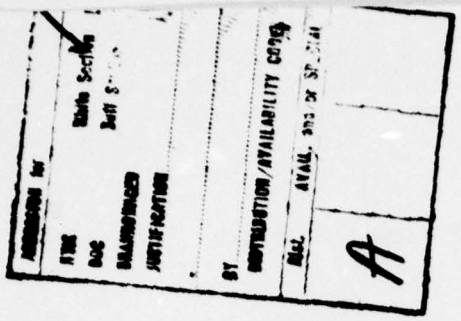

TABLE OF CONTENTS

		Page
	SUMMARY	1
	SCOPE OF WORK	2
	PART 1 NONDESTRUCTIVE TEST - FREQUENCY SWEEP METHOD	
1.1	PURPOSE OF NDT	3
1.2	DEVELOPMENT OF THE NDT THEORY	4
	a. Dynamic E-Value by Wave Velocity	4
	b. Dynamic Modulus of Pavement	5
	c. E-Value by Frequency Sweep NDT	7
1.3	DEVELOPMENT OF THE NDT PROCESS	11
	a. Early Field Experiments	11
	b. Newark, JFK and LaGuardia Airports	13
	c. Nashville, Portland and Raleigh-Durham Airports	13
	d. San Jose Municipal Airport	14
	e. Other Airports	14
1.4	RESEARCH ASPECTS OF NDT	21
	a. Correlation with Plate Bearing Tests	21
	b. Correlation with Soil Tests	23
	c. Magnification and System Damping	24
	d. Optimum Forcing Amplitude	25
	e. Pavement Surface Temperature	25
	f. Base and Subgrade Moisture	25
1.5	BASIC TESTER REQUIREMENTS	33
	a. Steady State of Vibration	33
	b. First Resonance and Frequency Range	33
	c. Vibratory Force	33
	d. Static Weight and Residual Force	34
	e. Resolution and System Error	35
	f. Filter and Damper Effects	36
1.6	DATA ACQUISITION	40
	a. Calibration of NDT Output	40
	b. Reliability	40
	c. Productivity and Monitoring Tolerance	41
	d. Planning Airport Tests	42
	e. Testing Procedure and Data Recording	43
1.7	DATA PROCESSING	46
	a. Input Files	46
	b. Initial Data Processing	46
	c. Reprocessing E-Value	47
	d. Inventory Files	47

1.8 PRACTICAL APPLICATION OF NDT 48
a. Traffic Patterns and Existing Pavement Strength 48
b. Existing Pavement Composition 48

1.9 COST OF NDT FOR AIRPORT PAVEMENTS 51

PART 2 SYSTEM DESIGN OF FUNCTIONAL PAVEMENTS

2.1 BASIC CONCEPT 52

2.2 FUNCTIONAL PAVEMENT REQUIREMENTS 54
a. Aircraft Movement and Demand Forecast 54
b. Aircraft Response and Pavement Surface 58
c. Progressive Deterioration of the Pavement Surface 59
d. Limiting Elastic Deflection of the Pavement Structure 61
e. Limiting Stress Level 62
f. Equivalent Single Type of Aircraft Operation 63
g. Present Functional Life 64

2.3 PAVEMENT THICKNESS AND COMPOSITION 70
a. Validity of Elastic Equilibrium Theory 70
b. Stress Analysis of Pavement Elements 71
c. Material Characterization 73
d. Differential Settlement 73
e. Temperature Variation 74
f. Pavement Design 74

2.4 COST/BENEFIT ANALYSIS 78
a. Initial Construction Cost 78
b. Annual Maintenance Cost 79
c. Indirect Operation Cost 80
d. Cash Flow and Financial Cost 80
e. Present Cash Value 81
f. Cost/Benefit Study 82

2.5 PRACTICAL APPLICATION OF DESIGN ANALYSIS 83

PART 3 COMPUTER INPUT AND OUTPUT LISTINGS

3.1 COMPUTER CODE AND DICTIONARY 84

3.2 NDT MACHINE DATA AND FIELD INPUTS 87
a. Offset Dictionary 87
b. Calibration Factors 87
c. Grid Dictionary 87
d. Test Identifications 87
e. Machine Data 88
f. Graphic of Machine Data 89

3.3 PROCESSED NDT DATA FILE 90
a. NDT Data by Test Number 90

b. NDT Data by Location 90
c. NDT Data by Date/Calibration 90
d. Graphic of NDT E-Value 91
e. NDT Inventory File 92

3.4 AIRCRAFT FILE AND DEMAND FORECAST 93

3.5 AIRPORT TRAFFIC DISTRIBUTION 94

3.6 MATERIAL FILE AND SYSTEM DEFAULT VALUES 95
a. System Default Values 95
b. Default System for FAM 95
c. Default System for PFL 96
d. DFLDI 96
e. Identification of Keel and Side 96
f. Navigation System, Dynamic Response and Velocity 96

3.7 COST FILE AND DEFAULT VALUES 97
a. Cost File 97
b. Component Characterization and Unit Price 97
c. ICC Component Default Values 97

3.8 EQUIVALENT AIRCRAFT OPERATION 98
a. Probability Distribution 98
b. Deflection and Stress of Default System 98
c. Aircraft Movement - First Year 99
d. Aircraft Movement - 20 Years 99
e. Equivalent Aircraft Operation 100

3.9 FUNCTIONAL REQUIREMENTS OF PAVEMENT 101

3.10 PRESENT FUNCTIONAL LIFE 102

3.11 THICKNESS DESIGN AND COST ANALYSIS 103
a. Grid System for Design Charts 103
b. Design Chart - Stress Criteria 103
c. Design Chart - Deflection Criteria 103
d. Pavement Design and Cost Analysis 104

3.12 COST BENEFIT STUDY 105

PART 4 RECOMMENDATIONS FOR FUTURE RESEARCH AND VALIDATION

4.1 MAJOR AREAS FOR FUTURE RESEARCH 106

4.2 VALIDATION PROGRAM OUTLINES 108

REFERENCES 109

APPENDIX A VIBRATION OF CIRCULAR PLATE ON ELASTIC SOIL 110
APPENDIX B A VIEW OF THEORETICAL FRAMEWORK FOR NDT ANALYSIS 123
APPENDIX C MAINTENANCE PRACTICE OF AIRPORT PAVEMENTS 126

LIST OF FIGURES

FIGURE		PAGE
1.1	Relation between E-value and Horizontal Velocity of Wave Propagation - Nashville Metropolitan Airport	10
1.2	Frequency Response Function - NDT at Newark	15
1.3	Frequency Response Function - Test on Taxiway Bridge	16
1.4	Frequency Response Function of Taxiway Bridge at JFK	17
1.5	A Typical Record of Vibratory Test at Newark	18
1.6	Frequency Response Function of NDT at Portland	19
1.7	Result of Plate Bearing Test at Newark Airport	27
1.8	Correlation between NDT and PBT at Nashville Airport	28
1.9	Correlation between NDT and PBT at San Jose	29
1.10	Logarithmic Decrement of Vibratory Amplitude	30
1.11	Optimum Forcing Amplitude of NDT at San Jose	31
1.12	Effect of Temperature on NDT - South Runway at Portland	32
1.13	NDT at Point B1, Runway at NAFEC	38
1.14	Effect of Filter on NDT at San Jose	39
1.15	Location of NDT	44
2.1	Structure of Pavement Computer Program	53
2.2	Flow Chart of First Subsystem	65
2.3	Transverse Distribution of Wheel Load	66
2.4	Longitudinal Distribution of Wheel Load	66
2.5	Aircraft Pavement Interaction	67
2.6	Progressive Deformation of Pavement Surface	68
2.7	Transfer Function - Longitudinal to Transverse Deformation	68
2.8	Deformation of Pavement	69
2.9	Transfer Function - Transverse Deformation to Elastic Deflection (log scale)	69
2.10	Measured Deflection vs Boussinesq Deflection	76
2.11	Measured Stress vs Boussinesq Stress	76
2.12	Surface Configuration due to Differential Settlement	77
2.13	Temperature Variation in Pavement	77

LIST OF TABLES

1.1	Summary of NDT at Six Civil Airports and WES Test Sites	20
1.2	Shell NDT Test on Subgrade at Newark Airport	27
1.3	Correlation of E-value at Nashville Airport	28
1.4	Correlation of NDT and Conventional Tests at San Jose	29
1.5	Experiment for Determining Optimum Forcing Amplitude	31
1.6	Effect of Tail Area at High Frequency Cut-off	37
1.7	A Sample of Original NDT Machine Print-out	45
1.8	Determination of E-value of Pavement Layers	50

NONDESTRUCTIVE EVALUATION OF CIVIL AIRPORT PAVEMENTS

SUMMARY

by Nai C. Yang

The nondestructive test (NDT) is used to define the physical conditions of an existing pavement system without destroying it. In 1968, frequency sweep NDT was introduced to replace conventional plate bearing tests. Since then, a 16 kip vibrator operated by the Waterways Experiment Station (WES) has conducted frequency sweep NDT at fifteen civil airports. The results from these tests confirmed the frequency sweep theory and the reliability of the data acquired under it. While conventional plate bearing tests took about 1½ days to complete at a direct cost of at least $800, frequency sweep NDT with identical or better results, took about 10 minutes and cost about $30. The reduced testing period minimized both airport interference and costs.

Test procedures have now been standardized and the entire pavement design system reported herein has been computerized. The computer program consists of three subsystems. The first subsystem relates aircraft response to pavement smoothness. The pavement structure's capacity to withstand repeated aircraft loadings is related to the user's requirements, the demand forecast, and the need for maintenance. The second subsystem determines the pavement thickness and composition required to meet the tolerances defined in the first subsystem. The third subsystem computes the present cash value of the initial pavement construction, and the annual maintenance and management costs for the anticipated service life of the pavement system. Cost/benefit studies are done to assist airport users in deciding upon an appropriate pavement construction/maintenance program. The end products of this study will provide the pavement designer a definite criteria in planning the public aviation facilities.

Prior to final adoption of this pavement design system, a validation program should be conducted at four airports representative of the various geographic and climatic conditions within the United States. The program should (1) implement use of the computer program, (2) further develop the transition from established design procedures to the computer-oriented process, (3) conduct technical seminars at the validation test sites, (4) obtain feed-back regarding improvements to the program's practical applications, and (5) prepare an operations manual to assist airport engineers in using the computer program.

SCOPE OF WORK

Faced with today's increasing traffic volume and new aircraft weights, there are definite indications that many airport pavements are not adequate. Extensive pavement testing and evaluation are necessary to develop meaningful rehabilitation and maintenance programs for airports in busy operation.

Since the nondestructive test (NDT) was conducted at the Port Authority's airports in New York and New Jersey in 1967, the air transport industry has recognized the advantages of NDT and has officially requested that the FAA sponsor research into this area. As a result, through a contract with the Waterways Experiment Station (WES), the writer was authorized by the FAA to complete the development and documentation of theoretical and experimental work involved in his evaluation procedure and pavement rehabilitation program.

Development of the NDT procedure is based on fundamental engineering principles and physical laws that accurately describe dynamic pavement response assuming that the damping characteristics of a multi-frequency response system can be treated as a single degree of freedom system. The entire NDT data processing and reduction have been computerized. Further development of computer simulation techniques for damping variables may improve the reliability of NDT data processing.

The processed NDT data together with the airport traffic demand forecast will be used to evaluate the present functional life of existing pavements and, if necessary, to design the system equilibrium and cost benefit aspects of a pavement rehabilitation program. The entire evaluation and design procedure have been computerized. A set of default values has been introduced to facilitate the operation of the computer program. The statistical relation and design analysis incorporated herein are valid for the construction practice and functional purposes studied. Attempts will be given to explain the limitations of these default values. Further research and validation are required.

Application of this technical report is clearly defined by its title: "Nondestructive Evaluation of Civil Airport Pavements". No attempt was made to correlate (1) NDT frequency sweep method with other dynamic pavement testings and (2) functional pavement design concept with other design procedures. They are not included in the scope of this study. In order to simplify the presentation of this report, the writer's early work will not be repeated herein but will be found in reference [1].

PART 1

NONDESTRUCTIVE TESTS - FREQUENCY SWEEP METHOD

1.1 PURPOSES OF NDT

The purpose of the nondestructive test (NDT) is to obtain the information necessary to define the physical properties of a structural member without destroying it. With this information, a rational engineering design can be applied to evaluate the mechanical behavior of that member under various loading and environmental conditions. Towards this end, NDT obtains the data necessary for determining the E-values to be used in the elastic theory of pavement design.

Additional purposes for using the current form of NDT are its advantages over conventional tests in the following areas.

Airport Operations Conventional CBR, plate load tests, and soil borings require long field testing periods which are reflected not only through increased operational costs, but also through interference with airport operations. NDT reduces testing time and therefore, minimizes costs and airport interference.

Conditions in the Field Conventional pavement tests reproduce field conditions in the laboratory. NDT is conducted under actual field conditions.

Simulation of Aircraft Loads Loading conditions for the conventional plate bearing test are, at best, reproductions of a stationary load. Since the effect of a moving load can be quite different from that of a static one, NDT simulates the dynamic effect of aircraft loads.

Quantitative Data Since practically all airport pavements were constructed in stages during airport growth, inherent variations are encountered in pavement composition as well as in subgrade support. This results in scattered service conditions for today's airport pavements. Any meaningful evaluation of such varied performances requires an adequate amount of data to optimize the design inputs. NDT is able to acquire such quantitative data.

Pavement Design and Evaluation The data acquired by NDT can be statistically processed to produce load-deformation information which can be used in the elastic theory for pavement design and evaluation.

1.2 DEVELOPMENT OF THE NDT THEORY

In the 1930's, Degebo [2] developed a vibrator which produced a periodic force by means of two rotating masses. When the mass and eccentricity were constant, the vibratory amplitude was proportional to the angular velocity squared. Under a steady state of forced vibration, the dynamic force F_s per unit area of the subgrade (assumed to consist of a uniform spring bed) was:

$$F_s = \omega^2(m_1 + m_s)/A \tag{1.1}$$

in which: ω = machine frequency when at resonance with the subgrade,
A = vibrating block area,
m_1 = vibrator mass,
m_s = unknown soil mass effectively participating in vibration.

The effective mass m_s, however, was related to the soil's damping factor. Degebo's vibrator and testing procedure did not offer a clear-cut solution to this problem.

a. Dynamic E-Value by Wave Velocity

Under the influence of a vibratory force, concentric waves are propagated away from the loaded area with a velocity v, governed by:

$$v = c\sqrt{G/\rho} \tag{1.2}$$

in which: ρ = homogeneous elastic mass density,
G = shear modulus,
c = a constant depending upon the nature of wave propagation.

Assuming the most probable waves to be Rayleigh waves, Young's modulus of elastic mass, $E = 2(1+\mu)G$, can be approximately expressed by:

$$E = 3\,v^2\,\rho \tag{1.3}$$

when $\mu=0.5$ and $c=1.0$. Because the elastic mass density varies within a very narrow range, the reliability of E-value computations depends primarily on the velocity measurements.

During wave velocity measurements, a ground pick-up moved away from the vibrator shows a steady increase in phase shift. At phase 2π, the distance between vibrator and pick-up is equal to the Rayleigh wave length of the elastic mass. The velocity of horizontal wave propagation in the elastic mass is equal to the wave length times the vibratory force frequency. For a multi-layered construction, different wave velocities are registered and knowledgeable judgment is required to distinguish the appropriate wave velocity for the individual layers.

In reviewing the velocity test, there are several limitations to its practical engineering applications:

(1) The measured velocity represents the horizontal elastic property of each distinctive layer. Any fluctuation in the horizontal layers would result in a fluctuation in measured wave velocity.
(2) According to Equation 1.3, E-value fluctuates about twice as much as the measured wave velocity. E-value reliability is influenced by this large fluctuation (see Section 1.5e).
(3) The E-value computed by Equation 1.3 does not represent the composite E-value in the vertical direction, as under the plate bearing test or rolling wheels, unless the elastic mass is homogeneous in three directions.

During the 1968 tests at JFK and Newark Airports, random fluctuations in wave velocity and sensitivity to pavement temperature were also observed. Tests made in 1972 at the Nashville Municipal Airport attempted to correlate E-values from plate bearing tests with those from wave velocity measurements. The scattered correlations shown in Figure 1.1 detract from the usefulness of velocity measurements until future research proves otherwise.

b. Dynamic Modulus of Pavement

Shell and other researchers [3 thru 7] have found that measurement of paving material strain can predict pavement life. Since the strain calculated from dynamic E-values agree well with the strain measured under rolling wheels, they accepted two sets of E-values for pavement design computations - the E-value determined in the laboratory under a static load and the dynamic E-value determined in the field under a simulated wheel load. Thus, the elastic theory for static load conditions could be applied to dynamic loadings as well.

Degebo's vibrator was used as their basic test machine. The eccentricity was made adjustable to compensate for the effect of rotation speed, and thus, a constant vibratory amplitude could be produced within a practical range of forcing frequencies. Double integration of the measured ground acceleration was considered to be the pavement "deflection". The ratio between the zero to peak force amplitude, F, and the resulting peak to peak deflection z, was called the dynamic stiffness:

$$S = 2F/z \tag{1.4}$$

In theory, the dynamic stiffness is:

$$S = k/X \tag{1.5}$$

$$X^2 = \frac{1}{(1-u^2)^2 + (2\beta u)^2} \tag{1.6}$$

in which: k = spring constant of the pavement system,
X = magnification factor of steady state of forced vibration,
β = structural damping coefficient
u = ω/p, the frequency ratio between the forcing function ω, and the pavement response function p.

Solving the structural damping problem, Shell researchers adopted the phase angle φ between the input forcing function F, and the measured deflection, z. The phase angle φ was defined as:

$$\tan\varphi = 2\beta u/(1-u^2) \tag{1.7}$$

Equations 1.6 and 1.7 show that both S and φ depend upon the frequency ratio u. Therefore, several frequency settings are required for a set of meaningful measurements of dynamic stiffness and phase angle. By plotting $S\cos\varphi$ against the forcing frequency ω, extension of that line to $\omega=0$ represents the spring constant k, of the pavement system. The elastic modulus E, of that system is:

$$E = k/2.5a \tag{1.8}$$

in which a = the load plate radius.

Because of practical limitations on mechanical vibrators, extrapolation of the ω-S line at low frequencies significantly affects E-value reliability. Multi-layered pavement systems encounter wide fluctuations in S-value measurements, which lead to less reliable E-value determinations.

In the mid 1950's, Foster [3] established a correlation between dynamic E-values in kg /cm^2 by the Shell machine and the CBR value by standard tests. On an average, the relationship is:

$$E_{dyn} = 110\ CBR \tag{1.9}$$

For individual soils, the factor ranges from 50 to 200. This correlation allowed application of CBR pavement experience to the NDT procedure.

In recent NDT studies [8], [9], extensive work has been devoted to equipment development and theoretical correlations. The most reliable load deflection relation by both theoretical and field analysis has been found to be encountered at a 15 Hz forcing frequency. Therefore, the Shell procedure for E-value determination was deleted, and the load deflection ratio at 15 Hz was defined as the dynamic stiffness modulus, DSM. Along the same lines advanced by Foster, a set of deflection-performance correlations was introduced. (pp.143-147, [8]).

In Appendix A, Veneziano independently reviewed the available theoretical results for forced vibration on a multi-layered soil system. For pavement tests using a heavy vibrator such as the one operated by

WES and the Shell Laboratory, Veneziano observed that the shear modulus of the response system is determined by:

$$G = \frac{\omega^2 \, m \, (1-\mu)}{4a} \qquad (1.10)$$

in which: ω = NDT resonant frequency,
m = effective vibration mass, including the free vibrator mass and an unknown portion of the response system,
μ = Poisson's ratio.
a = Radius of load plate.

The above equation is very similar to the Equation 1.1 used some 40 years ago. Veneziano commented that:

> The methods proposed above contain a few elements of uncertainty which express the degree to which the elastic half space and one degree of freedom are accurate in representing the actual physical system. The main sources of error are: (1) the effective mass of the soil should be added to the mass of the vibrator and footing (effective portion of the response system) in the one degree of freedom model, and (2) the material damping of the soil was neglected.
>
> Both approximations (neglecting the mass and the damping of the soil) make the measured resonant frequency smaller than the undamped natural frequency. In the approximation, the frequency ratio is assumed to be linear. The nonlinearity of the force-deformation relation have also effects of some importance.

c. E-Value by Frequency Sweep NDT

Shell researchers made two questionable assumptions in their NDT analysis, namely:

(1) The vibration and dynamic response characteristics of a multi-layered system could be ignored, and
(2) The dynamic response of a vibration system could be treated as its deflection under a given forcing amplitude.

Introduction of frequency sweep NDT by the writer in 1968 was aimed at modifying these assumptions. Frequency sweep output would automatically reflect the dynamic responses of a multi-frequency system, and individual "deflection" output could be treated as the spectral density of a pavement's response.

Under a steady state of vibration, the peak to peak response, z, of a pavement system can be expressed by (referring to Equations 1.4 and 1.5):

$$z(u) = \frac{2F_o(u)}{k} X(u) \qquad (1.11)$$

in which F_o is the equivalent force amplitude at zero frequency. When a constant forcing amplitude is used throughout the entire NDT series, the above equation becomes:

$$z(u) = \frac{2F}{k} X(u) \tag{1.12}$$

When NDT is conducted continuously at a small frequency interval du, integration of the dynamic response z(u), is equal to integration of the theoretical magnification factor as follows:

$$\frac{1}{2F}\int \frac{z(u)}{u}du = \frac{1}{k}\int \frac{X(u)}{u}du \tag{1.13}$$

Integration of the above equation can be made for a specific frequency range. Considering that (1) a low frequency vibrator is more difficult to build mechanically, and (2) the maximum dynamic response is normally encountered at first resonance somewhere between 5 and 12 Hz, the integration bounds are designed to be u=1 and ∞, or the first and and infinite resonant frequencies. The result is:

$$\frac{1}{2F}\int_1^{\infty} \frac{z(u)}{u}du = \frac{1}{2k} \ln\frac{1+\beta}{\beta} \tag{1.14}$$

Conventional plate bearing tests on a single elastic layer system will yield an E-value computed either by Boussinesq's or Burmister's elastic theory. (see pp.50-54 [1])

$$E = \frac{2pa}{w_o}(1-\mu^2) \tag{1.15a}$$

$$k = \frac{P}{w_o} = \frac{\pi aE}{2(1-\mu^2)} \tag{1.15b}$$

in which w_o is the surface deflection of the support system under a static load, $P=\pi pa^2$. To correlate plate bearing and frequency sweep NDT results, the k value of Equation 1.15b is introduced into Equation 1.14. The frequency sweep NDT E-value becomes:

$$E = \frac{1}{2a} \frac{1}{\frac{1}{2F}\int_1^{\infty}\frac{z(u)}{u}du} \frac{1-\mu^2}{\pi} \ln\frac{1+\beta}{\beta} \tag{1.16}$$

From experience (see Articles 1.4c and 2.3c), the μ-value ranges from 0.12 for a portland cement concrete slab, to 0.35 for a normal subgrade, while the structural damping coefficient β, varies from .025 for structural concrete, to .05 for the subgrade. Therefore the value $(1-\mu^2)/\pi \cdot \ln(1+\beta)/\beta$ ranges from 1.17 to 0.85 with a common value ranging from 1.05 to 0.95. Considering the machine output variability, the complex nature of the support system encountered, Equation 1.16 can be simplified to:

$$E = \frac{1}{2a} \frac{1}{\frac{1}{2F}\int_1^{\infty} \frac{z(u)}{u} du} \tag{1.17}$$

This equation governs frequency sweep NDT data acquisition and processing. Integration of the dynamic response $\int (z(u)/u)\, du$, is equivalent to summation of the spectral density of multi-frequency vibration. This equation also reflects the method of data acquisition that F represents the zero to peak forcing amplitude and z(u) represents the peak to peak dynamic response integrated from the velocity pickups of the tester. Two more contingencies should be considered in actual testing:

(1) In order to increase NDT productivity and efficiency, tolerance should be given to the frequency and amplitude settings. Experience indicates that a 2% tolerance will reduce the monitoring time to about one-third of that required when a 0.1% tolerance is observed. The total number of tests can therefore, be doubled without increasing the time and expense. However, to maintain data processing reliability, the dynamic response integration should be rearranged to:

$$\frac{1}{2F}\int_1^{\infty} \frac{z(u)}{u} du \quad \frac{1}{2}\int_1^{\infty} \frac{z(u)}{F(u)} \frac{1}{u} du \tag{1.18}$$

(2) Because of NDT equipment limitations, all tests have to terminate at a high frequency N. Equation 1.18 becomes:

$$\frac{1}{2}\int_1^{\infty} \frac{z(u)}{F(u)} \frac{1}{u} du = \frac{1}{2}\int_1^{N} \frac{z(u)}{F(u)} \frac{1}{u} du + \frac{1}{2}\int_N^{\infty} \frac{z(u)}{F(u)} \frac{1}{u} du \tag{1.19}$$

The last term of Equation 1.19 represents the tail area of the frequency sweep test. At high frequency vibration, Equation 1.12 approaches:

$$z(u) = \frac{2F}{k} \frac{1}{u^2} \tag{1.20}$$

Integration of the tail area leads to:

$$\frac{1}{2}\int_N^{\infty} \frac{z(u)}{F(u)} \frac{1}{u} du = \frac{z(N)}{2F(N)} N^2 \int_N^{\infty} \frac{1}{u^3} du = \frac{1}{4} \frac{z(N)}{F(N)} \tag{1.21}$$

In digital computations, summation of the dynamic response is coded as SUMZ, and is equal to:

$$SUMZ = \frac{z(1)}{2F(1)} \frac{H(2)+H(1)}{2H(1)} + \sum_2^{N-1} \frac{z(I)}{2F(I)} \frac{H(I+1)-H(I-1)}{2H(I)} + \frac{z(N)}{4F(N)} \tag{1.22}$$

in which H is the NDT forcing frequency in Hz. The composite E-value from Equation 1.17 of an assumed one layer response system becomes:

$$E = 1./(2.* a * SUMZ) \qquad (1.23)$$

which is equivalent to the E-value computed by the elastic theory from the load deflection data of a conventional plate bearing test using the assumptions stated on pp. 50-54 [1].

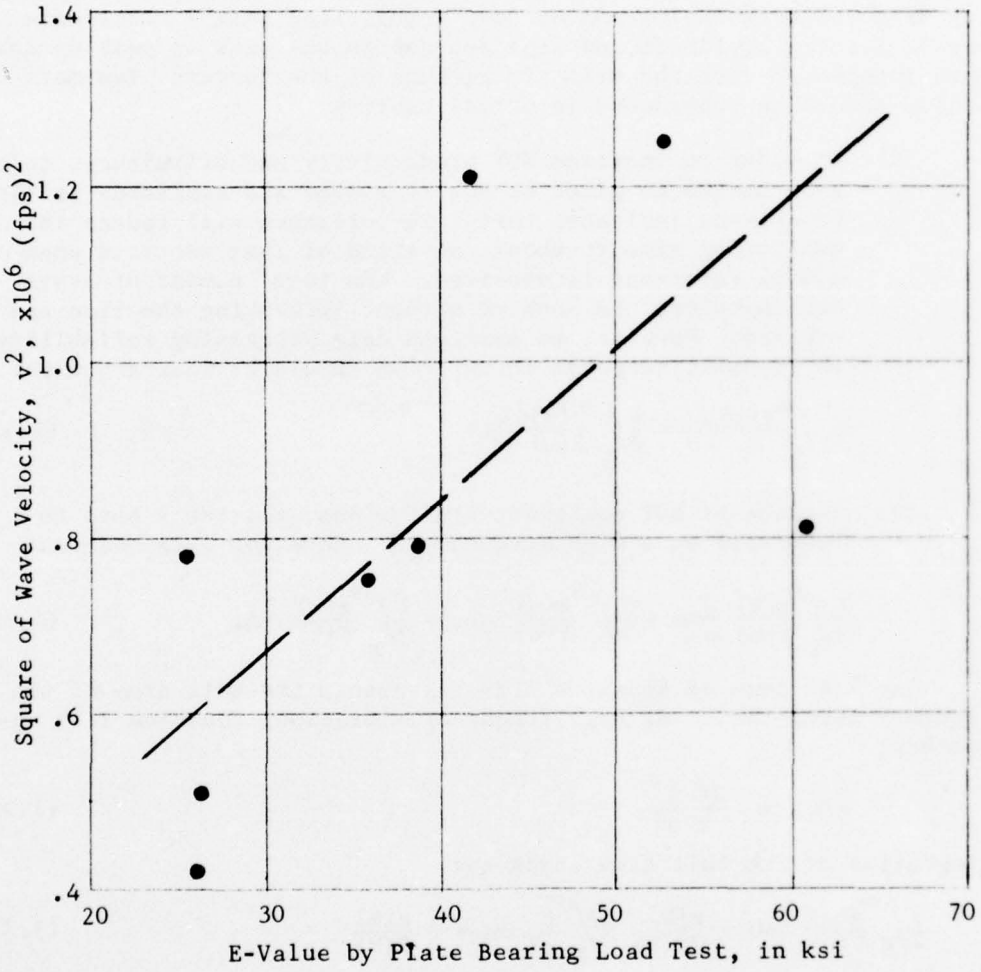

FIG. 1.1 RELATION BETWEEN E-VALUE AND HORIZONTAL VELOCITY OF WAVE PROPAGATION - NASHVILE METROPOLITAN AIRPORT

1.3 DEVELOPMENT OF THE NDT PROCESS

Since 1967, attempts have been made by the writer to improve pavement design methods through the use of NDT. Today, the entire design procedure from NDT data processing to pavement design and cost benefit optimization has been fully computerized. In order to understand the progress in NDT research and practical applications, a brief review of several airport jobs follows.

a. Early Field Experiments

In the fall of 1967, the mobile version of the Shell machine was used at Newark and JFK Airports. The self-powered, truck-mounted machine was equipped with a complete range of monitoring instruments, and independent low and medium frequency vibrators. Eccentric weights were attached in opposite positions inside each vibrator drum so that the horizontal forces of the rotating drums cancelled each other. The resultant vertical harmonic load was applied to the pavement surface through a steel contact plate 12 inches in diameter. An input-load range of 500 to 4000 kg, peak to peak, was obtained by adjusting the eccentricity of the rotating masses. A slot built into each vibrator drum allowed the load to be adjusted while the vibrator motors were in operation. The machine had an operation frequency of 5 to 20 Hz for the low-frequency (heavy mass) vibrator, and 16 to 80 Hz for the medium-frequency (light mass) vibrator. A separate but smaller machine with a maximum vibrational force of 1000 kg, peak to peak, and an operational frequency range of 60 to 200 Hz was also used in the experiment.

The contact plate housings of the low and medium frequency vibrators had three load cells which monitored the quasi-static load imposed upon the pavement. An accelerometer in contact with the loading plate monitored the acceleration of the ground vibration. The ground vibration amplitude was calculated by double integration of the g measurement through an analog computer.

Experiments on Subgrade The first experiments were conducted with the Shell tester on a subgrade reclaimed from marshland. From the surface to a depth of about 10 feet, the subgrade consisted of hydraulic sand fill. The grain size ranged from the No. 30 to No. 50 sieve sizes, with less than 10% retained on the No. 10 sieve and less than 3% of the particles passing the No. 200 sieve. The sand's density ranged from 108 to 112 lb/cu. ft. Below the sand fill, a meadow mat, 3 to 6 feet thick, consisted of a mixture of silt, sand and decayed vegetation. Below the meadow mat, the basement material consisted of red clay-sand. It was an original deposit, well compacted, and possibly preloaded by glaciers. The vibration test was conducted on the subgrade, with the vibratory machine directly on a 4 to 6 inch blanket of stone screenings as a work platform. The heavy vibrator was used for a range of

4 to 16 Hz, and the medium vibrator for 16 to 80 Hz. The forcing amplitude was kept constant (refer to equation 1.1). For each frequency selection, a steady state of vibration was attained. It required at least five forcing cycles to achieve steady state, but the vibrator was kept in the condition for about 20 to 30 seconds. At 20 seconds, the ground acceleration was monitored, the integration performed, and the ground displacement recorded. Output resolution was within $\pm$ 1% of rated capacity. The frequency interval were run from 1 to 2 Hz for the low frequency test and 3 to 4 Hz for the high frequency test.

The frequency vs. response results are shown in Figure 1.2. The peak response at 7 Hz possibly indicates the deflection in the meadow mat. The second resonance peak was not as clear as the first and occurred at 17 Hz. This could reflect the sand fill over the meadow mat. The third resonance, encountered at 52 Hz, could be the basement material.

Experiments on Test Pavements The next experiment was conducted on a Newark test pavement section consisting of a 3 inch asphaltic concrete surface on a 9 inch plant-mix, asphalt-stabilized stone base. The subbase consisted of 6 inches compacted screenings which served as a work platform for the paving equipment. The vibratory testing procedure was the same as described above except that the forcing amplitude was increased to 1000 and 2000 kg. The results are shown in Figure 1.2.

The surface deflection, SUMZ, by Equation 1.22 of the subgrade w_o (see Figure 1.2), was equal to 0.371 mm/kg x 10^{-3}. SUMZ of the test pavement w_z (see Figure 1.2), at a forcing load of 1000 kg was 0.142 mm/kg x 10^{-3}. From experience with the Newark test pavements, if the ratio of deflection between pavement and subgrade w_z/w_o, is known, then the ratio z/a can be determined by the Boussinesq Method. In this case, w_z/w_o = .142/.371 = .380, and therefore, z/a = 1.90. Since the radius a, of the Shell machine loading plate was 6 inches, the computed pavement thickness z, of the consolidated layers was 1.9a = 11.4 inches. The actual thickness of the test pavement was 3 inches asphaltic concrete plus 9 inches asphaltic plant mix stone base. It can be seen that the Shell test results can lead to an effective determination of pavement thickness when subgrade and pavement responses are measured.

Experiment on the Taxiway Bridge The third experiment was on a taxiway bridge over the Van Wyck Expressway at Kennedy International Airport. The bridge deck consisted of a concrete slab over 15 longitudinal steel beams spaced @ 6 foot intervals. The 130 foot long beams were supported by two abutments with a center pier, which divided the length into 2 spans of approximately 64 feet each. The Shell tester was first placed on the centerline of the bridge, mid-way between one abutment and the center pier. The machine was excited from 3½ to 20 Hz at about ½ Hz increments. Double amplitude of the forcing function was 500 kg. At each test frequency, the maximum vibration under the machine was monitored and plotted as shown in Figure 1.3.

The structure's first resonance occurred at about 6.1 Hz. The second mode of resonance was at 7.1 Hz, and the third mode at about 8.75 Hz. With the machine still at the same location, the next series of tests monitored the dynamic response of the concrete deck at 40 different points along the longitudinal centerline of the bridge. At 6.1 Hz, the response of one span was equal to the other's; that is, the two spans vibrated in harmonic motion (see Figure 1.4). The machine was next placed at the quarter-point of span from the center pier. The two spans vibrated harmonically at 6.1 Hz also, but the amplitude was different from when the machine was at the first test location. The machine was subsequently moved back to the first location and the exciting frequency set at 8.75 Hz, corresponding to the third resonance. The response in the span where the machine was located was the same as when the vibratory frequency was 6.1 Hz, but the adjacent span did not vibrate harmonically (see Figure 1.4). It can be seen that the pavement's response to a forcing function should be monitored under a wide frequency range.

These early experiments demonstrate that NDT is a useful tool for evaluating the deformation modulus of the subsoil, the existing pavement thickness, and the natural frequency of the response function.

b. Newark, JFK and LaGuardia Airports

In the fall of 1968, frequency sweep NDT was first applied at these three Port Authority airports. The mobile version of the Shell machine was imported again from the Netherlands. In a period of three months, 9000 measurements were made at 650 locations, covering practically all the aircraft pavements at Newark, JFK, and LaGuardia. The machine output pavement response (see Figure 1.5), which was then adjusted for the monitoring system's nonlinear performance and calibrated for the load cell's electric voltage against a static load, as determined previously in the laboratory. The final data deduced from the test represents the dynamic response (deflection) of the pavement surface in micrometers (10^{-3} mm) per kilogram.

c. Nashville, Portland and Raleigh-Durham Airports

Between 1972 and 1974, frequency sweep NDT was used to evaluate pavements at these airports. The basic engineering concept was similar to that applied at the three Port Authority airports.

The WES 16 kip machine was used for these tests. It is similar to the Shell machine but with a heavier electro-hydraulic forcing system and more efficient monitoring electronics. Frequency sweep ranged from 5 to 100 Hz at a constant amplitude of 4000 pounds (see Figure 14, p. 38 [8]). Approximately 100 tests were conducted at each airport and the test period lasted from 4 to 5 days. A typical plot of test results

is shown in Figure 1.6. Tests on runways and at busy intersections were carried out at night to minimize interference with airport operations. Close cooperation from the control tower kept airport operations normal during the entire NDT period. The night process of NDT was actually more efficient and yielded more reliable results because of the fairly constant night temperatures than day time testing.

d. San Jose Municipal Airport

Between September 9 and 24, 1975, 200 full frequency NDTs were performed by WES at San Jose Municipal Airport. There was no interference with operation schedules despite San Jose's being a one runway airport in the busy San Francisco Bay area. The practical and objective purpose for the NDT program at San Jose was to establish an inventory file on support conditions which could be integrated into the master computer program for pavement evaluation. Detailed discussion of this program will be given in Part II of this report.

e. Other Airports

At the beginning of this research contract, copies of 59 frequency sweep NDTs performed at 8 civil airports were supplied by WES. The tabulated frequencies, vibratory loads and dynamic responses were processed for the NDT E-value. The results are reproduced in Table 1.1. The airport codes are:

SRA	Shreveport Regional Airport
DFWRA	Dallas/Fort Worth Regional Airport
WESTTS	WES Temperature Test Section
NAFEC	National Aviation Facilities Experimental Center
WESSTS	WES Soil Stabilization Test Section
WDA	Wilmington, Delaware Airport
PIA	Philadelphia International Airport
BFA	Baltimore Friendship Airport
JMMA	Jackson Mississippi Municipal Airport

Test data from the Houston International Airport could not be processed by the NDT computer program because the dynamic response at first resonance was not monitored.

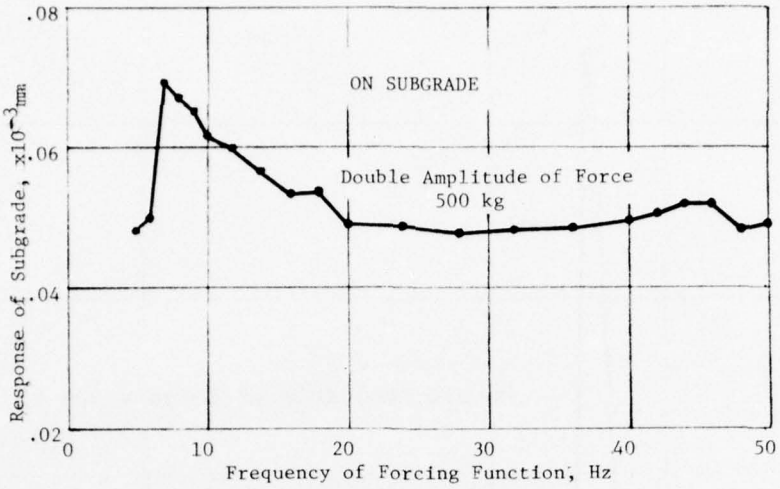

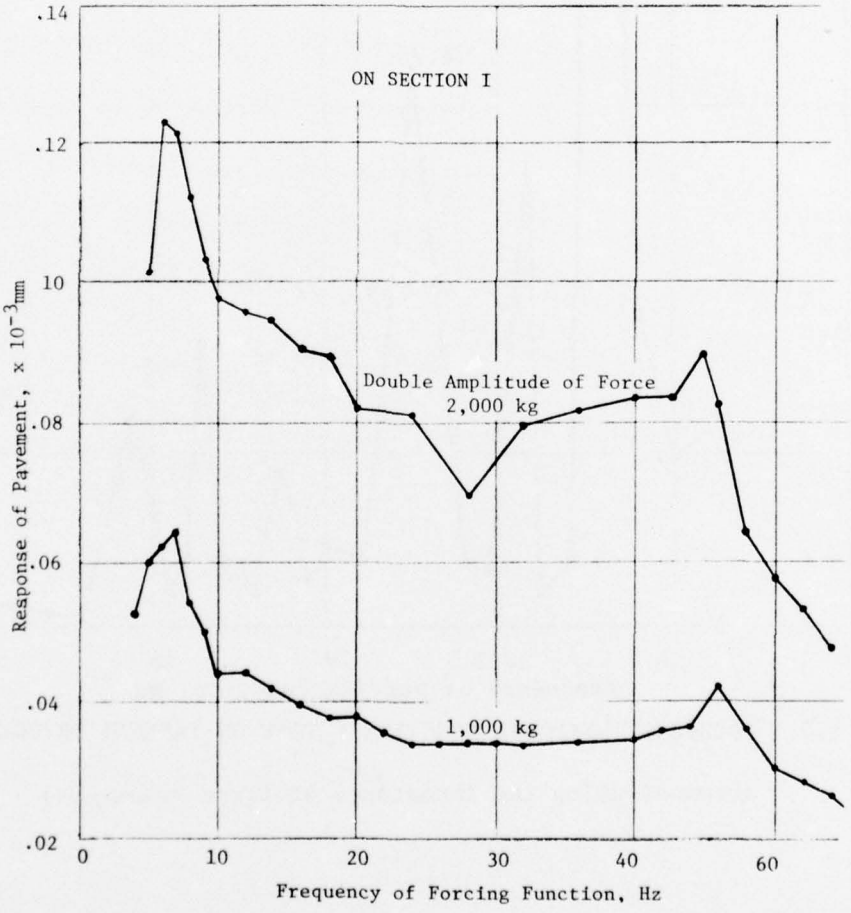

FIG. 1.2 FREQUENCY RESPONSE FUNCTION - NDT AT NEWARK

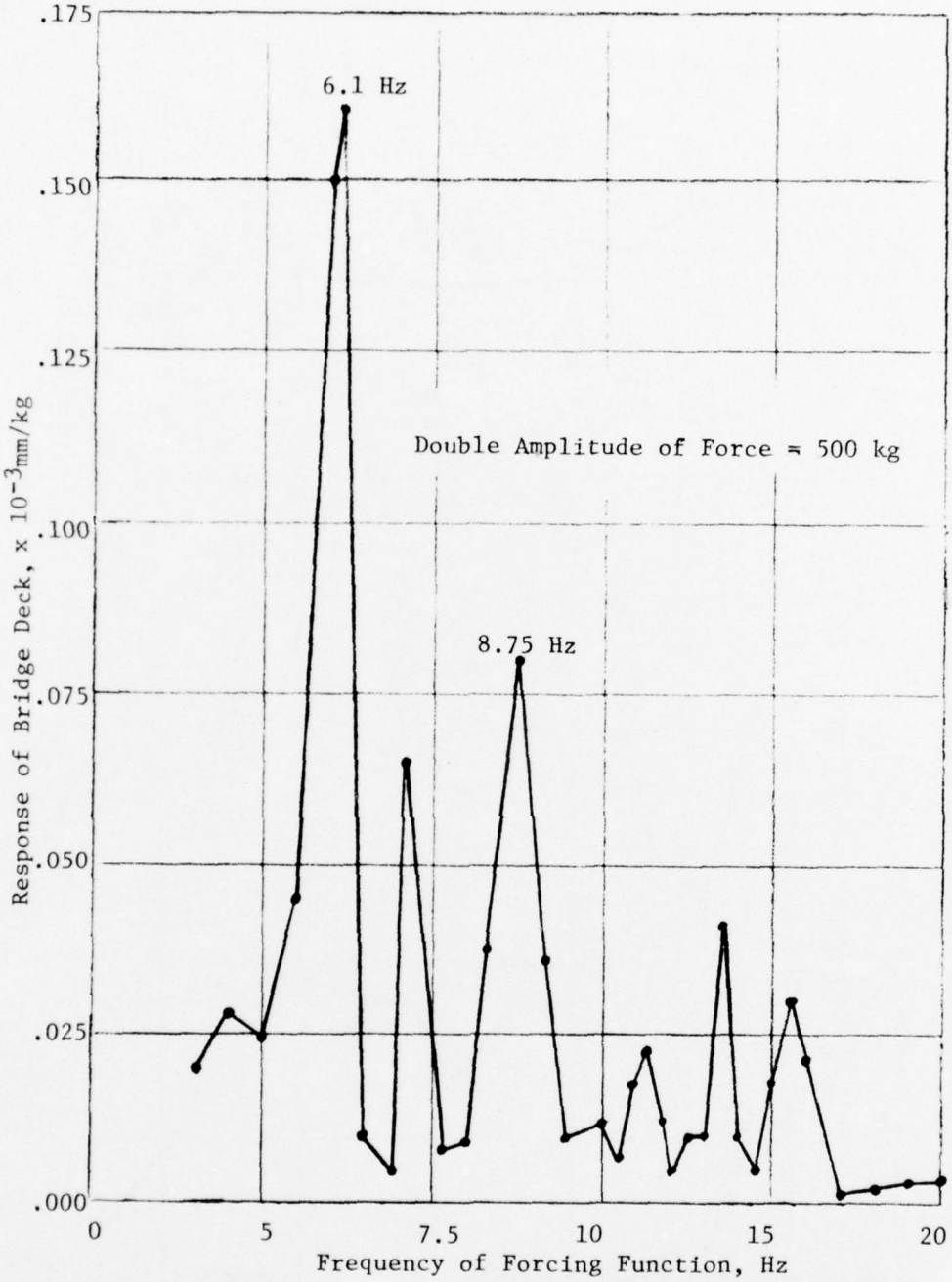

FIG. 1.3 FREQUENCY RESPONSE FUNCTION - TEST ON TAXIWAY BRIDGE

(Demonstrating the importance of first resonance)

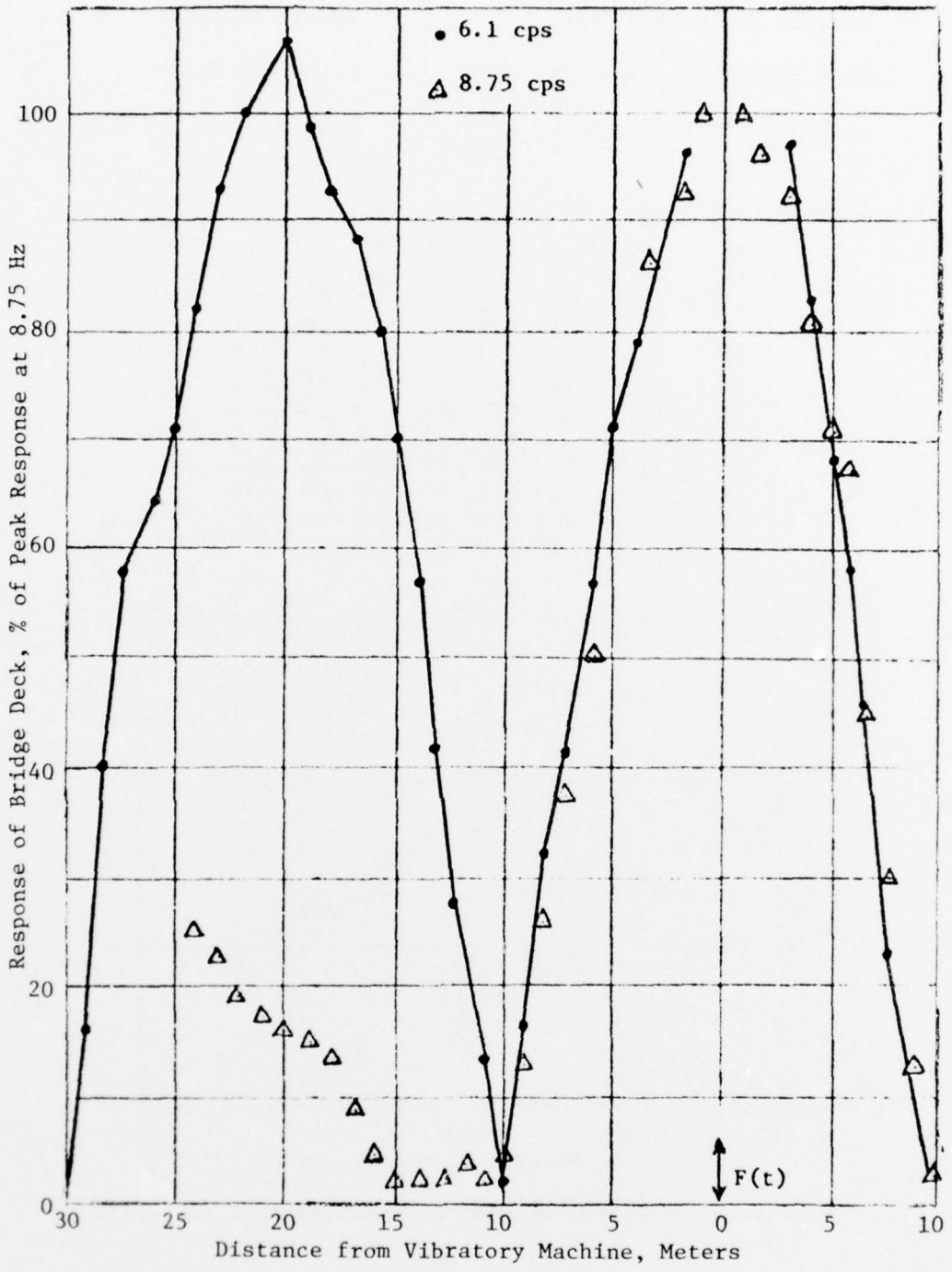

FIG. 1.4 FREQUENCY RESPONSE FUNCTION OF TAXIWAY BRIDGE AT JFK

Dynamic Deflection Test — Newark Airport

Date 10-1-68 — Temp Air 17°C — Area: R/W 4-22

Top 15

Weather: Clear — -3" 22.5 — Test No. 120

-6" 22.5

Symbol	Freq	Code	Fe	Fw	Zw	S	ϕ	Sc	1/Sc
Lo	10	10	1070	800	31	260	20	258	39×10^{-4}
	12	10	1050	800	29	205	14	276	36
	14	10	1150	795	31	265	15	257	39
	16	10	1230	820	34	250	19	242	41
	18	10	1300	800	33	255	24	243	41
Hi	20	12	800	810	32	252	26	253	39
	24	12	720	800	32	255	34	250	40
	28	12	630	810	33	253	38	245	41
	32	12	560	790	29	280	46	272	37
	36	12	570	815	27	300	46	302	33
	40	12	460	800	26	305	50	308	32
	44	12	370	820	24	350	48	342	29

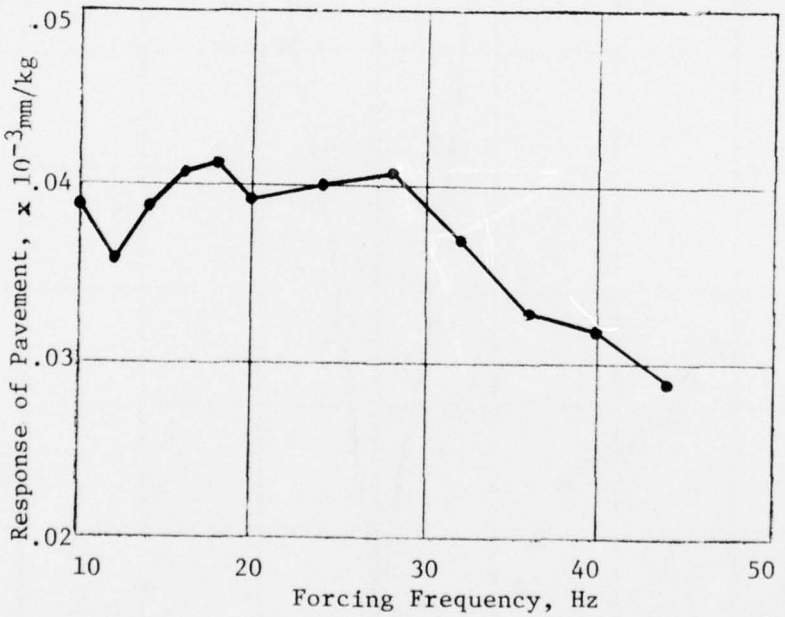

FIG. 1.5 A TYPICAL RECORD OF VIBRATORY TEST AT NEWARK

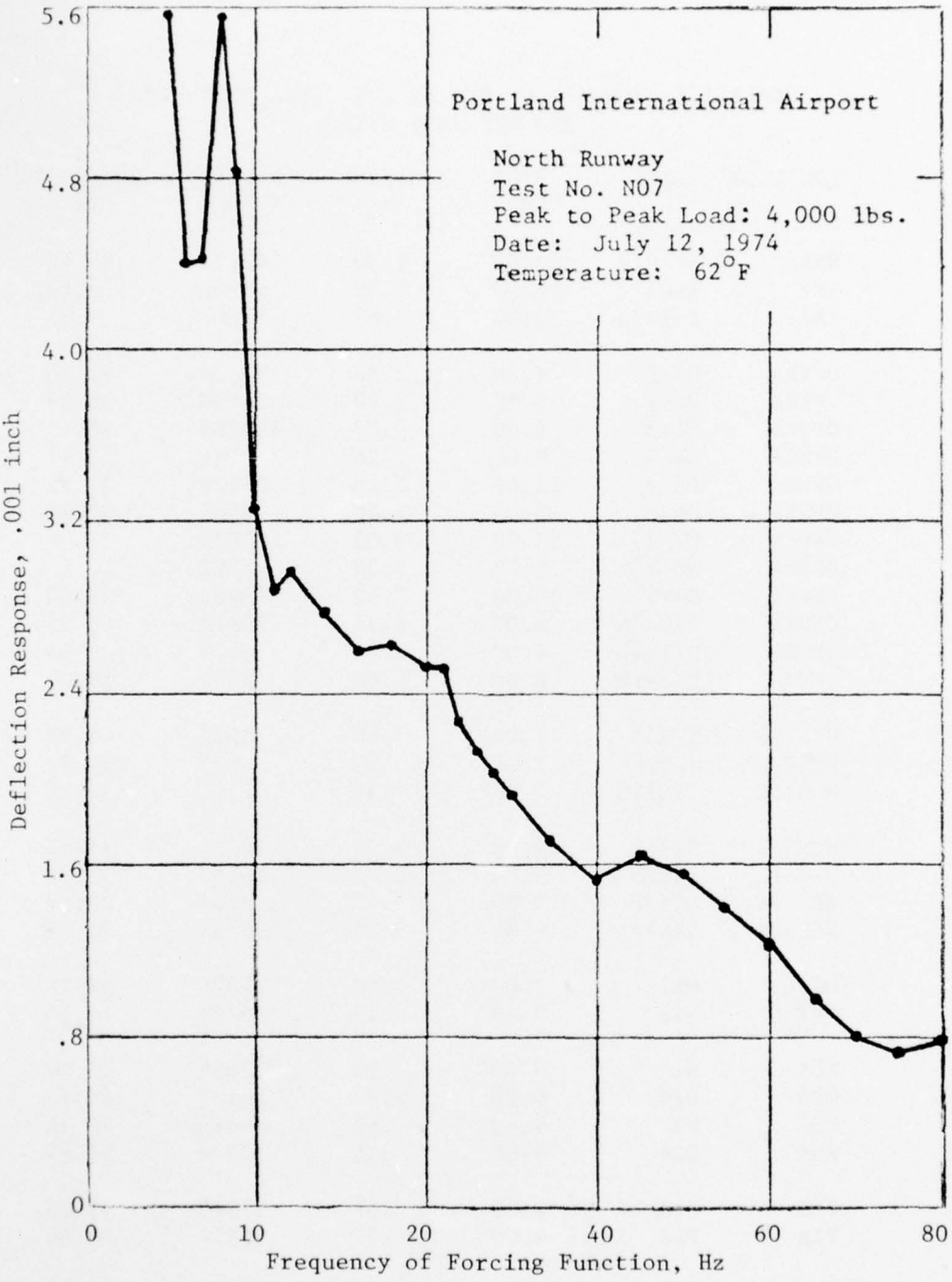

FIG. 1.6 FREQUENCY RESPONSE FUNCTION OF NDT AT PORTLAND

TABLE 1.1 SUMMARY OF NDT AT SIX CIVIL AIRPORTS AND WES TEST SITES

LOCATION	CODE	H(0) HZ	Z(N)/SUMZ %	E-VALUE PSI	DSM(0)/E IN
SRA	1-1072	10.00	5.30	47721.	35.42
SRA	1-0373	10.00	4.85	46202.	36.49
SRA	1-1073	10.00	2.68	57808.	29.01
DFWRA	D1-1	9.00	3.52	98536.	41.90
DFWRA	D2-2	9.00	2.98	78890.	31.59
DFWRA	D3-3	8.00	3.07	102659.	38.69
DFWRA	D4-4	9.00	3.16	110245.	35.67
DFWRA	D5-5	12.00	5.15	26423.	34.12
DFWRA	D6-6	5.00	2.48	4261.	47.34
DFWRA	D7-7	10.00	3.05	101022.	28.78
DFWRA	D8-8	8.00	3.08	31782.	40.66
DFWRA	D9-9	10.00	3.68	63965.	28.64
DFWRA	D10-14	8.00	3.31	28612.	40.65
DFWRA	D11-15	6.00	2.14	6079.	40.66
DFWRA	D12-18	6.00	1.66	9342.	39.37
WESTTS	TTS17	5.00	.30	8522	44.99
WESTTS	TTS18	7.00	.55	7425	34.52
WESTTS	TTS110	7.00	.39	7594	35.21
WESSTS	STS1P	9.00	4.34	24095	39.57
WESSTS	STS2P	9.00	3.27	30166	36.30
WESSTS	STS3P	10.00	3.43	63464	29.97
WESSTS	STS4P	10.00	3.38	65236	30.65
NAFEC	N11	7.00	1.80	17826	52.10
NAFEC	N18	9.00	3.45	18799	40.10
WDA	W1	8.00	.22	17689	38.84
WDA	W1A	8.00	1.39	16257	40.73
WDA	W2	9.00	.49	29414	36.36
WDA	W2A	9.00	.54	32570	35.01
PIA	P13	9.00	.57	37996	33.05
PIA	P14	9.00	.57	36577	36.64
BFA	B1A	9.00	1.06	29775	37.05
BFA	B2	8.00	.70	25037	40.07
BFA	B3	9.00	1.11	28029	40.68
JMMA	J1	9.00	.64	38731	31.77
JMMA	J2	10.00	.42	48973	30.87
JMMA	J3	9.00	.61	29601	34.62

1.4 RESEARCH ASPECTS OF NDT

Because NDT is still in its budding stage, whenever possible, additional research analysis was conducted during practical application of the NDT program. The results of such NDT research is discussed below.

a. Correlation with Plate Bearing Tests

The data processing method developed for frequency sweep NDT was designed to produce E-values equivalent to those obtained by the conventional plate bearing test. Correlation with the plate bearing test was established through experiments at the following airports.

Newark Test Pavements The test pavement shoulder consisted of 4 inches of stone screenings over a sand fill subgrade. Compaction of the sand and stone screenings was in the 97-100% maximum dry density range. There was no vehicle load on the shoulder except for occasional passenger automobiles. At completion of the test pavement construction in 1966, a plate bearing load test was conducted on the shoulder. The load-deformation data is plotted in Figure 1.7. According to the Boussinesq theory, the E-value by the plate bearing test can be computed by Equation 1.15a. For this test, the E-value was 12,900 psi when the μ-value was assumed to be 0.35.

About 18 months after the plate bearing test, NDT experiments with the Shell machine were conducted at the same location. The frequency sweep results are plotted in Figure 1.2 with the data processing details shown in Table 1.2. The computed NDT E-value is 12,500 psi, which represents a discrepancy of only 3% from the 12,900 psi value found by plate bearing tests.

This correlation confirmed for the first time the validity of frequency sweep NDT, and that NDT could be used to replace the conventional plate bearing test. In this case, the plate bearing test took about 1½ days to complete, at a direct cost of about $800. NDT with the Shell machine took about 10 minutes with a cost of about $30. In terms of time and money, NDT is very appealing to the pavement engineer.

Nashville and Portland Airports At Nashville Metropolitan Airport, nine plate bearing tests were conducted on the base course and subgrade while NDTs were carried out on the pavement surface. Theoretically, there is no correlation between these two types of tests, but based on the Newark test program experience, if the pavement structure and its subgrade support are known, the surface deflection of that pavement can be reasonably approximated through the Boussinesq theory. Consequently, the composite E-value of the pavement surface can be computed. The computed E-values are given in Table 1.3 and correlation with the NDT

E-values is shown in Figure 1.8. Except for locations A1 and B2, where wet subgrade was reported during the test, all NDT E-values agreed well with those computed from the plate bearing test. As a matter of fact, the NDT E-values for A1 and B2 had a much narrower range of variation which, from the statistical point of view, indicates a more realistic picture of the existing pavement.

At Portland International Airport, three plate bearing tests were conducted in 1971, to determine the support condition of the hydraulic sand fill. The E-values computed by Equation 1.15a range from 3700 to 6200 psi. In 1974, frequency sweep NDT yielded E-values ranging from 4000 to 5200 psi. The NDT locations did not coincide with those of the original plate bearing tests, but the soil conditions at the site were fairly uniform. The difference between the two E-value sets is small, with the NDT values having a much narrower range of variation.

San Jose Municipal Airport For NDT research, a series of plate bearing tests were conducted on the pavement surface, and then on its base and subgrade after a pit had been excavated at the test location. The average load test took about 3 days, with more than 5 weeks necessary to complete all the tests. In processing the results, the following standards were used:

(1) Normal rate of loading required the two-hour deflection reading after each load increment,
(2) Quick loading required the first 15-second deflection reading after each load increment,
(3) Repetitive loading required six successive 15-second deflection readings after each load increment, and
(4) The E-value computed by Equation 1.15a is assumed to have a μ-value of 0.30 for the existing pavement.

The E-values computed for all plate bearing tests are shown in columns 6 to 8 of Table 1.4. In studying these results, it is noted that:

(1) Except for two tests on concrete pavement, a large surface deflection (small E-value) was recorded for all tests, and
(2) The E-values at locations 68 and 69 seem unreasonable, i.e. saturated base rock seems stronger than unsaturated rock, and the asphalt pavement surface is nearly as strong as its base rock.

These discrepencies are possibly due to the asphalt surface heaving beyond the loaded plate during elevated ambient temperatures. Consequently, an excessive surface deflection was recorded.

Two plate bearing tests on concrete pavement correlated well with the NDT E-values, as shown in Figure 1.9. It should be pointed out that:

(1) The best correlation was encountered at a forcing function of 8000 pounds, which was also the most common double amplitude for the experiment;
(2) The plate bearing tests conducted at normal loading cycles correlated better with NDT results; and
(3) Reliable NDT E-values, such as those in column 4 of Table 1.4, can be obtained if the vibrator is properly calibrated for its velocity monitoring and amplitude recording.

Conclusions The correlation studies conducted at these four airports demonstrate that:

(1) The frequency sweep theory is valid. Correlations ranging from 0.95 to 1.05 with plate bearing test results have been experienced.
(2) The normal loading cycle of the plate bearing test reflects static load conditions and yields more reliable E-values than quick loading. This confirms the Shell researchers' observations that the E-value determined by the mechanical vibrator can be used in the elastic theory to analyze the stress-strain characterics of a pavement system as if it were under static loading conditions.
(3) NDT monitors the response of the entire pavement support system, from its surface to a greater subgrade depth than conventional plate bearing tests. The condition of the stone base support system at Nashville primarily affected the plate bearing test. The NDT deflection changed only slightly because the subgrade moisture remained constant.
(4) Based on San Jose's results (see Table 1.4), NDT is more reliable than the plate bearing test in monitoring the true deflection of an asphalt pavement at elevated ambient temperatures.
(5) As demonstrated by tests at Nashville and Portland, E-values from NDT have a much smaller standard deviation than those from plate bearing tests. NDT therefore, yields a more reliable representation of actual conditions.

b. Correlation with Soil Tests

Four core borings were made at San Jose Airport to extract undisturbed clay samples from the subgrade. The samples were prepared for the standard triaxial test and the E-values computed by Hooke's law are shown in column 9 of Table 1.4. As the rate of load application by this test is much slower than NDT's vibratory force, there seems to be no correlation between the E-value by NDT and the triaxial test.

A portion of the same set of clay samples was delivered to the

University of Illinois for resilient modulus testing. The results are shown in column 10 of Table 1.4. The soil samples were highly variable in texture, disturbance, and moisture content. The in-situ resilient moduli should be much greater than those measured from the tube samples. The laboratory tests indicated that the resilient moduli could be reduced by one-half if the sample moisture was high. This coincides with the experience that more pavement distresses are encountered when the clay base is wet. As the subgrade has a low moisture content and is undisturbed by NDT, the E-value by NDT should be correlated with the upper range of the resilient modulus. Considering the disturbance of the clay samples, NDT E-values correlate well with the resilient moduli.

c. Magnification and System Damping

The equation for E-value determination is derived from the assumption that:

$$(1-\mu^2)\cdot\ln((1+\beta)/\beta) = \pi \qquad (1.24)$$

in which β is the critical damping coefficient contributed by energy dispersion into the soil. Material damping is usually determined by the logarithmic decrement from free vibrations. For a one-degree-of-freedom system with viscous damping, successive decrements in vibratory amplitude for a full vibration cycle can be expressed by (see Figure 1.10):

$$\ln(x_1/x_2) = 2\pi\beta/\sqrt{1-\beta^2} = \delta \qquad (1.25)$$

in which the logarithmic decrement δ, is equal to $2\pi\beta$ when the β-value is very small.

Richard and Hall [10] indicate that the logarithmic decrement of sand ranges from 0.15 to 0.38. The corresponding β-value ranges from 0.024 to 0.060. The lower range represents the water saturated condition while the upper range reflects the dry condition.

During aircraft vibration tests at JFK Airport [11], the logarithmic decrement was measured through vibration of a steel platform on the subgrade. The β-value was about 0.02.

In our present state of knowledge, the β-value can be assumed to be between 0.02 and 0.06; $\ln(1+\beta)/\beta$ correspondingly ranges from 3.93 to 2.87. Richard and Hall [10] report the average logarithmic decrement of soils to be 0.25. The corresponding β-value is 0.04 and $\ln(1+\beta)/\beta$ is 3.26, only 4% greater than the π-value. Insofar as viscous damping is concerned, processing frequency sweep NDT data by Equation 1.17 will produce an E-value within $\pm 5\%$ of the theoretical value.

d. Optimum Forcing Amplitude

Seven sets of variable load frequency sweep tests were run at San Jose Municipal Airport to evaluate the effect of force amplitude on E-value reliability. The mean and average of log-E was determined for each test location under various loadings. The deviation of log E from the mean value is given in Table 1.5 and plotted in Figure 1.11. It can be seen that 8000 pounds double amplitude yielded the least variable results and the most conservative E-values.

e. Pavement Surface Temperature

Since asphalt is a temperature dependent material, a temperature correction factor was introduced into NDT at the New York-New Jersey airports in 1967-1968. At the same time, tests conducted by the Asphalt Institute [12] found the stiffness of an asphalt concrete mix at 100°F to be 22 to 25% of that at 70°F.

During NDT at Nashville in 1973, air temperature fluctuations did not significantly affect the E-values of asphalt pavements. At Portland, however, significant temperature fluctuations were encountered. Three sets of NDT was performed on two identical pavements at various air temperatures are plotted in Figure 1.12. The relation between air temperature and frequency sweep E-value is given below:

Test No.	Air Temperature	NDT E-value	Asphalt Layer
TRI-5	108°F	37,500 psi	10"
SQU-4	73°	40,300	10"
S07	108°	38,000	13"
S04	90°	35,600	12"
S15A	117°	52,500	13"
S15B	72°	58,500	13"

The E-value varies from -.23 to +.25% per degree change in air temperature. For air temperatures between 90° ± 20°F, the monitored NDT E-value can be expected to be between 95 and 105% of the average. Since a large portion of pavement deflection is contributed by the supporting soils and the subgrade support is less sensitive to temperature variations, E-values by frequency sweep NDT should be reasonably independent of temperature changes in the United States. Future research is required to determine the effect of extremely hot or cold temperatures on the E-values obtained from frequency sweep NDT.

f. Base and Subgrade Moisture

During NDT at San Jose, attempts were made to determine the effect of moisture on E-values of the base and subgrade. Portions of the

existing asphalt and concrete pavements were removed and NDT was conducted on the base rock (aggregate base) surface. NDT was repeated after the base was fully saturated. The results are given in Table 1.4. The E-value for a saturated base is about one-half that for an unsaturated base. These results are identical to those found by the plate bearing tests performed at Nashville and San Jose.

Experience at Nashville and San Jose also indicates that NDT conducted on the existing pavement surface does not detect base course moisture (see tests A1 and B2 in Figure 1.8 and Table 1.3). This is because NDT deflection is due primarily to the subgrade rather than the base course. Therefore, frequency sweep NDT yields the most reliable E-values for evaluating and characterizing the support conditions of a pavement.

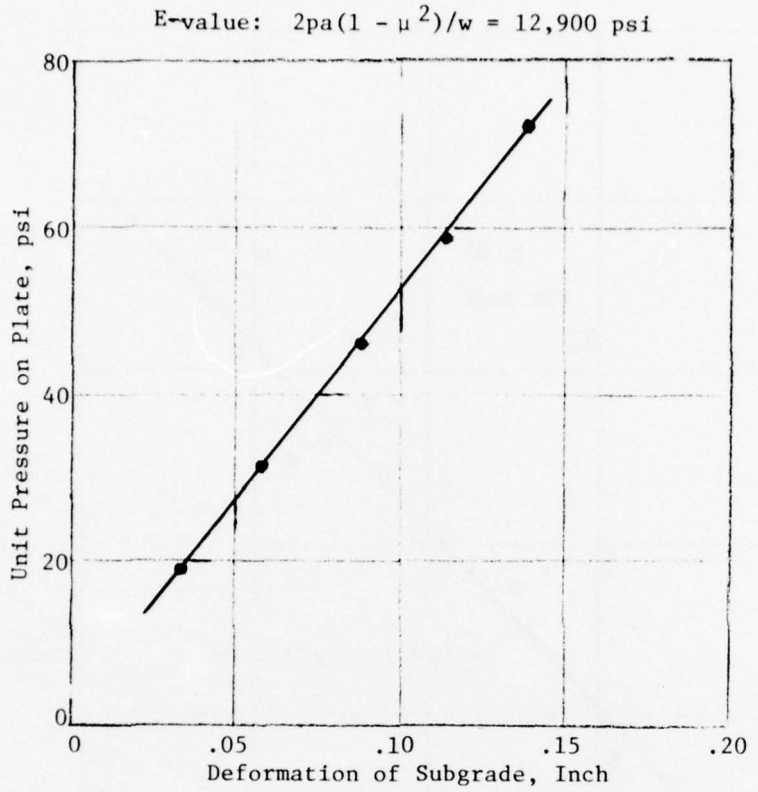

FIG. 1.7 RESULT OF PLATE BEARING TEST AT NEWARK AIRPORT

TABLE 1.2 SHELL NDT TEST ON SUBGRADE AT NEWARK AIRPORT

Double Amplitude of Forcing Function, F = 500 kg.
First mode of Resonance, p = 7 cps

Frequency ω, cps	u = ω/p	Response, z(u) x10^{-3} mm	z(u)/u x10^{-3} mm
7	1.0	69.0	69.0
14	2.0	57.6	28.8
21	3.0	49.0	16.3
28	4.0	48.4	12.1
35	5.0	50.0	10.0
42	6.0	51.2	8.5
49	7.0	52.6	7.5
56	8.0	50.6	6.3
63	9.0	50.0	25.0
		Σ z(u)/u	183.5

$$E = \frac{F}{2a} \cdot \frac{1}{\Sigma \frac{z(u)}{u}} = \frac{500 \times 2.2}{2 \times 6} \cdot \frac{1}{183.5 \times 10^{-6} \times 39.4} = 12{,}500 \text{ psi}$$

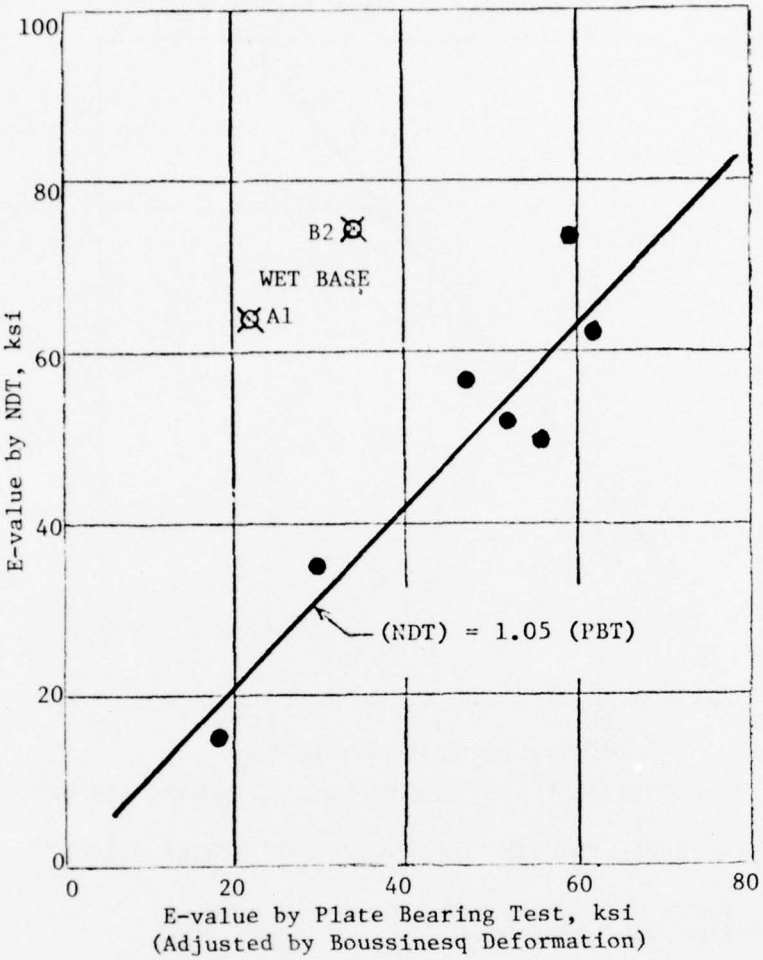

FIG. 1.8 CORRELATION BETWEEN NDT AND PBT AT NASHVILLE AIRPORT

TABLE 1.3 CORRELATION OF E-VALUE AT NASHVILLE AIRPORT

Location of Test	Thickness AC Top Inches	Thickness Base Inches	pa/w Subgrade psi	Surface Deflection Inch	E-value PBT psi	E-value NDT psi	Remarks
A1	14	8	5,930	.27	22,000	63,700	Wet base
A2	14	21	11,750	.21	56,000	49,700	
A3	13	25	8,800	.17	52,000	52,200	
A4	14	17	6,820	.23	30,000	35,500	
A5	8	12	5,530	.30	18,400	15,600	
A6	7	6	20,400	.43	47,400	57,400	
A7	18	12	13,100	.21	62,300	61,600	
B1	13	8	11,850	.20	59,200	74,000	
B2	13	9	7,150	.21	34,100	75,000	Wet base

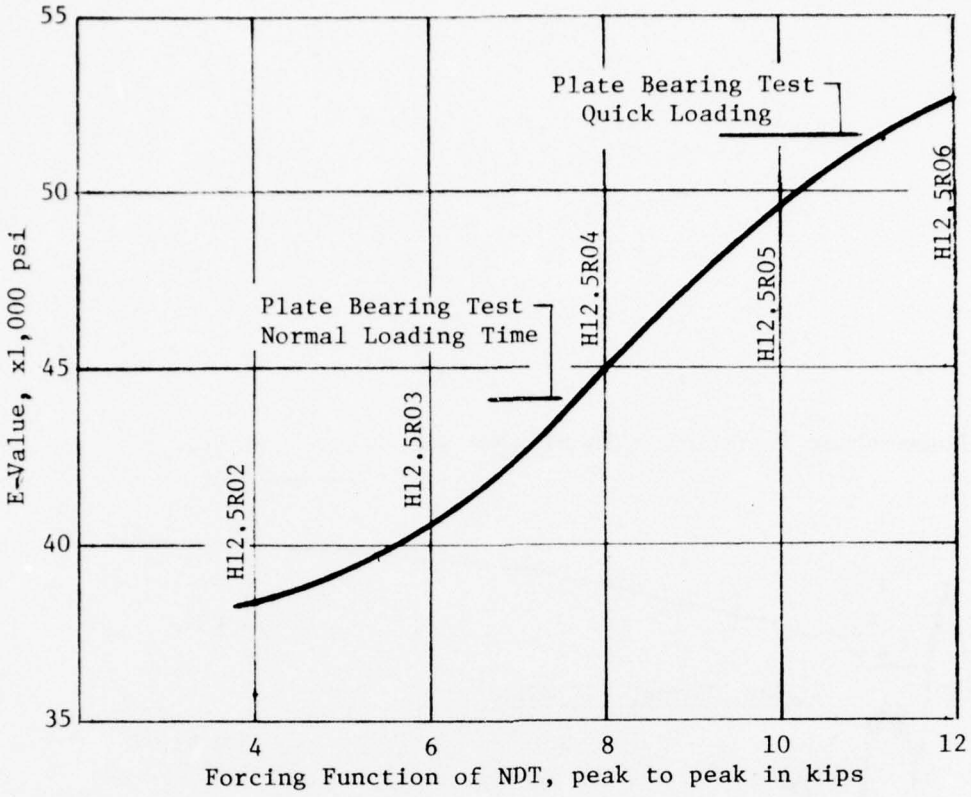

FIG. 1.9 CORRELATION BETWEEN NDT AND PBT AT SAN JOSE

TABLE 1.4 CORRELATION OF NDT AND CONVENTIONAL TESTS AT SAN JOSE

LOCATION	GRID	SURFACE MATERIAL	MODULUS OF ELASTICITY, E-VALUE in psi						
			BY NDT		PLATE BEARING TEST			TRIAXIAL	RESILIENT
			PRIOR TO*	AFTER**	NORMAL	QUICK	REPETITIVE	TEST	@ 10 psi
68	E38.5L14	Asphalt	34,700	47,900	14,400##	-	-	-	-
69	E37.1L2F	Base Rock(Unsaturated)	18,100	-	-	13,300##	6,700	-	-
69	E37.1L2F	Base Rock(Saturated)	-	12,300	-	15,900##	8,800	-	-
T/W	1,C,2,D	Subgrade	7,000	-	-	4,000	1,700	150-540	1900-4300
137	C10,8002	Shoulder-Subgrade	9,600	-	-	-	-	- -	-
109A	H12.5R06	Concrete	52,700	-	51,500	-	-	-	-
109B	H12.5R04	Concrete	44,900	-	44,600	-	-	-	-
110	H11.9R03	Base Rock(Unsaturated)	-	17,600	-	14,800	5,200	-	-
		Base Rock(Saturated)	-	-	-	5,300	2,700	-	-
		Subgrade	-	-	-	1,000	500	260-340	2600-4600
121	H54.5004	Concrete	-	124,900#	18,000	-	-	-	-
		Subgrade	-	-	-	-	-	500	3200-5500
145	D42.5004	Asphalt	-	41,800	15,300	-	-	-	-
		Subgrade	-	-	-	-	-	520	3500

* Tests completed prior to the break-down of NDT equipment on September 13, 1975.
** Tests resumed after the completion of equipment repairs on September 22, 1975.
# Tests were conducted on September 23, 1975, when the NDT equipment was repaired (reliability of equipment calibration was unknown).
Inconsistency in the result of plate bearing load tests.

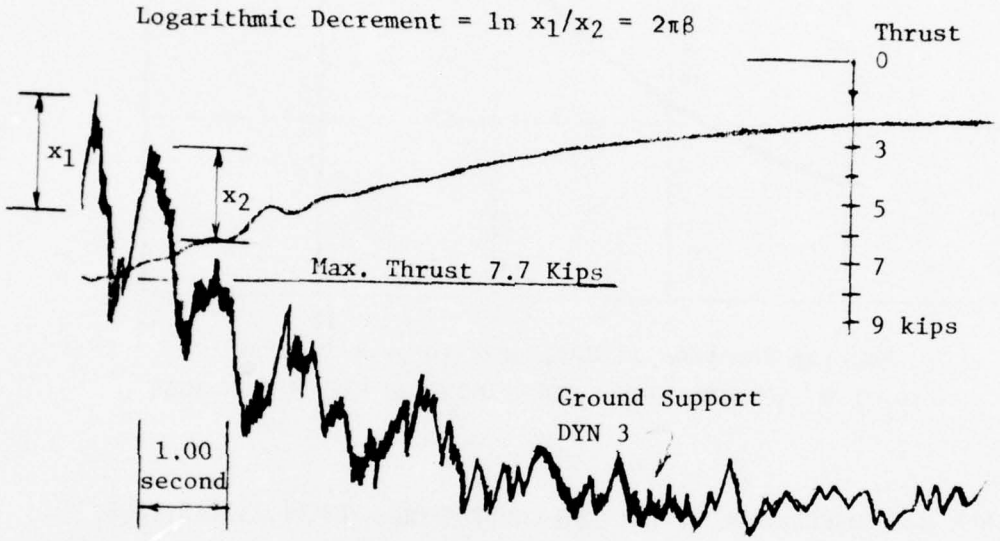

DC-8 Aircraft Test at JFK

FIG. 1.10 LOGARITHMIC DECREMENT OF VIBRATORY AMPLITUDE

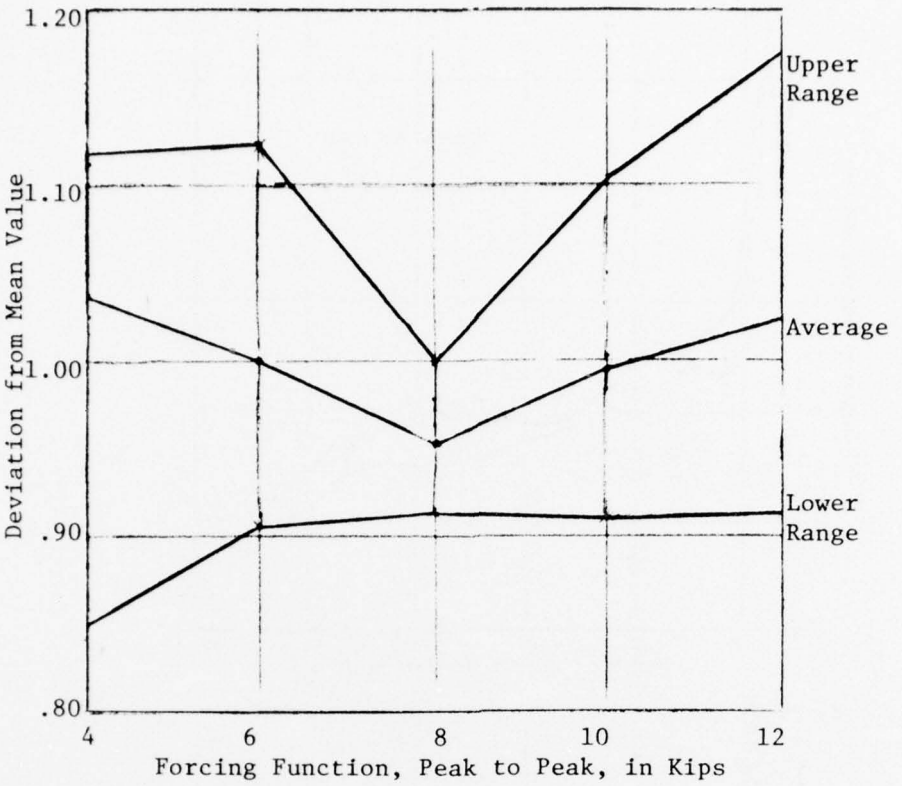

FIG. 1.11 OPTIMUM FORCING AMPLITUDE OF NDT AT SAN JOSE

TABLE 1.5 EXPERIMENT FOR DETERMINING OPTIMUM FORCING AMPLITUDE

DEVIATION FROM MEAN VALUE (ARITHMETIC SCALE)

H54.50	1.026	.953	.927	1.002	1.099
I54.50	1.094	1.012	.966	.986	.946
I36.50	1.050	1.023	.916	1.052	.971
H12.5R	.853	.906	1.000	1.102	1.175
E38.5L	1.019	.927	.973	.982	1.109
E38.5S	1.114	1.125	.918	.912	.951
D42.50	1.119	1.072	.977	.935	.914
Average	1.035	1.000	.955	.995	1.021
Upper Range	1.119	1.125	1.000	1.102	1.175
Lower Range	.853	.906	.916	.912	.914
Range	.266	.219	.084	.190	.261

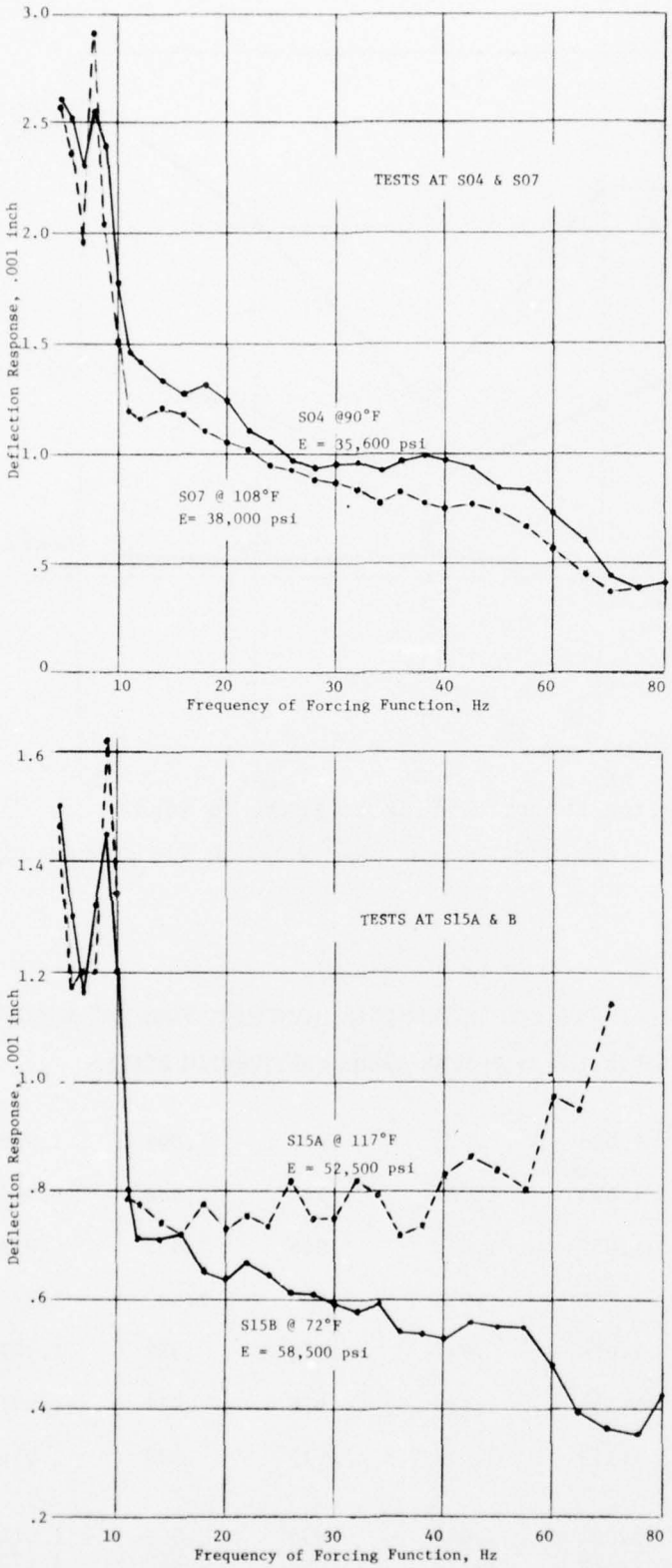

FIG. 1.12 EFFECT OF TEMPERATURE ON NDT - SOUTH RUNWAY AT PORTLAND

1.5 BASIC TESTER REQUIREMENTS

In NDT, the static load used in conventional plate bearing tests is replaced by a series of harmonic forces of constant amplitude vibrating steadily at all frequencies. Acquiring the dynamic response at first resonance is vital to the outcome of the entire test. These and other basic requirements govern the design of today's testers.

a. Steady State of Vibration

According to Equation 1.11, the pavement's dynamic response should be monitored under a steady state of vibration. This means that the tester should exert a constant forcing amplitude and frequency. The resultant ground acceleration or vertical velocity is then integrated by an analog computer to determine the vertical dynamic response (displacement). Any shift in the forcing frequency or amplitude will affect the accuracy of the integration.

b. First Resonance and Frequency Range

The E-value determined by Equation 1.17 from frequency sweep NDT is governed by summation of the pavement's dynamic response from frist resonance to infinity. If first resonance is missed, a higher E-value would be calculated. For normal pavement support, the lower range for first resonance is about 5 Hz. Therefore, the NDT machine should be capable of testing down to 5 Hz. If the pavement support is very soft, the machine should test down to about 4 Hz.

The upper frequency range should theoretically be infinite. However, it is difficult to build a high frequency vibrator with adequate amplitude. If the test is cut-off at a high frequency level, the tail area from that limit to infinity can be evaluated according to Equations 1.20 and 1.21, as shown in Table 1.6. Since high frequency vibrations above 60 Hz seem to contribute very little to the NDT E-value, the test can be cut off at 50 Hz with an anticipated error of 2%.

In summary, an adequate vibrator should be capable of sweeping from the lowest first resonance of the response system, say 5 Hz, up to a frequency of about 60 Hz.

c. Vibratory Force

In NDT, application of a series of harmonic forces simulates the effect of a static load. For airport design, the forcing amplitude should be closely related to the aircraft wheel loads. From aircraft and pavement experience, it is reasonable to assume that:

(1) the heaviest modern wheel load is 56,000 pounds,
(2) the natural frequency ratio between aircraft tires and pavement support is 1/6, and
(3) the critical damping coefficient of the pavement system is 0.05 (see Section 1.4c).

Since the dynamic impact factor for a moving aircraft is 1.03 (see pp. 318-320 [1]), the maximum dynamic wheel load is about 58,000 pounds. Using the damping coefficient, the NDT magnification factor is 10 when the forcing function vibrates steadily at the pavement system's first resonance, i.e., an NDT force of 5800 pounds double amplitude will have an effect on the pavement system similar to an aircraft with a maximum dynamic wheel load of 58,000 pounds. This double amplitude of force should be considered the minimum NDT requirement.

Since machine reliability depends primarily upon equipment resolution, the NDT force amplitude should also be within the optimum linearity and resolution range of the machine. Experience at Nashville, Portland, Raleigh-Durham and San Jose Airports indicates the optimum forcing function to be:

(1) 4000 lbs, peak to peak, for test on subgrade or badly cracked pavements,
(2) 8000 lbs, peak to peak, for tests on heavy asphalt pavements in good operational condition,
(3) 10,000 lbs, peak to peak, for tests on concrete pavements more than 12 inches thick.

The optimum forcing amplitude represents the practical operational range. The rated capacity of an NDT machine should be at least 1.2 times the upper range of the operational forcing function, i.e., at least 12,000 lbs.

d. Static Weight and Residual Force

The vibrator's static weight also affects NDT reliability. If the vibratory force is equal to or greater than the static weight of the vibrator, the vibrator itself will vibrate freely as an unsprung mass. Then, the monitored dynamic response would not be accurate. At several tests at NAFEC [13], the tester, a Road Rater #600, had a static weight of 2.5 kips with a maximum frequency range of 50 Hz. When a vibratory force of 1000 lbs was applied, the dynamic response at 40 Hz was about 40% below the peak response at 9 Hz. At 2000 lbs, the dynamic response at 50 Hz was about 30% higher than the peak response at first resonance at 7 Hz. Results of this second test do not necessarily suggest a large deflection, but may be due to operation of the tester at its upper frequency and amplitude range. Therefore, a large vertical movement was recorded due to the machine's free vibration (see Figure 1.13.).

To maintain NDT quality, the static weight or residual force of the vibrator should be at least 33% greater than the effective vibratory force. For ordinary test equipment, the resolution is best in the middle of the rated capacity. The static weight of the vibrator should therefore be around 14 kips.

e. Resolution and System Error

The WES 16 kip vibrator evaluates dynamic responses to six decimal places by processing the electronic signal from the velocity transducer through an analog integrator. The dynamic response resolution is therefore, related to velocity pick-up accuracy which cannot be evaluated directly (see Section 1.6a). Tests conducted by WES [8], indicate the computed deflection (dynamic response) resolution to be .0001 inch.

In order to maintain NDT accuracy, the forcing amplitude should be adjusted in the field to meet the following requirements:

(1) The minimum dynamic response (deflection) is to be .002 inch at the first resonant vibration, and
(2) The minimum dynamic response is to be .0002 inch and preferably .0005 inch at a steady state of vibration of 50 Hz.

Under normal NDT conditions, the vibratory forces outlined previously are adequate except for tests on very soft ground and/or very strong pavements.

All test outputs consist of the true test value R, plus the instrumental error, ε. Summation of all outputs will have an inherent error equivalent to the original instrument error:

$$\frac{1}{N}\sum^{N}(R+\varepsilon) = \overline{R} + \varepsilon \tag{1.26}$$

If the output is double integrated, as in the case of converting acceleration to response, the result can be expressed as:

$$(R+\varepsilon)^2 \sim R(R+2\varepsilon) \tag{1.27}$$

This means that after double integration, the computed error is twice that from the direct machine output. On the other hand, if the ratio of the two outputs is utilized, the error can be reduced:

$$(R_1+\varepsilon)/(R_2+\varepsilon) = (1+\varepsilon_r)\cdot R_1/R_2 \tag{1.28}$$

where R_1/R_2 is the true experimental ratio and ε_r is the error in the processed data:

$$\epsilon_r = \epsilon(R_2-R_1)/R_2R_1 \qquad (1.29)$$

If R_2 is equal to R_1, the instrumental error is eliminated. If R_2 is equal to $2R_1$, the error in the processed data is reduced to one-half that from the direct output. Equation 1.29 should be applied to data processing whenever possible.

f. Filter and Damper Effects

NDT data processed by the frequency sweep method automatically reflect the multi-frequency nature of dynamic responses and individual "deflection" outputs for a given frequency are treated as the spectral density of the total pavement response. Filtering or damping is therefore, not needed for frequency sweep NDT.

At the onset of NDT at San Jose Airport, an all-frequency filter was installed on the WES 16 kip vibrator to modify dynamic responses below 16 Hz. A typical set of test results is shown in Figure 1.14. The overestimation of NDT E-values by 53% would result in false optimism regarding existing pavement performance as well as premature deterioration of any reconstructed pavements. During the finals days of testing, from September 22 to 24, 1975, the high frequency range was reduced from 80 Hz to 50 Hz and the effect of filter damping was extended from 16 Hz to 36 Hz. High frequency cut-off resulted in 2% overestimation of NDT E-value, while installation of the low frequency filter and its extension to 36 Hz resulted in an increase of 178% in computed E-value.

"A mistake was made in calibration through use of wrong oscillator" WES reviewer explained, "therefore, incorrect data is being compared to correct data." Nevertheless, the experience suggests that:

(1) The installation of filter will complicate the NDT output;
(2) Calibration and integration of response signal are sensitive operation in NDT monitoring; and
(3) A reliable system of data recording is also an important requirement of NDT.

Counter	Frequency Hz	Force Amplitude lbs.	Dynamic Response inch	Ratio of E-value (see Note)
I	H	F	Z	
	5.06	2167.0	.001920	
	6.02	2114.4	.002139	
	7.12	2218.4	.003093	
1	7.87	2061.0	.003497	2.32
2	8.99	2120.8	.000913	1.90
3	9.97	2185.0	.001179	1.74
4	11.52	2274.3	.001444	1.60
5	12.72	2109.9	.001492	1.48
6	14.77	2073.7	.001550	1.38
7	16.93	2032.9	.001544	1.29
8	18.92	2108.1	.001746	1.20
9	20.59	2189.4	.001872	1.15
10	22.40	2160.3	.001654	1.13
11	24.57	2165.0	.001449	1.12
12	26.51	2125.7	.001320	1.10
13	28.62	2103.5	.001170	1.09
14	30.77	2094.0	.001093	1.08
15	32.52	2088.6	.001012	1.07
16	34.43	2113.5	.000972	1.06
17	36.58	2123.2	.000944	1.05
18	38.51	2131.3	.000962	1.04
19	40.62	2092.3	.000912	1.03
20	45.35	2131.5	.000804	1.03
21	50.22	2216.0	.000787	1.02
22	54.79	2213.2	.000747	1.01
23	59.72	2052.2	.000649	1.00
24	64.77	2108.2	.000533	1.00
25	69.43	2232.0	.000479	1.00
26	74.75	2548.9	.000522	1.00
27	79.57	2549.7	.000404	1.00

Note: E-values shown in this column represent the NDT data reduction by Equation (23) from the first resonance, 7.87 Hz, to a high frequency cut-off. For instance, if the NDT is cut-off at 14.77 Hz, the computed E-value is 1.38 times that cut-off at 59.72 Hz.

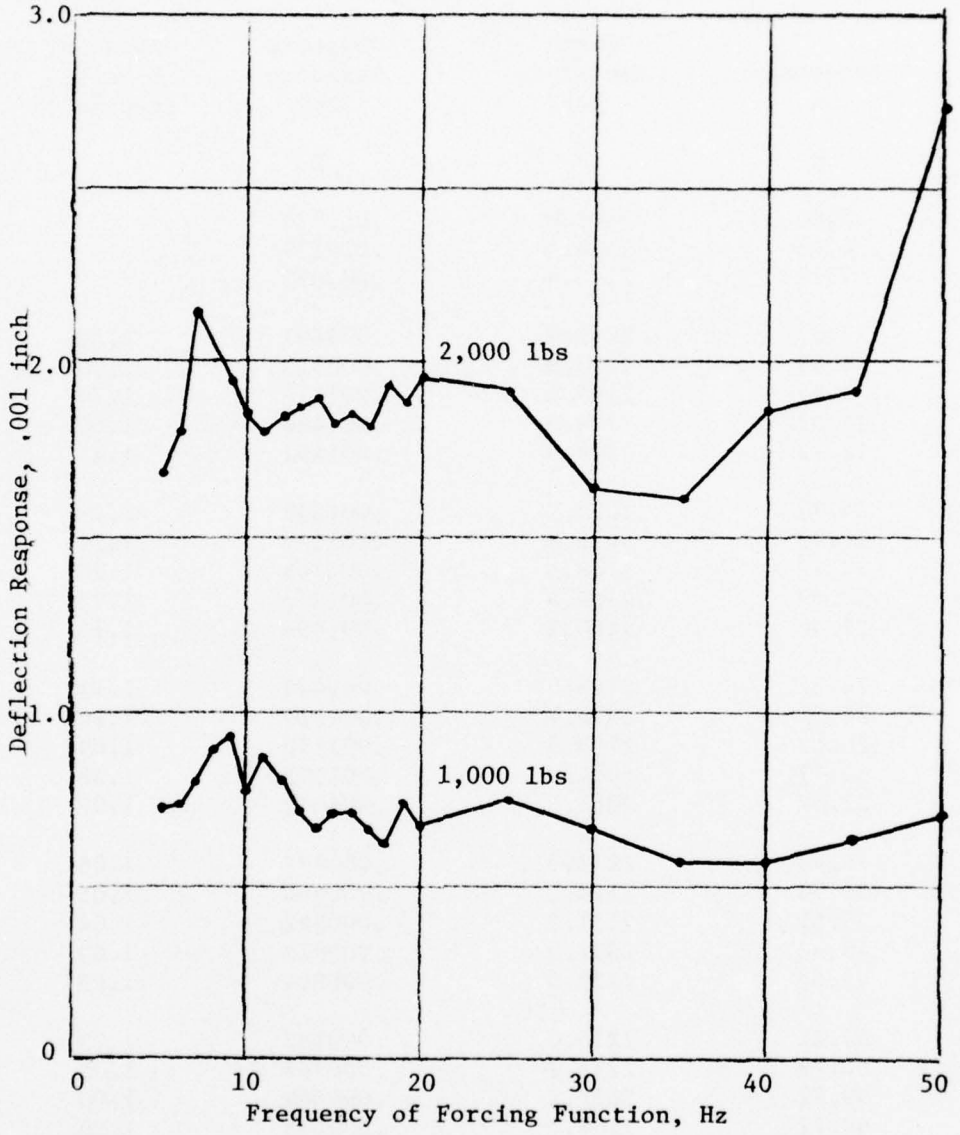

FIG. 1.13 NDT AT POINT B1, RUNWAY AT NAFEC

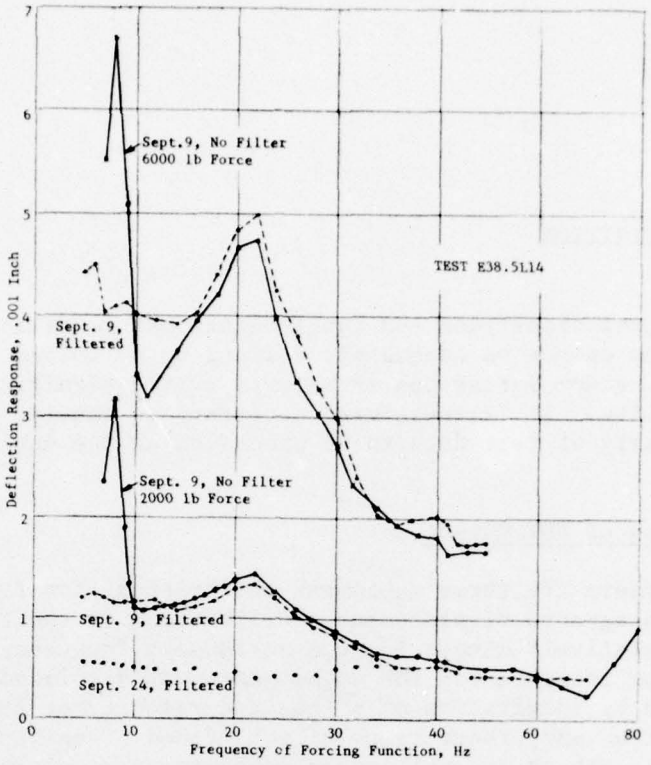

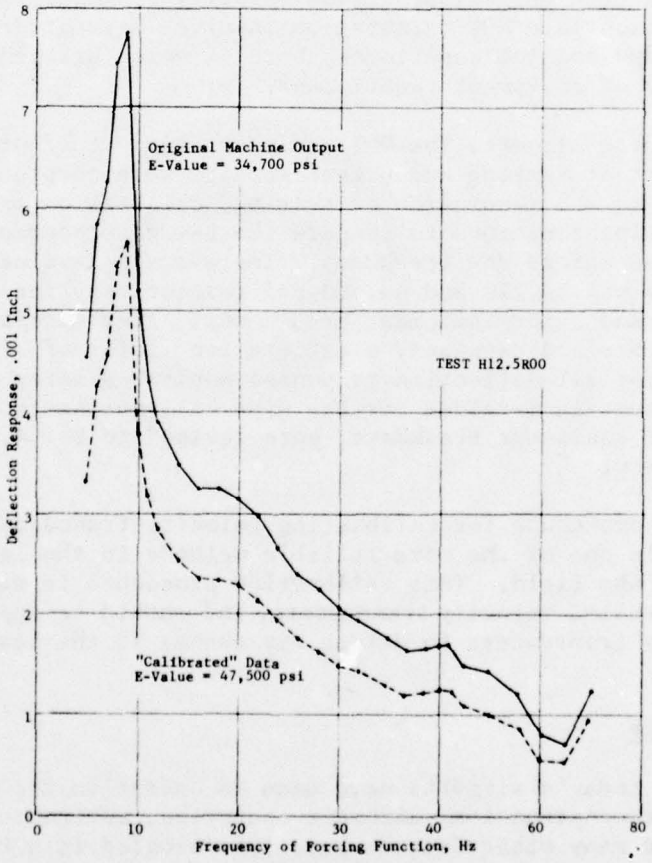

FIG. 1.14 EFFECT OF FILTER ON NDT AT SAN JOSE

1.6 DATA ACQUISITION

The support conditions and conglomerate nature of a pavement - subgrade system cannot be adequately defined by a limited number of tests because random variations in natural events significantly reduce their reliability. It is therefore, necessary to acquire a sufficiently large quantity of test data to be processed as the design inputs.

a. Calibration of NDT Output

In NDT there are three equipment calibrations for frequency, amplitude and integrated displacement. Calibration of the first two elements is relatively simple because a standard frequency and load analyzer can be utilized for the adjustment. As displacement is normally obtained by integration of either the velocity or acceleration monitored at the test, there is no direct method of calibrating the monitored data with the actual ground velocity or acceleration. Consequently, appropriate NDT calibration involves a great deal of engineering knowledge and job experience, both of which are generally beyond the capability of equipment technicians.

At San Jose Airport, the NDT equipment was out of order during the latter part of testing and urgent repairs were completed in the field. Prior to the resumption of testing, calibration tests were conducted at nine locations to compare the new displacement data with those monitored before the breakdown. The average E-value at these nine locations was 34,220 and 48,660 psi respectively for tests conducted before and after equipment breakdown. After careful study of the displacements and E-values, a calibration factor of .73 was used as a divisor for all deflection responses monitored after equipment repair. The average E-values for the nine calibration tests for before and after equipment breakdown, were revised to be 34,220 and 35,520 psi respectively.

The WES procedure for calibrating velocity transducers reported by Hall [8], is one of the more reliable methods in the laboratory, as well as in the field. This calibration procedure is mandatory for all newly installed velocity transducers, and should be applied to all other velocity transducers to detect any change in the instrumentation.

b. Reliability

Many of today's airports have been in operation for many years. Maintenance, reconstruction, aircraft operation, environmental deterioration, and many other factors have intermingled in a random pattern. The degree of randomness is indicated by the coefficient of variance, i.e.:

NDT Conducted at Airports	Coefficient of Variance E-value by NDT
Newark	.18 - .21
Nashville	.15 - .40
Portland	.08 - .32
Raleigh-Durham	.12 - .29

The coefficient of variance in the above list is actually the combination of all variation in the form:

$$\sigma_s = \sqrt{c_1\sigma_1^2 + c_2\sigma_2^2 + \cdots\cdots} \qquad (1.30)$$

in which σ_1, σ_2, ... respectively represent the coefficient of variation in pavement components, subgrade support, human factors, mechanical factors, method of computation, and other pertinent factors in testing, and c_1, c_2, ... are the weighted contributions from each variable. According to pavement construction experience, the lower range for σ is .08 and .12 respectively for the compressive strength of concrete (or asphalt) pavements and the supporting capacity of the pavement base. Since the coefficient of variance's lower range for NDT E-values at Portland and Raleigh-Durham is about the same as the material variance, it indicates that NDTs are of extremely high quality and are very reliable in repetitive tests. The true coefficient of variance due to human and mechanical factors in NDT is likely to be less than .05.

c. Productivity and Monitoring Tolerance

The first NDT experiment at Newark in 1967, took about two hours to complete one comprehensive test series. NDT with the same Shell tester in 1968, took only about 25 minutes. The forcing function had a constant amplitude of 1000 kg and a frequency sweep of 5 to 50 Hz.

At Nashville, NDT was carried out with the efficient WES 16 kip machine. Four velocity monitoring systems were used. The average testing time was about 17 minutes. The forcing function had a constant amplitude of 4000 pounds with a frequency sweep from 5 to 50 Hz.

Similar testing procedures were used at Portland, except that only one velocity gauge was used. The average testing time was about 16 minutes.

At Raleigh-Durham, NDT was carried out by the same WES crew with the 16 kip machine. The average testing time was reduced to less than 10 minutes. The test procedure and output data were basically identical to those used at Nashville and Portland, except that the frequency and load dials were not turned to exact round numbers. A variance of $\pm$.02

and ±.05 was allowed for frequency and load respectively. NDT production was thus increased by more than 50%. Because the output data now reflected the actual rather than specified frequency and forcing function, the NDT data became too cumbersome to process manually. Since fluctuations in frequency and load can be processed without seriously affecting the accuracy of the computed results, a computer program was developed to process the data (see Section 1.2c).

For San Jose, the Raleigh-Durham experience was incorporated into the NDT program. From September 9 to 24, 1975, 200 frequency sweep NDTs were performed on the airport. The total testing time was about 27.5 hours, with an average testing time of 8.4 minutes per test. All tests on active runways and taxiways were conducted during the slack period at night.

d. Planning Airport Tests

Planning the NDT program prior to field testing has a significant effect on testing quality and efficiency. Since each airport has its own unique conditions, there can be no standard NDT program. The following are general guidelines for pre-planning field work:

(1) Positive communication should be established between the airport control tower and the NDT operator. A 10 minute warning should be given to the NDT operator before entering or clearing the aircraft operational area.
(2) Test locations should be spaced 100 to 200 feet apart when within 2000 feet of the runway end, and 200 to 500 feet apart when in the center portion of runways and taxiways.
(3) Additional tests should be made in heavily trafficked areas and areas with pavement problems.
(4) The primary runway and taxiway areas should have at least four tests performed on areas of identical pavement construction and operational background. The test location should be offset 10 to 15 feet to the right or left of the taxiway or runway centerline.
(5) At least two cross-sections with an offset distance from the centerline to the pavement edge, should be taken for each runway and taxiway.
(6) Special tests, such as variable load frequency sweep NDT, can be conducted in areas where no interference to aircraft operation is anticipated.
(7) Important tests, such as those on runways where tower control is mandatory, should be performed early in the testing program and preferably at night.
(8) An identification drawing and listing should be prepared to indicate the location and counter number of each test as shown in Figure 1.15.

e. Test Procedures and Data Recording

Actual test procedures are outlined as follows:

(1) Calibrate the system output for forcing frequency, forcing amplitude, and dynamic response (displacement). The pre-test calibration record should be kept as an integral part of the NDT data file.
(2) No filters or dampers should be employed for any forcing frequency lower than 80 Hz so that all measurements reflect the true response of the ground support.
(3) The equipment should be warmed up prior to use.
(4) Calibration of both the force monitoring system and the response (displacement) integrator in the field should be checked.
(5) Set the forcing function at a pre-defined, constant load level (double amplitude). A variation of ±5% is tolerable. For example, if the pre-defined constant load is 6000 pounds, the actual test load may range from 5700 to 6300 pounds.
(6) Maintain the input force at a steady state of vibration for at least 2 seconds. The response (displacement) is then recorded.
(7) Switch to another frequency and repeat the steady state vibration test.

Frequency Range	Intervals	Tolerance
5 to 15 Hz	1.0 Hz	±.1 Hz
16 to 28 Hz	2.0 Hz	±.4 Hz
30 to 60 Hz	5.0 Hz	±1.0 Hz

(8) Recheck the calibration of the force monitoring system and the response (displacement) integrator. Record any change in the calibration factor, time of the change, and the name of the specialist who sponsored the change.
(9) Measure the pavement temperature at several locations at 2 hour intervals during the testing period.
(10) For the first batch of printouts, channel identifications should be made for frequency, force amplitude, and response (displacement), and their respective calibration factors should be properly indicated as shown in Table 1.7. Pertinent information such as time, location, temperature, and type of tester should be noted. No other modifications should be made on the original machine printouts, which should be kept as source data records.

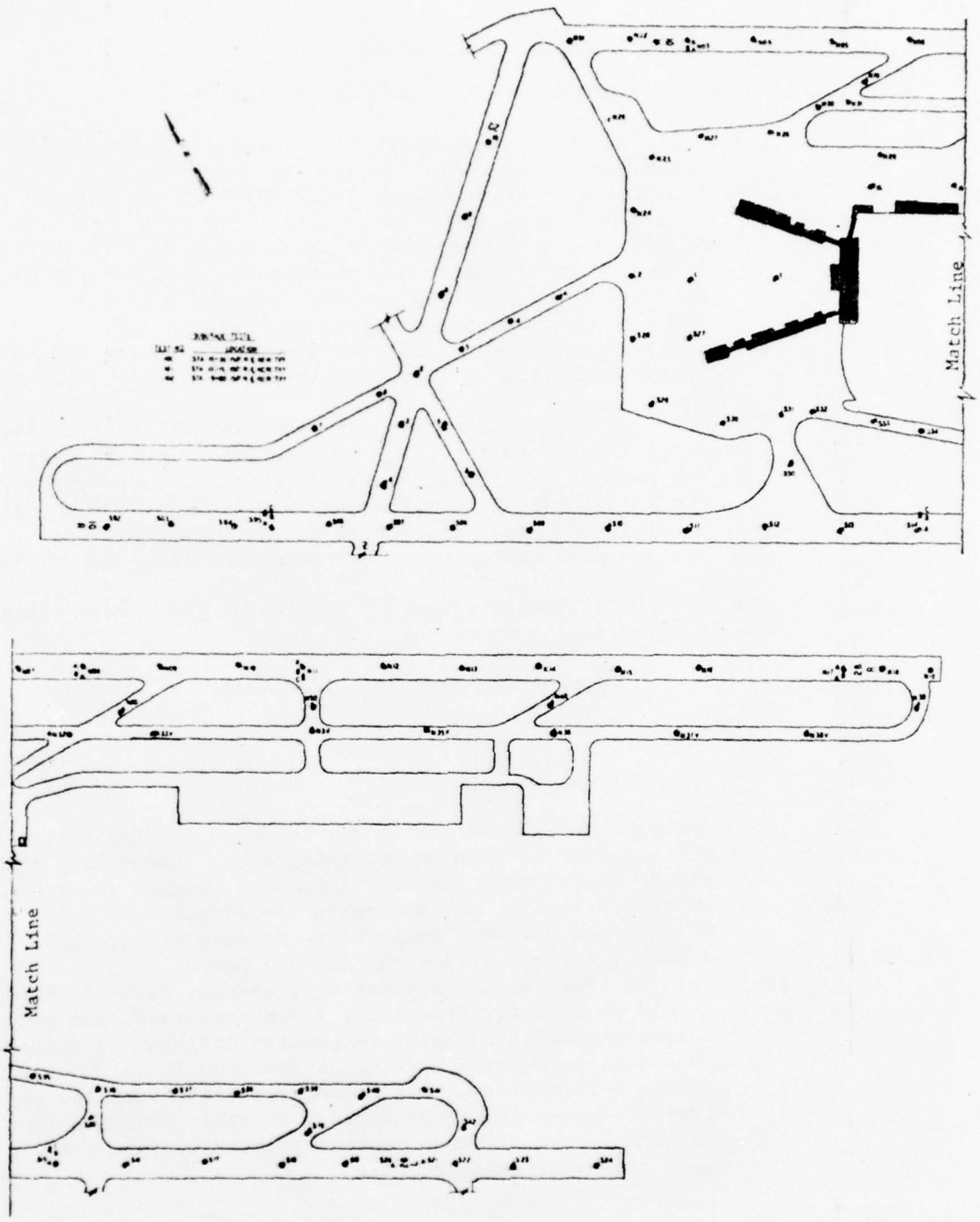

FIG. 1.15 LOCATION OF NDT

TABLE 1.7 A SAMPLE OF ORIGINAL NDT MACHINE PRINT-OUT

NEW ORLEANS 19MAY 76 Project Date
0921 HRS RWY 1-19 Time Facility
TEST LOC 3 Test No.
T = 77.6°F Temperature

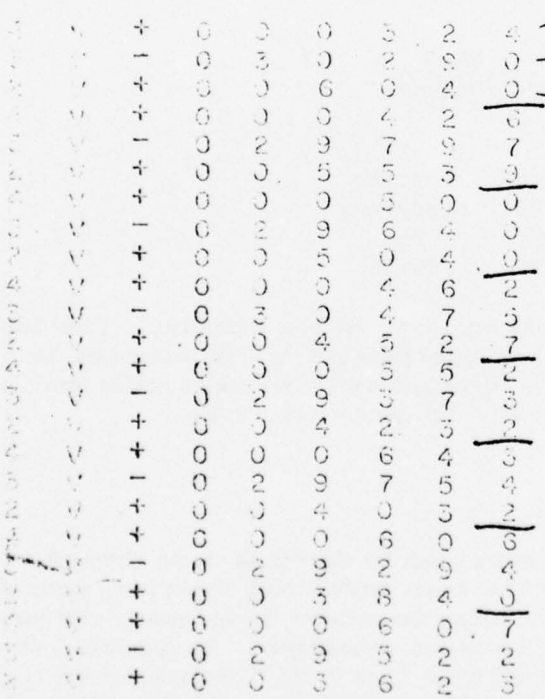

Response .000324 in.
Amplitude 3,029.0 lbs.
Frequency 60.40 Hz

1.7 DATA PROCESSING

The NDT data processing procedure has been fully computerized on the Univac 1108. This computer program is divided into four segments: input files, initial data processing, reprocessing E-values and establishing the inventory file for pavement design.

a. Input Files

The first input file consists of the test counter (I), location, date time, calibration code and temperature. The first two items are copied from the original test schedule except for those modified during the field test. The remaining items are obtained from the NDT machine printout having field notes marked. A sample input listing is shown in Section 3.2a through d.

The second input file consists of the NDT machine printout frequency, force amplitude and response (displacement). Each input card is indentified by the test counter. A sample input listing is shown in Section 3.2e and should be interpreted as follows:

Computer Listing:

No.	RESPNS	AMPL	FREQ
1	000246	030028	006042

Translation:

Test No.	Response Inch	Force Amplitude lbs.	Forcing Frequency Hz
1	.000246	3002.8	60.42

Data translation and calibration are done in the computer. The input listing shown in Section 3.2e has been plotted by the computer in Section 3.2f in which Z is the pavement response and F is the double amplitude of force and HSTEP is the increment of frequency in Hz.

b. Initial Data Processing

The processed data are summarized in Sections 3.3a through c. The columns 1, 2, 3 and 4 indicate the test number and location, date calibration and temperature at NDT. Data in column 5 represent the pavement frequency at the first mode of resonant vibration. In general, thin pavements over a weak subgrade vibrate from 5 to 6 Hz and heavy concrete pavements over a strong subgrade vibrate from 11 to 13 Hz. However, these ranges are not always true as there are many factors which contribute to variations in the first resonance. Values in column 6 represent the influence of high frequency vibration cut-off. The smaller the

percentage, the more reliable the processed E-value which is shown in the last column. This E-value is not a theoretical value, but can replace that found by the plate bearing test. In general, the subgrade has an E-value of 3000 to 10,000 psi; the subbase a value of 10,000 to 30,000 and a good concrete pavement a value of 80,000 to 160,000 psi.

c. Reprocessing E-Value

The reprocessed E-value is sorted again by facility location, as shown in Section 3.3b to introduce statistical reliability into pavement design and evaluation. The pavement support conditions are then divided into a number of groups according to:

(1) histroy of pavement construction,
(2) pavement composition,
(3) pattern of aircraft movement and
(4) inspection of pavement performance.

All the E-values in one pavement group are processed for the mean value, standard deviation and the mean value minus one standard deviation. This last value is called AREA E and is marked by X in Section 3.3d.

d. Inventory Files

The processed data are stored in computer inventory files which greatly facilitate data retrieval and compilation. The inventory consists of the input files, processed NDT data files, strength profile and cross-section files. Data in the last listing is shown in Section 3.3e and is ready to be used for determining the present pavement performance life and the need for overlay or new construction. These NDT inventory files are an important component of the master file for the pavement design and evaluation program.

1.8 PRACTICAL APPLICATIONS OF NDT

For the practical applications of NDT two jobs will be discussed below. They are not directly related to pavement design.

a. Traffic Patterns and Existing Pavement Strength

The first step towards practical NDT application is to understand the computer printouts as shown in Sect.3.3d. The pavement surface's E-values vary from point to point just as do those of the subgrade soil. However, the variation pattern is closely related to the traffic pattern on the existing pavement surface. As each aircraft movement tends to compact the subgrade under the wheelpath, the supporting soil may have a slight rise in bearing strength. Consequently, the pavement E-value may progressively increase during its service life. Runway traffic is reasonably channelized - the nose wheel may wander 10 feet from the center line while the B727 landing gear wanders in a strip of 10-20 ft at either side of the runway center line. The strength in terms of NDT E-value for a runway cross-section confirms this analysis - the E-value 10 to 20 feet off the center line is about 10% higher than that at the center line.

The wheelpath of a taxiing aircraft is also normally chanelized. The nose wheel may wander three ft while the B727 landing gear wanders about 15 feet to either side of the taxiway center line. NDTs at Portland and Raleigh-Durham Airports confirm these results, but San Jose Airport indicated some deviation. The difference can be traced in detail to San Jose's history of traffic density and pavement maintenance programs and their effects on pavement strength.

The strength profile of a normal runway is also closely related to the longitudinal distribution of aircraft operations. At both ends of a runway, take-off and landing impacts (see pp. 300-303 [1]) are significant and the E-value is relatively high. In the mid-portion of the runway, aircraft weight has a reduced effect because of wing-lift at take-off speeds (see p. 306 [1]). This analysis has been confirmed by NDT at all the airports studied by the writer. For studies at San Jose Airport,the traffic pattern history indicates that more than 85% of the take-offs and landings were on Runway 12R-30L, of which the original threshold was at Station 25+00. The field NDT E-values confirm these traffic patterns.

b. Existing Pavement Composition

Theoretically, frequency sweep NDT measures the composite E-value of a pavement structure, including the subgrade's elastic property. As elastic deflection of the subgrade contributes a significant portion of

total elastic pavement deflection, physical characteristics of the pavement elements other than its overall thickness, have only a minor contribution to the composite E-value of a pavement structure.

At Raleigh-Durham Airport, the following E-values for various pavement sections were observed.

PAVEMENT COMPOSITION

Location	Asphalt	Concrete	Stone	Sub-base	E-value
A1	14-1/2"	-	-	6"	20,400 psi
A2	-	6-1/2"	2-1/2"	-	16,420
A3	8"	6"	4"	-	18,960
A4	8"	6"	4"	-	23,670
R18	16-1/2"	8"	12"	-	61,460
R19	16-1/2"	8"	12"	-	46,230
R20	16"	-	12"	-	41,180
R21	16"	-	12"	-	51,610

At test locations A1, A3 and A4, the total pavement thickness was about the same and their E-values were within a narrow range regardless of of the significant differences in the physical properties of the asphalt and concrete pavement elements. When the total thickness was different, as in the case of R18 and R19 versus R20 and R21, the E-values were different. A definite interpretation of these results is not possible unless the subgrade conditions are carefully evaluated.

With the elastic layer computer program, the above NDT data can be used to precisely analyze the pavement structure. If NDT is conducted on the subgrade support, the computed E-value represents the overall subgrade load-deformation. When a base course is placed on the subgrade, the NDT E-value on top of that base represents the combination of the elastic modulus E, layer thickness h, and Poisson's ratio μ. Assuming a given μ and h for the subgrade to be infinite, the remaining variables are the E-values of the subgrade and base course, and the latter's thickness, which can be measured in the field. If one of the E-values is known (by NDT on the subgrade or laboratory determination of the base course E-value), the other value can be computed by the elastic layer program.

When another layer of known thickness is subsequently placed on the base course, the E-value of that layer can be computed by the elastic layer program using the NDT E-value from the top of that layer. Similar computations can be made for all necessary layers. During frequency sweep NDT at the Dallas/Fort Worth and Shreveport Regional Airports, WES conducted studies on the subbase, base (existing support at Shreveport), and subsequent pavement layers. The computed E-value for each pavement layer is shown in Table 1.8.

TABLE 1.8 DETERMINATION OF E-VALUE OF PAVEMENT LAYERS

DALLAS/FORT WORTH REGIONAL AIRPORT

COMPONENT	THICKNESS Inches	E-VALUE psi	POISSON'S RATIO	NDT-E psi	TEST No.
Cement Concrete	15	6,500,000*	.15	78,890	D2
Base	9	2,100,000*	.30	26,423	D5
Lime Stabilization	9	8,000	.35	4,261	D6
Subgrade	Infinite	2,820*	.35		

SHREVEPORT REGIONAL AIRPORT

COMPONENT	THICKNESS Inches	E-VALUE psi	POISSON'S RATIO	NDT-E psi
Asphalt Overlay	4.75	450,000*	.30	57,800
Asphalt Overlay	3.50	310,000*	.30	47,700
Concrete Slab	10.00	3,500,000	.20	46,200
Sub-Base	7.00	15,000	.30	
Granular Subgrade	6.00	6,000	.35	
Subgrade	Infinite	4,500*	.35	

Notes: 1. The E-value and Poisson's ratio of all pavement layers are to be assumed for theoretical analysis except those * mark which are determined by MWELP (multi-wheel elastic layer program).
2. NDT-E denotes the E-value computed from the output of nondestructive test at the test location on top of the referenced layer.

1.9 COST OF NDT FOR AIRPORT PAVEMENTS

At this stage of development, it is premature to estimate the cost of NDT for airport pavements. The following information is provided for reference only. The annual cost, in 1976 dollar, for testing pavements at 12 airports is likely to be:

Direct Labor:	Two technicians	$46,000.	
	One engineer, half time	14,000.	$ 60,000.
Overhead:	Social Security, Insurance, Benefits		25,000.
Travel:	Transportation and Subsistence		25,000.
General and Administrative Expenses:			40,000.
		TOTAL LABOR:	$150,000.
Equipment:	Amortization and Depreciation of Tester		40,000.
	Operation and Maintenance		30,000.
General and Administrative Expenses:			20,000.
		TOTAL EQUIPMENT:	$ 90,000.

Without considering the cost of research, engineering, etc., the NDT cost for a two runway airport ranges:

Direct labor:	$12,000. - 16,000.
NDT Equipment:	7,000. - 9,000.

Duration of the test would be about five to eight days at the airport and two to four days on the road.

PART 2

SYSTEM DESIGN OF FUNCTIONAL PAVEMENTS

2.1 BASIC CONCEPT

The design system, flow charted as shown in Figure 2.1, consists of three subsystems. The first subsystem deals with the interaction between aircraft and pavement, and relates aircraft response to pavement roughness. Pavement roughness and the need for maintenance are related to progressive deterioration of the materials' stress sustaining capacity under repetitive loadings. For pavement engineering analysis, the functional criteria are translated into the limiting elastic deflection and the requirements to maintain the limiting stress level during the anticipated pavement service life.

The second subsystem makes use of design theories to determine the pavement thickness which would allow the distribution of aircraft load over the subgrade and would cause an elastic deflection and stress level in the materials within a tolerance defined in the first subsystem.

The third subsystem focuses entirely on the economic aspects of the pavement system. It begins with estimation of the unit cost of each pavement element followed by evaluation of the maintenance and operational costs. With the financial cost data, the total service cost of a pavement system is computed in terms of present cash value. The present cash values and the anticipated service performances of design alternatives will help the pavement users reach an appropriate decision on the pavement system design.

This system defies traditional design practice. All computer input parameters should be specified by the user. If he fails to do so, a set of "default values" will be used to yield tentative design and economic analysis. If the principle of computer simulation is applied to the analysis, an appropriate pavement solution can be developed even if certain design parameters are less reliable.

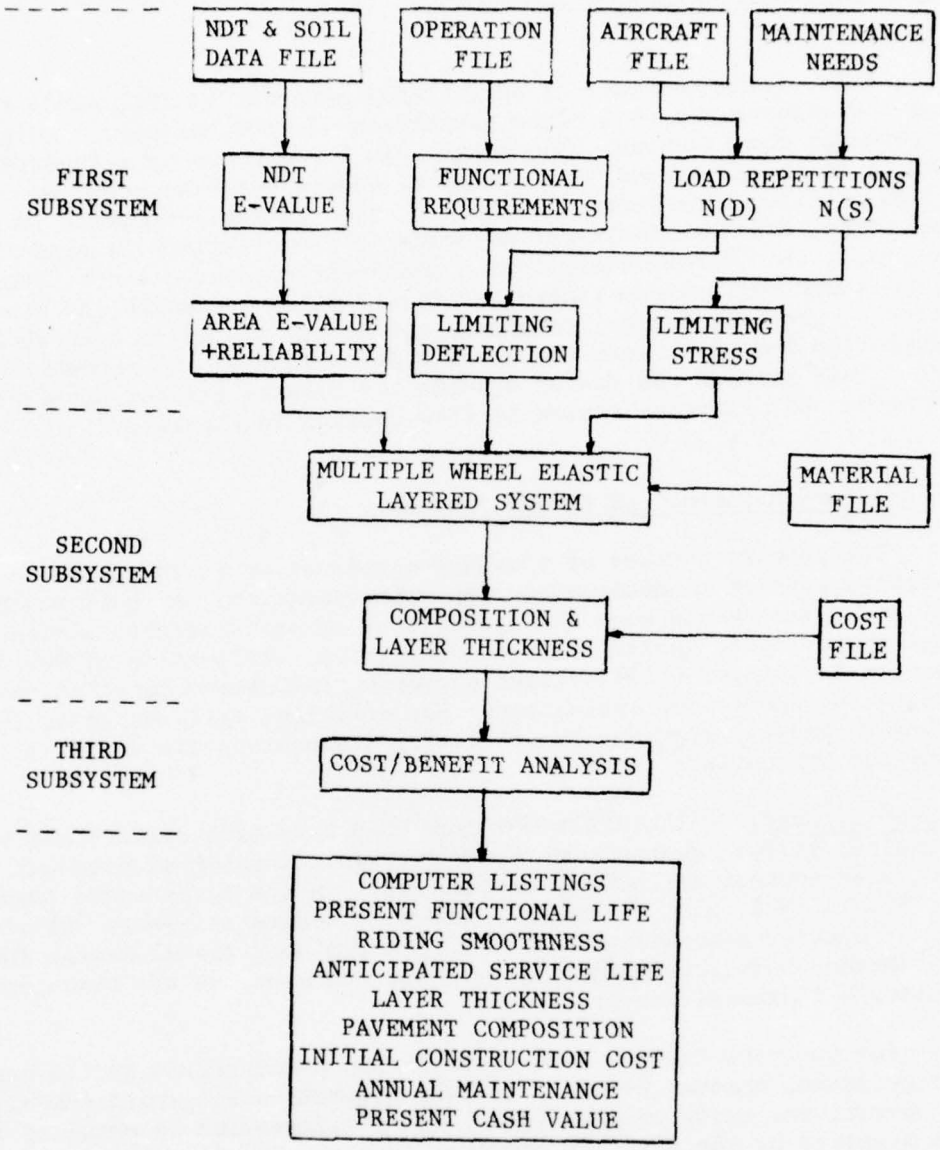

Fig. 2.1 Structure of Pavement Computer Program

2.2 FUNCTIONAL PAVEMENT REQUIREMENTS

Safe riding response of operational aircraft is the user's requirement and maintenance of surface performance is the engineer's objective of pavement construction. The longitudinal roughness of a functional surface is characterized by a series of random waves governed by the design profile, construction tolerance, the inelastic behavior of system components, characteristics of subgrade, the variability of pavement materials, the traffic distribution and environmental factors. Based on the known performance record and test results at Newark and Kennedy Airports, the longitudinal roughness can be translated in transverse deformation and then, into the elastic deflection of the pavement structure. This permits the use of elastic theories to predict pavement performance. The first subsystem is flow charted in Figure 2.2.

a. Aircraft Movement and Demand Forecast

The primary purpose of pavement construction is to provide a cost effective surface to accommodate aircraft operation. Airport management and users should know the operational aircraft weight, airline fleet composition, ground aviation facilities, utilization of Public Aviation Facilities (PAF), flight patterns, and demand forecast, prior to pavement design and evaluation. For efficient utilization of the pavement computer program, the following discussions are aimed as a guide for appropriate inputs.

Type of Aircraft The B727, B707 and DC-8 have made significant contributions to the development of the jet age. Insofar as pavement design is concerned, the predominant aircraft in the foreseeable future, say 1985 to 1990, will be the B727 and wide-bodied tri-jets. Development of heavier aircraft will depend upon its operational costs, fuel consumption, noise/environmental factors, and upon the air transport industry's financial resources.

For pavement design, each aircraft is characterized by its gear configuration, maximum take-off (MTOW), maximum landing-roll (MLRW), and operational empty weights (OEW). This information is compiled from data supplied by the aircraft industry (see pp. 288-290 [1]). The actual take-off weight (TOW) is usually smaller than the MTOW and should be determined by the airport and airline engineers for each operational aircraft. If the user fails to input the operational landing-roll weight (LRW), or the impact load at touch down (TDW), the computer program is designed to compute them as follows:

$$LRW = (MLRW - OEW) * (TOW - OEW)/(MTOW - OEW) + OEW \qquad (2.1)$$

$$TDW = 1.5 * LRW \qquad (2.2)$$

The touchdown impact factor is equivalent to the drop test at a sinking velocity of about 4 fps (see pp. 295, 307-308 [1]).

A computer input file has been established for the following aircraft:

Long Haul Group: B747, DC-10/30, DC-10/10, L1011, B707, DC-8
Intermediate Group: B720 B727-200, B727-100
Short Haul Group: DC-9, B737, F27

Data for the Air Bus, Concorde and other aircraft can be included in file without any programming difficulties.

Utilization of PAF Utilization of Public Aviation Facilities (PAF) depnds on such factors as flight patterns, terminal facilities, navigation systems and runway lengths. Each airport has its own unique pattern of PAF utilization and traffic distribution which should be properly analyzed prior to pavement evaluation. The first computer inputs are estimated landing roll (LR) and take-off (TO) frequencies for the three aircraft groups. The estimates are expressed as percentage of total aircraft movement at the airport. Traffic distribution on a runway is programmed by its station at "ZERO" and "END" and the station length of the touchdown "ZONE". The longitudinal traffic distribution by aircraft weight on a runway (I)R (I+18)L is as follows (see pp. 300-303 [1]):

Runway Station:

From	To	TOW	LRW	TDW
ZERO	ZERO+ZONE	TO(I)R+O	LR(I)R+LR(I+18)L	LR(I)R
ZERO+ZONE	END-ZONE	TO(I)R+TO(I+18)L	LR(I)R+LR(I+18)L	O
END-ZONE	END	O+TO(I+18)L	LR(I)R+LR(I+18)L	LR(I+18)L

The second inputs are the ground navigation facilities and flight patterns. For runways under Cat II, instrument landing systems (ILS), all aircraft movements are confined to a narrow band. Therefore, pavements with centerline lights under ILS rule will be subjected to more load repetitions within that band than pavements under a visual navigation system. An FAA research project [14], reported bandwidths computed from data on the average standard deviation of traffic concentration, to range from 11 to 19, and 25 to 42 feet respectively, for taxiways and runways at nine airports across the nation. The FAA test did not, however, identify the navigation aids at the monitoring.

The bandwidths at three New York-New Jersey Airports (see pp. 299-300 [1]), were observed to be:

	Runway	Taxiway
Normal Visual System	35 - 45 feet	12 - 20 feet
Centerline Lights/ILS	15 - 25 feet	6 - 12 feet

If there are no bandwidth inputs, the computer program will use the following bandwidths, defined as containing 98% of the aircraft movements:

	Runway	Taxiway	Holding Pad
Normal/Visual in feet	40	16	16
Lights/ILS in feet	20	10	16

The computer program also includes information on the longitudinal distribution of aircraft impact on touchdown. The input data is based on observations at three New York-New Jersey airports. The center of landing impact was 1200 to 1300 feet from the threshold and 90% of the landings took place within a 1500 feet zone. The FAA [14] reported a slightly scattered touchdown distribution. The center of impact was reported to be 1500 to 1600 feet from the threshold, with 80% touchdowns. Similar to landings and take-offs, navigation aids were not reported.

Demand Forecast Present pavement design practice does not require precise traffic demand forecast. Instead, the pavement structure is designed for anticipated aircraft weights. When the B747 was introduced in 1969, aircraft weights increased from 350,000 lbs. to 700,000 lbs., and elaborate analysis indicated that future aircraft weight may range from one to two million pounds. Consequently, new pavements at some major hub airports were designed and constructed for these hypothetical aircraft. To save the extra costs involved in such construction, a realistic traffic demand forecast should be developed.

Today, there are two sets of airport demand forecasts. The set prepared by the Air Transport Association (ATA) is based on (1) the demand-supply of seat capacity, (2) the fleet composition of major airlines, (3) the route structure, and (4) economic projection of the air transport industry. It is a realistic and basic traffic demand forecast. However, the ATA forecast does not include non-scheduled flights and, sometimes, does not closely reflect the economic growth of a particular air trade area.

The other set of forecasts are normally prepared by the airport operator. This traffic forecast is usually related to the airport master plan and economic development of the air trade area. It is necessary to review both sets of forecasts and then, develop a working set which will include the outstanding features of both.

In preparing the demand forecast, the following definitions will be used:

Aircraft Movement - one aircraft landing and one take-off.
Average Daily Movement - the average daily aircraft movement in the peak month of the year.
Peak Hour Movement - the maximum number of aircraft movements at the peak hour in the peak month.

A demand forecast should be prepared for each type of aircraft in operation in the following form:

Type of Aircraft
Operational Take-off Weight
Average Daily Movement, Last Year
Present
5 Years
10 Years
15 Years
20 Years

Load Repetitions Aircraft movement on a taxiway or runway assumes a random distribution across the transverse direction. The load repetition at a given point is governed by the tire width and the traffic concentration. Observations at 9 airports [14], demonstrate that the probability of wheel load repetition on runways and taxiways assumes a normal distribution curve. For the bandwidth (BW) having 98% traffic concentration, the standard deviation is equal to BW/4.652. Using the principle of super-position (see Figure 2.3), the area of probability APX, for multi-wheel aircraft movement is:

$$APX = 1.8553\sqrt{\pi}(a/BW)\ \Sigma \exp\ (-10.8167\ (x/BW)^2) \qquad (2.3)$$

in which x is the transverse wheel spacing, and a is the radius of the wheel. All units are in inches. The APX value is applicable to aircraft take-offs and landing rolls. The distribution of touchdown impact depends largely upon the airport's climatic and geometric environment, as well as navigational aids and ground facilities. Under typical landing conditions, aircraft come down at a glide slope of 2 to 3^0. Over the threshold, the aircraft is about 50 feet above the landing surface when the pilot brings the aircraft into a landing position and the aircraft flares to a horizontal position within about 1200 to 1300 feet from the threshold. The landing impact zone is clearly marked on the runway surface as shown in Figure 2.4. In general, the landing impact assumes a random distribution within the marked landing strip. From observations at the New York-New Jersey airports and by the FAA [14], the landing impact is normally distributed with a standard deviation of 450 feet. The longitudinal area of probability APY, for a multi-wheel impact is:

$$APY = .00007387\sqrt{\pi}a\ \Sigma \exp\ (-(y/5400)^2/2) \qquad (2.4)$$

in which y is the longitudinal wheel spacing. Considering the transverse probability of load distribution APX, and the longitudinal distribution APY, the overall landing impact probability is equal to APX* APY. For today's aircraft, it takes several hundred landings to produce one landing impact at the same spot on a runway.

In 1967, the concept of keel construction was introduced into the

pavement design and evaluation at NY&NJ airports. The width of the keel WK, of a taxiway or runway is:

$$WK = BW + x_{max} \tag{2.5}$$

in which x_{max} is the distance between the outermost wheels. 98% of the anticipated aircraft load repetitions occur within the keel. The pavement area beyond the keel is defined as the runway or taxiway sides and has a traffic volume equivalent to 1% of the load repetitions in the keel area. Adoption of the keel concept at the New York-New Jersey and other airports has resulted in about a 10% savings of the normally accepted uniform depth of pavement across the entire runway or taxiway.

b. Aircraft Response and Pavement Surface

Aircraft-pavement interactions can be expressed mathematically by (see Figure 2.5):

$$F(\Delta, L, N) \simeq P(\overline{DI}, f, \beta, v) \tag{2.6}$$

where the pavement surface F, is a function of the surface deviation Δ, the wavelength L, and its functional life as represented by the number of load repetitions N. The functional surface condition is represented by the aircraft response P, which is characterized by the dynamic increment $\overline{DI}$, of aircraft at interface with the pavement, the natural frequency (mass-spring) f, the damping β, of aircraft at interface, and the velocity v, of aircraft travelling on the pavement surface. The theory of random vibrations was introduced to define the dynamic aircraft response (see pp. 313-344 [1]):

$$\overline{DI}^2 = \Phi(1/L) \cdot \pi f/4\beta \tag{2.7}$$

where $\overline{DI}$ = average dynamic aircraft response at interface,
$\Phi(1/L)$ = Power Spectral Density (PSD) of the pavement surface for a wavelength L,
$\pi f/4\beta$ = transfer function of the dynamic test.

The peak aircraft response occurs when the pavement surface wavelength is equal to the aircraft velocity per cycle of vibration. Thus:

$$L = v/f \tag{2.8}$$

For a discrete wavelength, the functional pavement surface can be defined by a straight-edge criteria (pp. 340-341 [1]):

$$\Delta_n = KL^{\frac{1}{2}} \tag{2.9}$$

where the K value is a function of the aircraft operation characteristics expressed by:

$$K = T(f,\beta)\ \overline{DI}_n/(v\sqrt{f}) \qquad (2.10)$$

the subscript n represents the incremental change in Δ and $\overline{DI}$ after the N-th aircraft load repetition.

The transfer function $T(f,\beta)$ used in the computer program was deduced from the FAA aircraft tests at JFK Airport (pp. 342-343 [1]). The validity of such tests depends largely on the instrumentation for monitoring the interface response of moving aircraft and a precise, level survey of the pavement surface. Arbitrary disturbance of the pavement surface, such as runway or taxiway crossings, will affect the transfer function.

The above analysis represents the introduction of dynamic aircraft response into the definition of functional pavement requirements. There is little information available to define the operational characteristics of the aircraft in Equation 2.10. In the computer program, the following data are used (pp. 388-390 [1]):

v - Aircraft Speed:

Normal Taxiing	30 to 50 MPH
High Speed taxiing	50 to 80 MPH
Normal Landing	130 to 150 knots
Normal Take-off	120 to 140 knots

f - Fundamental Aircraft Frequency at Interface (according to the drop test of main landing gear assemblies):

B727 Stretch and DC-8-63	1.5 to 2.0 Hz
Most Commercial Aircraft	1.1 to 1.5 Hz
DC-10, L1011	0.9 to 1.3 Hz

$2\pi\beta$ - Efficiency of the Shock Absorber System:

Pneumatic Tires	0.45 to 0.47
Oleo-pneumatic Struts	0.75 to 0.80
Gear System (Tires and Struct)	0.85 to 0.92

$\overline{DI}_n$ - Increment of Aircraft Vibration after the N-th load repetition, over and above the vibration level on an as-built or as-is pavement surface (pp. 340-341 [1]):

.12 g	Smooth riding surface
.18 g	Operational surface
.25 g	Upper limit of roughness tolerance
.30 g	Major surface rehabilitation required.

c. Progressive Deterioration of the Pavement Surface

The performance of a functional surface after the N-th load repetition is the ultimate goal for pavement construction. There are two major causes for pavement deterioration. One is the environment or natural conditions, such as temperature, moisture, and differential settlement of the pavement support. These are random events, and local

experience is the most reliable design parameter. The other major cause is the load repetitions on the pavement system. The extent of surface deterioration depends on three physical conditions. Firstly, if the traffic load is non-uniformly distributed over the pavement's width, rutting and excessive deformation will occur in the heavily trafficked areas. Secondly, because of the inherent heterogeneity of the subgrade and pavement components, the surface deterioration is not evenly distributed throughout the pavement layers. Thirdly, due to the inelastic behavior of the pavement and subgrade, the magnitude and extent of pavement damage vary. Consequently, the degree of permanent deformation may vary widely.

The inelastic behavior of materials and subgrade has a greater influence on a transverse cross section than the two factors, the traffic load and material variations. At the Newark test, the progressive deformation with respect to traffic repetitions of a transverse cross-section was observed to be a gentle curve. If the surface deformation is not excessive, that means, nearly in the elastic state of equilibrium, the following relation can be assumed:

$$D_n = D_1 + D_o \log N \tag{2.11}$$

where D_n is the transverse permanent deformation after the N-th load repetition, D_1 is the initial deformation, and D_o is the rate of progressive transverse permanent deformation, expressed in feet per log cycle of load repetition (see Figure 2.6). This equation is very similar to the one used for evaluating the fatigue strength of materials.

The surface deflection is closely related to the deflection basin selected in the study. Theoretically, pavement deflection extends an infinite distance from the load. Practically, it is necessary to define the significant transverse deflection basin. Since the subgrade contributes more than 85% of the total pavement deflection, it becomes logical to use 85% of the total deflection as a guideline in determining the width of the transverse deflection basin, which for semi-infinite elastic solids, theoretically corresponds to a point 3.3a from the wheel load edge, when a is the radius of the contact area. Thus, the straight-edge length XX, of the transverse deflection basin becomes:

$$XX = (2.0 + 6.6)\, a + x_o \tag{2.12}$$

in which x_o is the transverse wheel spacing of the landing gear. In the future, the effective straight-edge length should be computed by the multi-layered elastic system. Based on several computer runs, the XX-value of Equation 2.12 is slightly conservative.

At the Newark pavement test, comprehensive measurements were made on transverse and longitudinal deformations with respect to the significant wave length (pp. 374-375 [1]). The transfer function deduced from the test is in the form (see Figure 2.7):

$$D_n/\sqrt{XX} = A_1 \cdot (\Delta_n/\sqrt{L} - A_2) \qquad (2.13)$$

in which A_1 is the rate of progressive longitudinal deformation and A_2 indicates the deformation at the beginning of pavement service life. Introducing Equation 2.9, the above transfer function can be rewritten as:

$$D_n/\sqrt{XX} = A_1 \cdot (K - A_2) \qquad (2.14)$$

Thus, the transverse permanent deformation is related to the functional aircraft requirements.

d. Limiting Elastic Deflection of the Pavement Surface

Translation of the longitudinal permanent deformation into transverse permanent deformation is an important step in the development of a functional design method. However, all engineering theories are based on the elastic state of pavement equilibrium. In order to utilize these well established theories, it is necessary to translate permanent deformation into linear elastic deflection. For a visco-elastic pavement system, the classic theory can be applied if the system is segmented into a group of elastic subsystems having the boundary conditions defined for continuity with respect to stress or strain level.

Under the influence of a moving load, the pavement surface deforms and then, rebounds when the load is removed. Because of the inelastic behavior of the pavement system, the rebound is always incomplete. Accumulation of the non-recoverable portion of pavement deflection contributes to the progressive longitudinal and transverse surface roughness. The rate of accumulation of non-recoverable pavement deflection is related to the total deflection under the load and the shape of the deflection basin (see Figure 2.8).

Pavement deflection can be directly related to the stress-strain behavior of pavement materials, including the subgrade. At the lower range of the stress-strain setting, a large portion of the load-deflection is recoverable. At the higher range of the stress-strain setting, the stress/strain ratio decreases while the non-recoverable deflection increases. During the Newark pavement test, efforts were made to measure the recoverable deflection and the corresponding rate of progressive permanent deformation of fourteen test pavements. The rate of progressive deformation observed at the test is indicated by the parameter D_o, and the recoverable deflection of the same pavement is expressed by w_z. Because more than 85% of the pavement surface deflection is contributed by deformation in its subgrade, the elastic deflection of the subgrade w_o, is used to compute two dimensionless parameters D_o/w_o and w_z/w_o. The transfer function between these two parameters is determined by multiple regression. In the computer program, a logarithmic scale of the parameters is used and the transfer function is in the form (see

Figure 2.9):

$$\log(D_o/w_o) = d_2(\log(w_z/w_o) - \log d_1) \qquad (2.15)$$

Considering the parameters involved in $w_o(p,a,E)$ and $D_o(N,\overline{DI},h,E_n)$, it can be stated that the recoverable pavement deflection w_z, is governed by the load parameters p and a, the dynamic response of the moving aircraft $\overline{DI}$, the anticipated functional life of the pavement structure N, the physical property of the subgrade E, and the pavement composition h, and E_n. The E and E_n values are assumed to be constant and independent of traffic load repetitions. Evaluation of the recoverable deflection w_z, will facilitate utilization of the elastic theory for load-deflection analysis and, ultimately, the determination of pavement thickness and composition.

e. Limiting Stress Level

Presently, many pavement designs are based on stress computations for determining the thickness and composition of a pavement structure. The crucial decision in the whole process is the assignment of an allowable working stress. The allowable working stress is governed by the formation of structural cracks, the rate of crack propagation, and the need for structural maintenance. Although pavement performance is not significantly affected by the early stages of crack formation, the propagation of cracks and disintegration of material from around the cracks will eventually affect aircraft safety and riding qualities. Therefore, preventive pavement maintenance becomes necessary and the frequency of maintenance becomes a function of the pavement's stress level.

In the computer program, the concept used in estimating the limit of working stress (pp. 122-123 [1]), is:

$$\sigma_t = (1 - c\ \log N)\cdot(1+s_o)\cdot(1-\nu)\cdot(s_t\sqrt{E})\ /\ (1+\overline{DI}) \qquad (2.16)$$

in which σ_t = limiting tensile stress of the pavement component,
c = coefficient relating to the material fatigue strength,
N = number of load repetitions,
s_o = overstress factor for (1) permissible maintenance, (2) less traffic volume and (3) time or temperature dependent properties of the material,
ν = coefficient of variance of material strength,
E = elastic modulus of material,
s_t = coefficient for converting E-value to the material tensile strength,
$\overline{DI}$ = dynamic impact factor of the aircraft wheel load.

A set of default values for the above parameters has been carefully developed for each type of pavement material. If more realistic and reliable values are developed in the future, replacement can be made when its effect on the entire set of default values is evaluated.

f. Equivalent Single Type of Aircraft Operation

Using the above analysis, the pavement engineer is able to define the limits of pavement deflection and working stress to meet the functional requirements ($\overline{DI}$,v) for an anticipated number (N) of aircraft movements (f,β,p,a). However, operation at all modern civil airports consists of a fleet of mixed aircraft. Their effect on pavement structures should be equated to that of a single type of aircraft.

The first step in equivalency analysis is to determine the critical stress and surface deflection of a model pavement under an actual aircraft load. Model pavement composition should be identical to the pavement structure to be evaluated or designed.

According to Equation 2.16, the number of load repetitions governed by the pavement stress level can be expressed by:

$$\log N(i,j) = (\sigma_y - \sigma_t(i,j))/c\,\sigma_y \qquad (2.17)$$

in which: $\sigma_y = (1+s_o)\cdot(1-\nu)\cdot(s_t\sqrt{E})/(1+\overline{DI})$ (2.18)

Equivalent aircraft operation with respect to the limiting stress becomes:

$$\log (N(i,j)/N(m,n)) = (\sigma_t(m,n) - \sigma_t(i,j))/c\,\sigma_y \qquad (2.19)$$

The value $\sigma_t(i,j)$ is the model pavement stress under the aircraft weight which is considered to be the design standard, and $\sigma_t(m,n)$ is the pavement stress under the other aircraft to be equalized. For example, the normal pavement stress under the DC-10, B727 and DC-9 is computed by the multi-wheel elastic layer program to be 456.3, 488.3 and 366.3 psi respectively. The corresponding N(i,j)/N(m,n) value is .2864, 1.0000 and .0085 when the B727 is used as the standard aircraft. This means that one DC-10 or DC-9 movement is equivalent to .2864 or .0085 times the B727 movement.

Similarly, equivalent aircraft operations with respect to the limiting deflection by Equations 2.11, 2.14, and 2.15 are in the form:

$$\log N(i,j) = (D_n - D_1)\,(d_1)^{d_2}\,w_o(i,j)^{(d_2-1)}\,w_z(i,j)^{-d_2} \qquad (2.20)$$

and
$$\log(N(i,j)/N(m,n)) = (\log N(i,j) - \log N(m,n)) \log(ATM(m,n)\cdot APX(m,n))/\log N(i,j) \qquad (2.21)$$

in which (i,j) is the model aircraft and (m,n) is the one to be equilized.
ATM(m,n) is the demand forecast of the aircraft movement to be equalized, and APX(m,n) is its probability area of wheel load repetition in the transverse direction. The last two terms are used to equalize the computations for actual aircraft volume.

The equivalent operation of a fleet of mixed aircraft by Equations

2.19 and 2.21 has been written into the program. Systemization of aircraft load repetitions is an important step in pavement design.

g. Present Functional Life

Pavement performance life is measured with respect to the need for maintenance, and the surface riding quality. Service performance was previously measured by crack formation which, in turn, was related to the need for pavement maintenance. The annual maintenance cost reflected the pavement condition. For many modern highway and airport pavements, the riding quality becomes an important consideration for safe vehicle and aircraft operation. For instance, runways 22L and 31L at JFK Airport required major surface rehabilitation not because of structural disintegration, but because of its rough riding quality.

From the discussion on functional surfaces (Equation 2.10), it can be seen that progressive deformation (Equation 2.11), transverse deflection (Equations 2.14 and 2.15), and the pavement's functional life are closely related to its elastic deflection measured by NDT in the field. The sequence of computations is governed by the following equation:

$$\log(\text{ANDA}) = (A_1(K-A_2)\sqrt{XX} - D_1) \;/\; w_z^{d3} \qquad (2.22)$$

in which ANDA is the number of load repetitions where the aircraft will not vibrate in excess of the defined dynamic response DI. The present functional life is equal to ANDA divided by the present annual load repetition, as determined by Equations 2.20 and 2.21 (see sample computer printout in Section 3.10).

The computer program calculates the present functional life for four different classifications of riding quality. A functional life of three years or more is simply expressed as 3.++. Computer output on the present functional life should be used as a general guideline for pavement evaluation. As shown in the sample computer printout, riding quality is a very important parameter. Abnormal aircraft vibration may occur occasionally at landing and take-off if the aircraft weight and gear or maneuvering pattern are significantly changed. Therefore, this program should not be used to predict aircraft vibration.

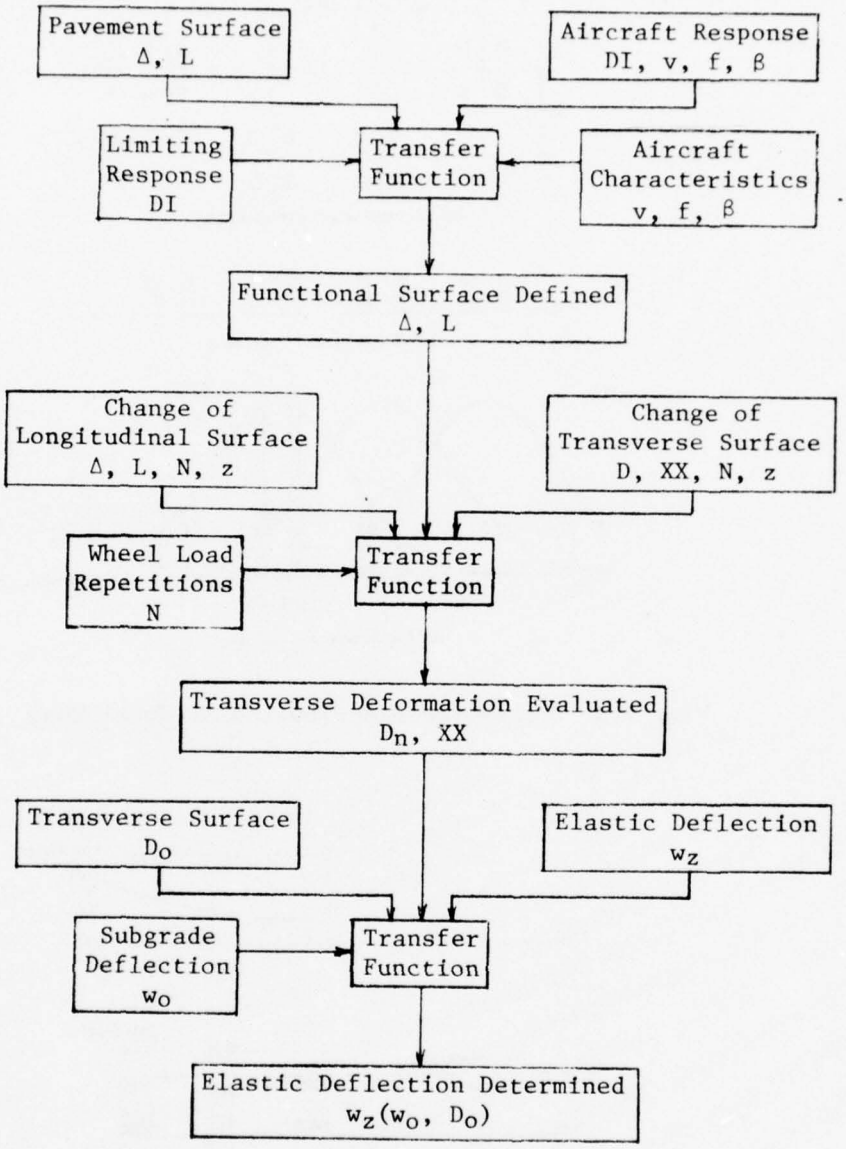

Fig. 2.2 Flow Chart of First Subsystem

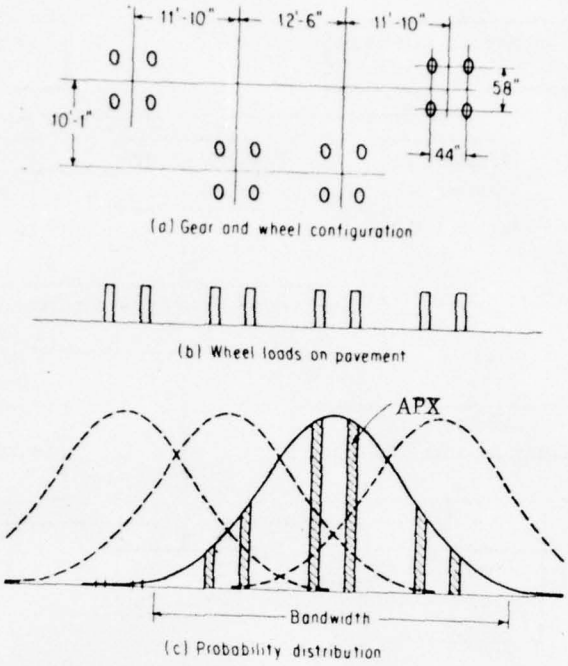

Fig. 2.3 Transverse Distribution of Wheel Load

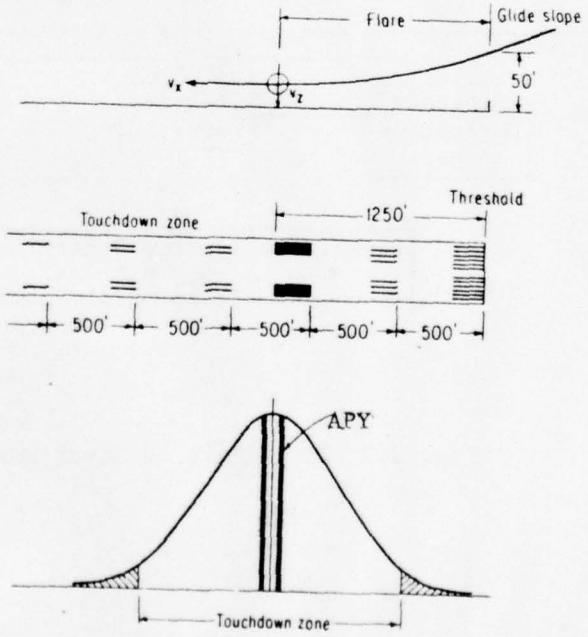

Fig. 2.4 Longitudinal Distribution of Wheel Load

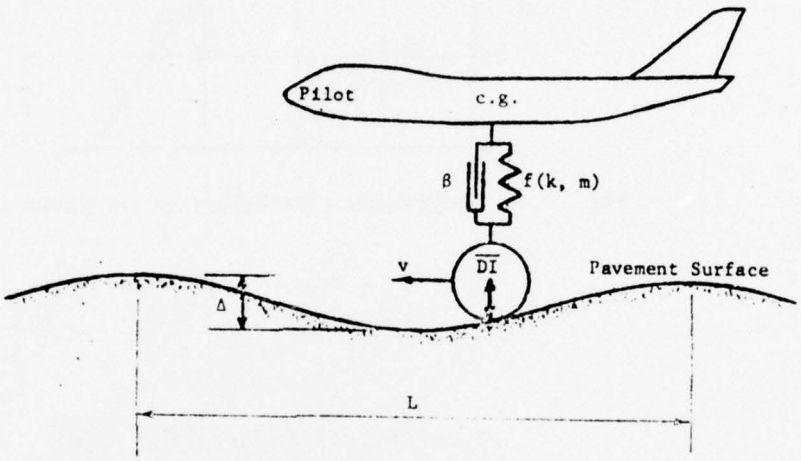

Fig. 2.5 Aircraft Pavement Interaction

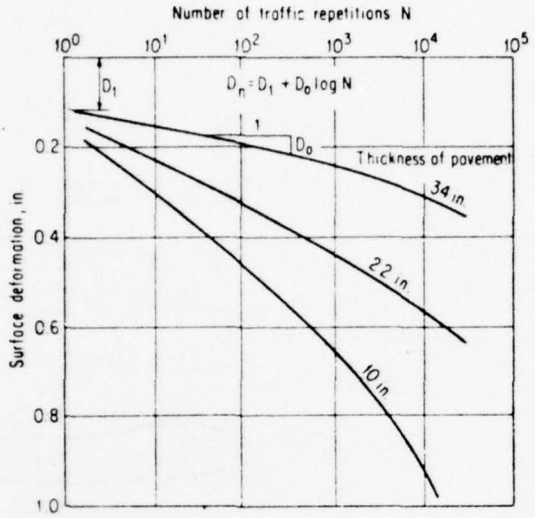

Fig. 2.6 Progressive Deformation of Pavement Surface

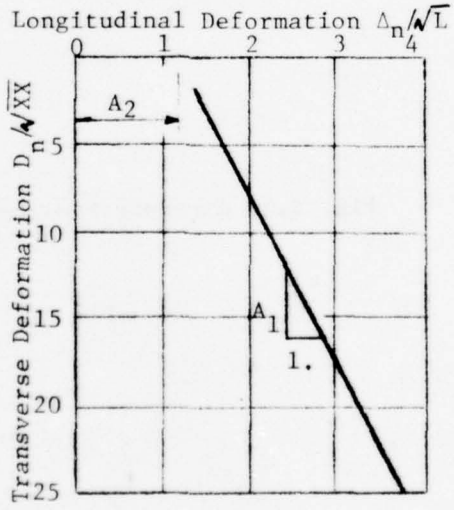

Fig. 2.7 Transfer Function - Longitudinal to Transverse Deformation

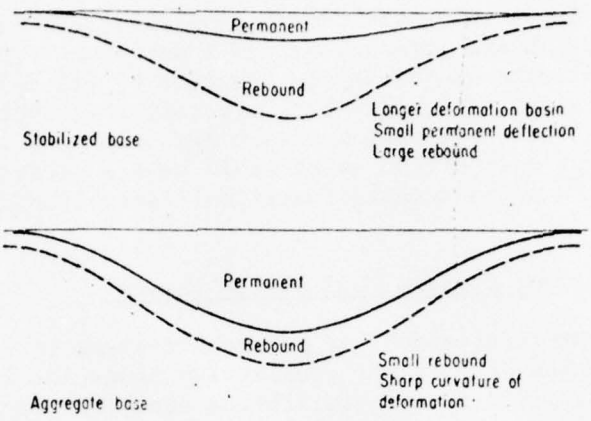

Fig. 2.8 Deformation of Pavement

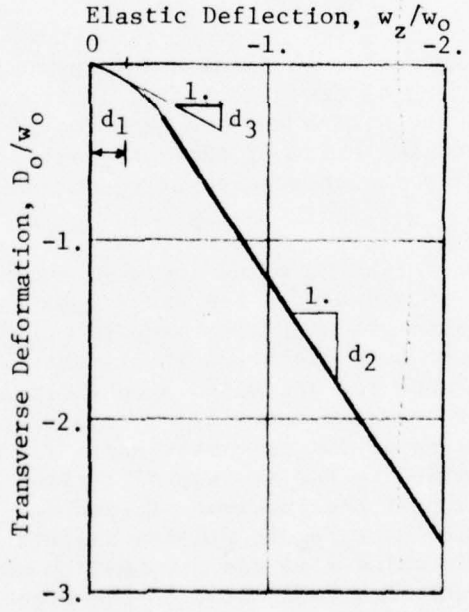

Fig. 2.9 Transfer Function - Transverse Deformation to Elastic Deflection (log scale)

2.3 PAVEMENT THICKNESS AND COMPOSITION

The first subsystem developed a tolerance for the limiting elastic deflection and stress level of a pavement system. The second subsystem will make use of design theories to (1) determine the pavement thickness which will distribute aircraft load over the subgrade and cause an elastic deflection within the tolerance level and (2) analyze the pavement composition which would have a stress sustaining capacity resulting in a predictable functional life without major maintenance.

a. Validity of Elastic Equilibrium Theory

Mathematical models of pavement systems (reviewed in [1]) stress the importance of pavement equilibrium under the influence of external loads. The first set of equilibrium equations was solved by J. Boussinesq in 1885. It was a purely mathematical solution of the stress-strain conditions in a semi-infinite elastic solid. In the late 1930's the theory was introduced into pavement design. Because of the problems in characterizing the modulus of elasticity of the subgrade and pavement elements, application of the Boussinesq theory met with limited success.

In 1945, Burmister introduced the layered system theory to analyze pavement consisting of several layers. Here, general equilibrium was translated into the stress and displacement in the layers. Tedious computations and complexity of the mathematical model have prevented many engineers from using this powerful method to solve pavement problems.

In the early 1960's, extensive research and tests were carried out by Vesic [16] to evaluate the Boussinesq theory. During the Newark pavement test, attempts were also made to verify this theory. LVDT displacement gages were installed in 11 test pavements, with a permanent steel reference rod driven to a nonyielding layer. During the test, nine gages operated normally. These gages directly measured the surface deformation of the test sections. The measured surface deflection w_z, was divided by the surface deflection of the subgrade w_o, prior to placement of the pavement structure. In Figure 2.10, the dimensionless parameter w_z/w_o is plotted against another dimensionless parameter z/a, in which z is the pavement thickness and a is the radius of the load wheel. The solid line in the figure represents the theoretical Boussinesq deflection distribution. The measured deflections are within 85% of those computed by the Boussinesq equation.

Concurrent with the Vesic study and Newark tests, significant progress was made towards computer solution of the layered system. Jones and Peattie produced coefficient tables which allowed evaluation of two and three layered systems, while the Chevron Research Company developed a computer program (see original references in [1]). A re-

vised program with free form input was subsequently developed by Barenberg, to solve the multi-layered system under the influence of multiple wheeled aircraft loads. This multi-wheel-elastic-layer program (MWELP) was developed independently after the Newark tests, and it is not possible to evaluate the theoretical deflection against the ones measured at Newark because the E and μ values of some pavement layers were not measured.

Computer reliability depends largely upon validity of the input characteristics, and particularly, the subgrade's E-value. However, the deflection encountered in the subgrade ranges from .95 to .80, with the most common value at .85 of the surface deflection of the pavement structure. This result indicates that if the physical properties of the subgrade only are properly characterized, MWELP can still output reasonable elastic deflections.

In a current FAA research project [17], Crawford, Hopkins and Smith reported that the multi-layered elastic system predicts the peak stress and displacement of concrete pavement. This finding confirms the computation Procedures outlined in Sections 2.3f and 3.11, and the original intention for utilizing MWELP to calculate the peak stress and displacement.

Due to improved computer techniques, many investigators have turned to finite element methods FEM (see original reference pp. 212-218 [1]), to solve problems in nonlinear elastic systems. There are several features of FEM that are better than the MWELP, but the FEM input assignments and mesh size are computer oriented problems. Program refinement will depend upon the discipline with which the appropriate material characteristics are assigned.

MWELP analyzes the theoretical deflection of a pavement system consisting of linear elastic-layer materials. Nonlinear elastic systems can be solved by discretizing the stress-strain curves into a series of tangent segments for each particular stress domain. The central processing unit (CPU) time required to develop the final answer would be several times longer. A similar process can also be applied to the temperature or time dependent elastic properties of pavement materials.

b. Stress Analysis of Pavement Elements

The concept of stress analysis is the basic step in structural design. Westergaard followed this approach in solving the bending stress of an elastic plate. The Newark pavement tests studied the basic assumptions of the Westergaard theory, such as k-value validity, equilibrium of the subgrade support, and material bending stress (see pp. 219, 238-240, 411-413 [1]). Saxena introduced the concept of equilibrium in the subgrade support and modified the finite element model developed by Hudson and Matlock (see pp. 233-236, 256-272 [1]). This

is probably the most advanced mathematical model for stress analysis of an elastic plate on the Boussinesq foundation. Saxena's computer program output the axial and shear forces, and the bending moment of the plate. Bending stress is determined by M·c/I. The slab is assumed to be isotropic and homogeneous, with a linear stress-strain relationship. Validity of the computation depends upon the assumption that the bending deformation of the slab is large when compared with the shear deformation. This means that the computation is applicable to a thin slab.

From an engineering point of view, the bending stress can be used to judge the probability of crack formation, which in an ordinary structure system, represents an unsafe service condition. Stress crack formation does not have an immediate effect on a pavement's functional performance. Many smooth functional pavements, particularly of portland cement concrete, are initially constructed with expansion, construction or contraction joints, and may subsequently exhibit the formation of shrinkage, stress and other kinds of cracks. Stress cracks normally indicate the need for pavement maintenance and, consequently, the cost of pavement service. Insofar as airport pavements are concerned, the purpose of stress analysis is to (1) design pavement for a functional life without major maintenance and (2) estimate the need and cost for pavement maintenance.

During construction of the Newark test pavement, layer components were compacted at various stages of construction and gage outputs were monitored when the pneumatic tire compactor moved directly over the gages. Four sets of readings were obtained for every gage at each construction stage. In order to make the analysis more useful, dimensionless parameters were formed; the stress σ_z was divided by the tire pressure p, and the depth z, to the gage was divided by a, the radius of the test load. The actual test results are plotted in this manner, in Figure 2.11. Note that the stress distribution in the subgrade under the aggregate base closely follows the Boussinesq pattern of stress distribution, as shown by the solid line. Stress readings in the stabilized base range from 25 to 50% of the Boussinesq stress pattern.

Stress analysis by the multi-layered elastic system yields a peak stress which closely agrees with observed ones [17]. The advantages in using MWELP for stress analysis are that (1) only a single program is necessary to compute the limits of elastic deflection and stress level in a pavement, (2) the k-value and its required modifications are not applicable (see pp. 412-413 [1]), and (3) common assumptions for the bending stress and elastic stiffness of a concrete beam can be by-passed. Stress analysis by MWELP is a straight forward computation, but its reliability depends upon the input parameters, including the subgrade support.

c. Material Characterization

For structural engineering analysis, construction materials are characterized by their strength and stress-strain properties. There are three distinctive stress-strain relationships: the linear elastic, plastic state of equilibrium, and stress-hardening stage. The rate of excessive strain in the last two stages is usually related to the load duration and intensity, as well as temperature. The basic material property, known as the modulus of elasticity, is expressed by Hooke's law which serves as the foundation for all structural analysis. Other related material properties are the tensile, compressive, and fatigue strengths. Nonlinear elastic materials can be characterized as consisting of linear elastic elements with defined boundary conditions relating to the time, temperature and/or load intensity.

In pavement design analysis, characterization of material properties is not strictly observed. Consequently, the basic engineering principles cannot be applied to all types of pavement structures. A theory that is good for concrete pavement is not necessarily good for asphalt, and vice versa.

In order to provide a meaningful cost/benefit study of various pavement systems, the programmed design procedure determines the pavement system equilibrium. Characterization of pavement layer materials will be governed by their basic stress-strain properties, with an emphasis on tensile elongation. The tensile and fatigue strengths can then be related to the modulus of elasticity. The subgrade can now be considered an integral part of pavement system, and characterized by its basic stress-strain property, with an emphasis on the compressive displacement.

d. Differential Settlement

Although the MWELP can be used to estimate pavement stress due to static aircraft loading, there are several environmental factors which also influence pavement stress. At many modern airports, if subsidence of the ground occurs, it is not uniform, and the resulting differential settlement of the subgrade support creates a deflection basin in the pavement. If the pavement is continuous and strong enough to resist progressive deformation in the subgrade, the pavement will be in a better position to maintain its smoothness.

The deformation configuration due to differential settlement is assumed to be a harmonic curve, as shown in Figure 2.12. L is the wavelength, and Δ is the maximum differential settlement. The maximum tensile stress at the bottom of the critical pavement layer is:

$$\sigma_d = 6.5\ E'(\Delta/L^2)\ h \qquad (2.23)$$

in which E' is the plastic state of the stress-strain modulus, and h the thickness of the pavement layer (see pp. 171-180 [1]). In pavement design analysis, the σ_d value should be deducted from the working stress limit as expressed by Equation 2.16. The settlement coordinates have been oversimplified in this analysis. However, considering the magnitude of the stress developed in the pavement due to differential settlement, the equation provides a simple but reasonable estimate of pavement stress.

e. Temperature Variation

An environmental factor other than aircraft load which affects pavement stress is the fluctuation of pavement temperature. Whether it is daily of seasonal fluctuation, the critical condition should be studied. Since the pavement surface is exposed to changes in ambient temperature while below the surface the temperature is more stable, a thermal gradient is encountered in the pavement from the surface down to the subgrade. This change in temperature with depth can cause warping and thus result in pavement stress. Insofar as pavement crack formation is concerned, cold weather temperature variations are the most critical. Pavement stresses caused by temperature variation (see pp. 139-150 [1]), are approximated by:

$$\sigma_T = .33\ E \cdot \varepsilon \cdot h \cdot (dt/dz) \qquad (2.24)$$

in which ε = coefficient of thermal pavement shrinkage,
(dt/dz) = seasonal thermal gradient with respect to pavement depth in cold weather (see Figure 2.13).

The computed σ_t value should be deducted from the working stress limit computed by Eq.2.16. Similar to the stress formula for differential settlement, the above equation is also oversimplified for stress analysis.

f. Pavement Design

There are three normal stresses, three shear stresses and three displacements at the boundary or interface of each pavement layer as programmed in the MWELP. Continuity conditions at the interface produce six more strain outputs (eliminating two horizontal displacements). For a five-layer pavement system, there are 117 stress-strain-displacement outputs for every point under a single static wheel load. If a minimum of ten iterations are required for thickness or composition determination, at least 20,000 outputs would be printed. These design computations are straight forward mechanical operations, but can be time consuming and expensive. Several modifications have been made to streamline the iteration process and thus reduce CPU time.

MWELP used at Portland International Airport in 1972, was modified to iterate only the vertical surface displacements and horizontal normal stresses. For pavement evaluation at San Jose Municipal Airport in 1975, the MWELP iteration process was replaced by a set of computer files which contained the peak stress, peak deflection, thickness and E-value of each pavement element. A significant reduction in computer time resulted.

Under the present setup, the computer program can handle pavements consisting of 15 structural layers under an aircraft having 35 wheels. The program is big enough to handle today's and the foreseeable future's airport operations. Airport experience and computer analysis indicate that runway pavement thickness and composition is normally governed by the limiting elastic deflection, that is, the functional requirements of aircraft operation. On the other hand, taxiway pavement thickness and composition is likely to be, but not always, governed by the limiting stress level, that is, by the need for facility maintenance and pavement crack formation.

Insofar as pavement materials are concerned, computer analysis indicates that the thickness of a portland cement concrete layer is most likely governed by the limiting stress level (formation of cracks). The thickness of an asphalt concrete layer however, is usually governed by the limiting inelastic deformation (surface deformation of the pavement). The pavement support quality also has a significant effect on thickness determination.

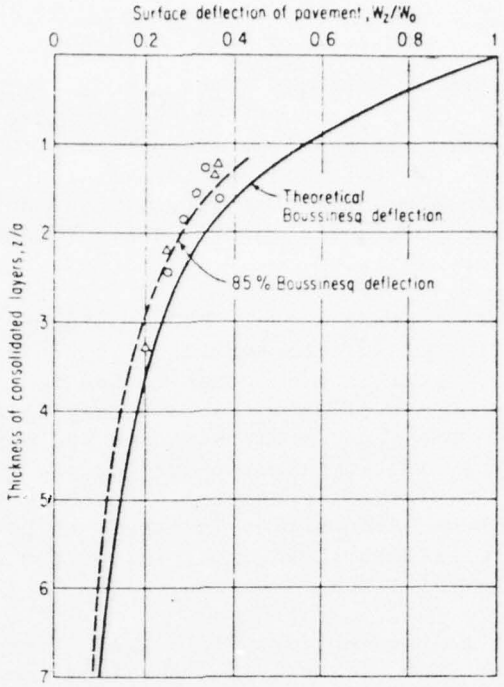

Fig. 2.10 Measured Deflection vs Boussinesq Deflection

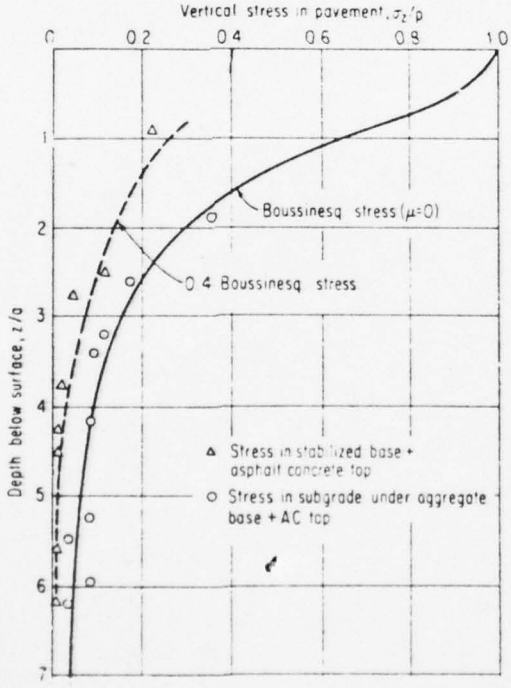

Fig. 2.11 Measured Stress vs Boussinesq Stress

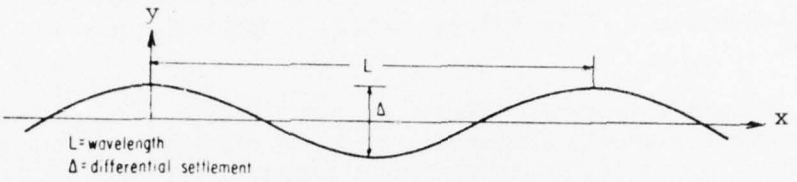

Fig. 2.12 Surface Configuration due to Differential Settlement

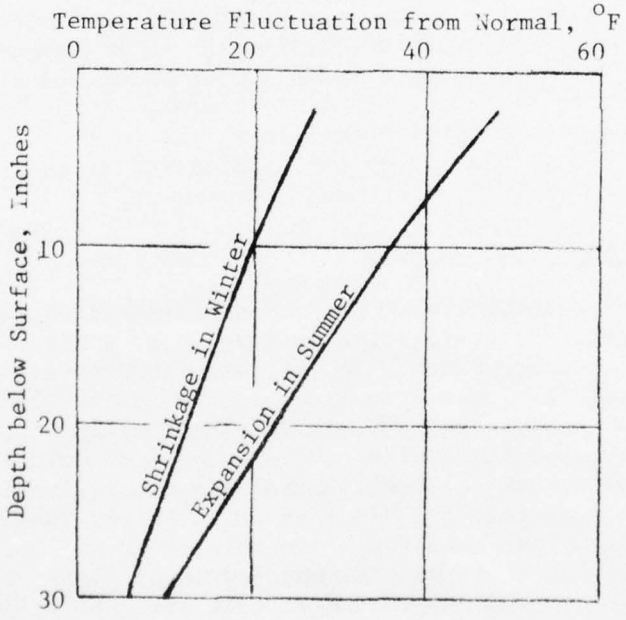

Fig. 2.13 Temperature Variation in Pavement

2.4 COST/BENEFIT ANALYSIS

Pavement construction costs consist of (1) the initial construction cost, (2) the direct cost of repair and maintenance, and (3) the indirect cost due to service interruption. This last item is very important for today's busy airports. Airport management tends to prefer construction of better pavements in order to reduce maintenance needs.

Economic study in today's pavement design program is actually its weakest element. Pavement engineers can estimate the initial construction costs, but they cannot properly evaluate the subsequent maintenance costs. At the Newark pavement test, an objective cost/benefit study was conducted to determine the most desirable pavement system. The result was a substantial savings in construction costs, leading to less participation by the FAA's Airport Development Aid Program (ADAP), and a lower mortgage payment by the users. Similar pavement design and economic studies were adopted by Zurich, Portland, and other airports. Construction cost savings ranging from 20 to 60% were reported.

A set of default values are programmed for each economic event. All dollar value analyses are "ball park" estimates only. However, the relative dollar values can provide a meaningful index for comparing the cost/benefits of different pavement systems. Because of regional variation and local construction practices, the default values should be objectively modified prior to its application at an airport.

a. Initial Construction Cost

Initial construction cost estimates should be logically made by the contractor. However, there is frequently a wide variation in bids from different contractors. In the computer program, the initial construction cost is broken down into (1) materials, (2) direct labor and equipment for processing, (3) direct labor, equipment, and transportation for placement and finish, (4) general and administrative, (5) overhead and profit, and (6) mobilization and demobilization costs. Except for the last cost breakdown which is fairly independent of job size, the other five breakdowns are related to the basic material and labor costs. For instance, the unit price of plain portland cement concrete pavement PCC, expressed in cost per inch thickness per square yard, is the sum of the following items:

.0433 x unit price of coarse aggregate, $/ton
.0181 x unit price of fine aggregate, $/ton
.1430 x unit price of construction lumber, $/BM
.0102 x unit price of portland cement, $/ton (bulk)
.0321 x hourly rate of common labor, $
.0127 x hourly rate of skilled equipment operator, $.

The last two items include rental of the yard equipment, mixing plant, transportation, placement equipment, finishing and water curing. Overhead, general and administrative, and profit are added to all items. A 5 to 15% fluctuation from this "ball park" estimate should be anticipated.

For actual job applications, the unit price of materials and labor should be mandatory inputs for each airport. A set of default values for each cost item has been carefully developed for fourteen types of pavement materials. These values reflect the general construction condition at major cities in the U.S. and should be adjusted for the specific job condition.

b. Annual Maintenance Cost

For modern airports, runway and taxiway maintenance which requires closedowns is a very serious operation. When a runway maintenance program is scheduled, distant airports and the air transport industry are informed several weeks in advance. During emergency repairs, air traffic can be tied up at distant airports and inbound flight delay may become costly and difficult to manage. The monetary loss of operational revenues and the inconvienence to the travelling public cannot be accurately measured.

Pavement maintenance costs are generally included in the overall operation and maintenance programs. At some airports, a separate account is kept for materials, equipment and labor costs for pavement maintenance. Under the scope of this research contract, a series of field surveys were conducted by Sutherland on the administrative and fiscal policies pertaining to pavement maintenance at twelve domestic airports. His complete report is given in Appendix C. Sutherland reported that annual pavement maintenance costs range from $0.10 to 0.14 per square yard for most airports, to $0.75 to 1.62 per square yard for airports where regional subsidence is pronounced.

The computer program computes the annual maintenance costs at a common airport on the following assumptions:

Ultimate Material Strength, ULSTR = (1-COVAR)*STRESS*$\sqrt{E}$
Allowable Working Stress, WOSTR = ULSTR(1-FATIST*ALOG10(AANA))
Computed Pavement Stress, ACSTR = Output of computer analysis
Annual Maintenance Cost, AMC = ICC*COVAR*(ULSTR-WOSTR)/(ULSTR-ACSTR)

in which ICC is the initial pavement construction cost, COVAR is the coefficient of variance of the material strength, FATIST is the coefficient of the material's fatigue strength, and AANS is the anticipated number of wheel load repetitions. If the concept of a limiting stress level is applied to pavement design analysis, the annual maintenance cost ranges between $0.05 to 0.18 per square yard.

c. Indirect Operational Cost

In addition to the direct costs of pavement maintenance and repair, there are the indirect costs due to interruption of airport operations and the additional cost of standby manpower and equipment. As today's airport construction is paid primarily by the users (the ADAP fund is paid for by the air travel public through the user's tax), indirect operational costs should also be considered in pavement design analysis.

The indirect operational cost, in general, is less critical for multi-runway and medium hub airports than for intersecting runways at major hub airports. There is no definitive method in estimating the indirect operational costs, but several job examples offered below can be used for reference.

At JFK Airport, more than 50% of the landing and take-off traffic is from runway 31L. Shutdown of this runway could cause delays which could run well over 60 minutes. At a major hub airport in the mid-west, the average cost would be about $10.00 plus 19 gallons of fuel per minute delay on an average inbound flight. The indirect costs for inbound flight delays alone could run into six figures for a one-day operation [15].

During pavement reconstruction of the single runway at a medium hub airport, airport authorities can temporarily divert air traffic to neighboring airports. The additional cost in providing ground transportation is not prohibitive. A general provision cannot be made in the computer program for estimating the indirect operational costs.

d. Cash Flow and Financial Cost

The concept of cash flow and financial cost analysis was introduced by Vittas [15] for the Nashville Metropolitan Airport. The capital investment for construction costs is assumed to be paid for by revenue bonds P, which are amortized by an annual payment for n-years at an interest rate, i. The annual mortgage payment p, is:

$$p = P/\sum_{N=1}^{n} 1/(1+i)^N \qquad (2.25)$$

In the next cost analysis step, the annual mortgage payment plus the cost for incidental or scheduled maintenance works are converted into discounted cash flow. For a constant annual payment q, for m-years, at a cash discount rate r, the discounted cash value CV, is:

$$CV = q \sum_{N=1}^{m} (1-r)^{N-1} \qquad (2.26)$$

If the cash discount rate r, is greater than the bond interest rate i, p=q and m=n, the discounted cash value CV, will be smaller than the capital investment for construction costs. Under the present market conditions, the interest rate for municipal revenue bonds floated by the airport authority, is about 2% less than the cash discount rate. For a 30 year bond, the savings in initial construction cost is about 21%. This is an additional incentive for designing a better pavement for the initial construction and, thereby, reducing future maintenance costs.

e. Present Cash Value

The computer program calculates the present cash value for the initial construction cost using:

$$PCVICC = (ICC) * \sum_{N=1}^{NBL} (1-ARCD)^{N-1} / \sum_{N=1}^{NBL} 1/(1+AIRB)^{N} \qquad (2.27)$$

The present cash value for annual maintenance costs is:

$$PCVAMC = \sum_{N=1}^{NSLP} (AMC) * ((1+ASCMC+ASCCC) * (1-ARCD))^{N-1} \qquad (2.28)$$

The present cash value for the entire pavement service package is:

$$PCV(I) = PCVICC + PCVAMC \qquad (2.29)$$

in which ICC = Initial construction cost of total pavement, $/s.y.,
AMC = Annual maintenance cost, $/s.y.,
ASCMC = Annual escalation rate of maintenance needs
ASCCC = Annual escalation rate of construction costs,
NBL = Revenue bond maturity, years
AIRB = Annual interest rate of bonds
ARCD = Annual rate of cash discount,
NSLP = Effective service life of pavement, years
PCV(I) = Present cash value during service life, $/s.y.

In the actual computer program, the power series is simplified:

$$\sum_{N=1}^{n} x^{(N-1)} = \frac{1 - x^{n}}{1 - x} \qquad (2.30)$$

It becomes simpler and more accurate to compute PCV by indicating the value of each pavement segment. Vittas [15] stated: "Discount cash flow analyses are valid techniques to be used in exploring the economic aspects of design alternatives, particularly when one or both involves capital investments at some future date."

f. Cost/Benefit Study

Present cash values obtained from the above computations are weighted by the width and length of the pavement section as follows:

$$PCV = (\Sigma PCVKEEL(I)*L(I)(WK)+ \Sigma PCVSIDE(I)*L(I)(WD-WK))/(L*WD) \quad (2.31)$$

in which:
- L = total pavement facility length,
- L(I) = pavement segment length,
- PCVKEEL(I) = PCV of the segment's keel portion,
- PCVSIDE(I) = PCV of the segment's side portion,
- WD = total pavement facility width,
- WK = keel width by Equation 2.5.

The PCV in the above equation represents the weighted average of the pavement facility's present cash value. It is the most meaningful dollar value for studying the relative costs of different pavement systems. This information provides a good background to airport managment, users, and administrators regarding the cost of pavement systems.

Insofar as benefits of a pavement system are concerned, they can be expressed by:

(1) Length of pavement's performance life without major maintenance, in years,
(2) Option of an in-pavement navigation and light system,
(3) Pavement surface quality with respect to smooth aircraft riding,
(4) Demand forecast of aircraft movements both in aircraft size and volume.

In the computer program, there are eight types of pavement systems which have been used for cost/benefit studies. There are three types of pavements for new constructions on the subgrade: portland cement concrete, asphalt cement concrete, and the stabilized LCF system. Five types of pavement are programmed for use in rehabilitation: reinforced portland cement concrete overlay, asphalt concrete overlay, LCF overlay, and portland cement concrete, or LCF in the keel section with asphalt concrete overlay for the sides. New pavement systems, if required, can easily be programmed. The computer is capable of accepting reasonably flexible input regarding the thickness and composition of the pavement structure to be designed.

2.5 PRACTICAL APPLICATION OF DESIGN ANALYSIS

In the above design analysis, two very important factors were not considered. They are the pavement surface geometry and the surface and subsurface drainage condition. In establishing the new profile and side slope, it is necessary to consider (1) the minimum overlay thickness, (2) its bonding to the existing surface, and (3) the material durability. For all practical purposes, an asphalt overlay should not be less than three inches, and a portland cement concrete overlay should not be less than six inches.

Insofar as pavement drainage is concerned, the computer program has no provisions for anything in this area. Experience with NDT at all the airports mentioned in this study, shows that the supporting capacity of a pavement system will be reduced by 50% when its base is wet and saturated. A good pavement maintenance policy is to seal the joints and cracks, thus preventing surface water penetration and the lateral migration of ground moisture.

In the final stages of pavement design, there are several important considerations, such as construction practice, material utilization and fiscal management which are beyond the scope of this study. Some information on these factors can be found in Reference [1]. Insofar as the relative cost of pavement design alternatives, the third subsystem of this computer program provides a solid background from which airport management will be able to formulate a pavement construction program tailored to the financial situation of the airport.

Finally, the most important item in the whole design system is the sound judgment of a well informed designer. All human beings make mistakes, however, and an appropriate factor of safety should be used in the final design process. To improve the reliability of the pavement design system, computer analysis as discussed in this study should be extensively used to iterate any questionable variables with respect to the functional performance and total cost of a pavement project.

PART 3

COMPUTER INPUT AND OUTPUT LISTINGS

3.1 COMPUTER CODE AND DICTIONARY

A. TYPE OF PAVEMENT

ASPHLT	ASPHALT PAVEMENT
ASPOV	ASPHALT OVERLAY
CONC	CONCRETE PAVEMENT
CONCOV	CONCRETE OVERLAY
LCF	LIME-CEMENT-FLYASH PAVEMENT
LCFOV	LCF OVERLAY

B. PAVEMENT COMPONENTS

AGBS	AGGREGATE BASE COURSE, P-206 TO P-214, P-217
ASBS	ASPHALT BASE COURSE, P-201
ASTB	ASPHALT TREATED BASE, P-215, P-216
ASTOP	ASPHALT TOP COURSE, P-401, P-408
CTB	CEMENT TREATED BASE, P-301, P-304
LCFA	LCF-A MIX
LCFB	LCF-B MIX
LCFC	LCF-C MIX
LTSUB	LIME TREATED SUBGRADE, P-155
PAV	EXISTING PAVEMENT
PAVDF	EXISTING PAVEMENT LAYER FOR PSL STRESS
PCC	PORTLAND CEMENT CONCRETE, P-501
PCCR	REINFORCED PORTLAND CEMENT CONCRETE, P-501, P-610
RLC	ROLLED LEAN CONCRETE
SSBS	SELECTED SUB-BASE, P-154
SUB	SUBGRADE SOIL

C. PAVEMENT AREA

END	END PORTION OF RUNWAY AT LANDING ROLL
HP	HOLDING PAD
KEEL	CENTER STRIP OF RUNWAY OR TAXIWAY
MID	MID PORTION OF RUNWAY OR TAXIWAY
SIDE	SIDE STRIPES OF RUNWAY OR TAXIWAY
TD	TOUCH DOWN AREA

D. FUNCTIONAL CONDITION

A1,A2	COEFFICIENTS OF TRANSFER FUNCTION (TRANSVERSE TO LONG. DEFLECTION)
AAND	EQUIVALENT LOAD REPETITIONS OF ALL AIRCRAFT - DEFLECTION CRITERIA
AANS	EQUIVALENT LOAD REPETITIONS OF ALL AIRCRAFT - STRESS CRITERIA
AND	EQUIVALENT LOAD REPETITIONS OF ONE TYPE OF AIRCRAFT - DEFLECTION
ANDA	ANTICIPATED SERVICE LIFE IN LOAD REPETITIONS - DEFLECTION CRITERIA
ANS	EQUIVALENT LOAD REPETITIONS OF ONE TYPE OF AIRCRAFT - STRESS CRITERIA
APX	TRANSVERSE DIRECTION PROBABILITY DISTRIBUTION OF WHEEL LOAD
APY	LONGITUDINAL DIRECTION PROBABILITY DISTRIBUTION OF LANDING IMPACT
D1,D2	COEFFICIENTS OF TRANSFER FUNCTION (ELASTIC TO CUMULATIVE DEFORMATION)
ILS	INSTRUMENT LANDING SYSTEM
LIGHTS	IN PAVEMENT LIGHTING SYSTEM
NORM	NORMAL AIRPORT NAVIGATION SIGNS
NSLP	EFFECTIVE SERVICE LIFE OF PAVEMENT, NUMBER OF YEARS
PFL	PRESENT FUNCTIONAL LIFE IN YEARS
SERVYR	DESIGN SERVICE LIFE IN YEARS
VISUAL	VISUAL LANDING SYSTEM

E. AIRCRAFT FILE

DI	DYNAMIC INCREMENT OF AIRCRAFT VIBRATION AT PAVEMENT-WHEEL INTERFACE
EPW	OPERATING EMPTY WEIGHT OF AIRCRAFT
ESW	EQUIVALENT SINGLE WHEEL LOAD
FACTOR	INFLUENCE FACTOR OF ALL AIRCRAFT WHEELS
FREQ	NATURAL FREQUENCY OF AIRCRAFT GEAR SUPPORT ON PAVEMENT
LRW	LANDING ROLL WEIGHT
MLG	MAIN LANDING GEAR LOAD OF AIRCRAFT
MLRW	MAX. LANDING WEIGHT OF AIRCRAFT
MTOW	MAX. TAKE-OFF WEIGHT OF AIRCRAFT
NWHEEL	NUMBER OF MLG WHEELS PER AIRCRAFT
OEW	OPERATIONAL EMPTY WEIGHT OF AIRCRAFT
PLF	BOARDING FACTOR
PSI	TIRE PRESSURE
RADIUS	RADIUS OF CONTACT AREA OF AIRCRAFT MLG WHEEL
RANGE	DISTANCE RANGE OF AIRCRAFT(SHORT,MEDIUM,LONG)
RGF	RANGE FACTOR
RPWT	RAMP WEIGHT OF AIRCRAFT
TDW	TOUCH-DOWN WEIGHT
TOW	TAKE-OFF WEIGHT
VEL	VELOCITY OF AIRCRAFT EQUIVALENT TO FULL STATIC LOAD WITHOUT WING LIFT
WGT	WEIGHT OF MLG PER TIRE

F. MATERIAL FILE

ACSTR	ACTUAL WORKING TENSILE STRESS
COVAR	COEFFICIENT OF VARIANCE - MATERIAL STRENGTH
EPAV	E-VALUE OF EXISTING PAVEMENT
ESUB	E-VALUE OF SUBGRADE
E-SUP	E-VALUE OF PAVEMENT SUPPORT (SUBGRADE OR EXISTING PAVEMENT)
FATIGT	COEFFICIENT OF FATIGUE STRESS (LOG CYCLE)
OVSFKL	OVERSTRESS FACTOR FOR KEEL OR OTHER UNDEFINED AREA
OVSFSD	OVERSTRESS FACTOR FOR SIDES
SIGMA	HORIZONTAL STRESS IN PAVEMENT COMPONENT
SIGMAT	HORIZONTAL TENSILE STRESS IN PAVEMENT COMPONENT
STRESS	CONVERSION FACTOR E-VALUE TO TENSILE STRESS
ULSTR	ULTIMATE SAFE TENSILE STRESS
WOSTR	SAFE WORKING TENSILE STRESS
WZ	SURFACE DEFLECTION OF PAVEMENT
WZERO	WZ AT X = 0, Y = 0

G. COST FILE

AIRB	ANNUAL INTEREST RATE OF BOND
AMC	ANNUAL MAINTENANCE COST, $/S.Y.
ARCD	ANNUAL RATE OF CASH DISCOUNT
ASCCC	RATE OF ANNUAL ESCALATION OF CONSTRUCTION COST
ASCLT	COST OF ASPHALT OIL, CAR LOAD PER TON
ASCMC	RATE OF ANNUAL ESCALATION OF MAINTENANCE NEED
CLHR	RATE OF COMMON LABOR PER HOUR
COAGT	COST OF COARSE AGGREGATE PER TON
FIAGT	COST OF FINE AGGREGATE PER TON
HLBT	COST OF HYDRATED LIME, BULK PER TON
ICC	INITIAL CONSTRUCTION COST OF TOTAL PAVEMENT, $/S.Y.
LBBM	COST OF CONSTRUCTION LUMBER PER BOARD MEASURE
NRL	MATURITY OF REVENUE BOND, NUMBER OF YEARS
PCBT	COST OF PORTLAND CEMENT, BULK PER TON
PCV	PRESENT CASH VALUE OF TOTAL PAVEMENT DURING SERVICE LIFE, $/S.Y.
POZBT	COST OF POZZOLAN OR FLYASH, BULK PER TON
RSWLB	COST OF REINFORCING STEEL (WIRE MESH) PER POUND
SFST	COST OF SELECTED FILL SAND PER TON
SLEHR	RATE OF SKILLED EQUIPMENT OPERATOR PER HOUR
WAPCV	WEIGHTED AVERAGE OF PRESENT CASH VALUE

H. NDT DATA FILE

AREA-E	(MEAN - ONE STANDARD DEVIATION) OF A GROUP OF E-VALUE
Z(I)	DYNAMIC RESPONSE OF SUB OR PAV IN INCH AT ITH TEST
DSM(1)	F(1)/Z(1) AT FIRST RESONANCE
EVALUE	MODULUS OF ELASTICITY OF RESPONSE SYSTEM IN NDT PROGRAM
F(I)	FORCING FUNCTION, DOUBLE AMPLITUDE IN POUNDS
H(I)	FREQUENCY OF FORCING FUNCTION IN HZ AT ITH TEST
H(1)	H(I) AT FIRST RESONANCE, HZ
NDT	NONDESTRUCTIVE TEST

I. FORECAST FILE

ADM	AVERAGE DAILY MOVEMENT
ADMSUG	AVERAGE DAILY MOVEMENT SUGGESTED FOR PAVEMENT DESIGN
ADMATA	AVERAGE DAILY MOVEMENT PREPARED BY ATA
ADMAPO	AVERAGE DAILY MOVEMENT PREPARED BY AIRPORT OPERATOR
ADMFAA	AVERAGE DAILY MOVEMENT PREPARED BY FAA
ATD	AIRPORT TRAFFIC DISTRIBUTION
ATDSUG	AIRPORT TRAFFIC DISTRIBUTION SUGGESTED FOR PAVEMENT DESIGN
ATDAPO	AIRPORT TRAFFIC DISTRIBUTION PREPARED BY AIRPORT OPERATOR
FAM	FORECAST OF AIRCRAFT MOVEMENT
FAMSUG	FORECAST OF AIRCRAFT MOVEMENT SUGGESTED FOR PAVEMENT DESIGN
FAMAPO	FORECAST OF AIRCRAFT MOVEMENT PREPARED BY AIRPORT OPERATOR

3.2 NDT MACHINE DATA AND FIELD INPUTS

a. OFFSET DICTIONARY

C	CENTER LINE
R	RIGHT OF CENTER LINE
L	LEFT OF CENTER LINE

b. CALIBRATION FACTORS

DATE	TIME CODE	RESPONSE E-6	AMPLITUDE E-1	FREQUENCY E-2
5/18/76	1/0850/1	.99570	2.00290	.99670
5/18/76	1/1151/2	.99240	2.00020	.99930
5/18/76	1/1617/3	.98720	1.99200	1.00270
5/19/76	2/0845/1	1.00140	2.00180	.99930
5/19/76	2/1004/2	.99930	1.99820	.99930
5/19/76	2/1322/3	.99750	2.00280	.99800
5/19/76	2/1617/4	1.00310	2.00460	.99870
5/20/76	3/1208/1	1.00730	2.00710	1.00130
5/21/76	4/0910/1	1.00730	1.99190	.99870
5/21/76	4/1302/2	.99930	2.00130	1.00270
5/22/76	5/0500/1	.99420	1.99040	1.00270
5/23/76	6/0847/1	1.00640	2.00340	.99870
5/23/76	6/1250/2	1.00880	2.00150	1.00330

c. GRID DICTIONARY

A	RUNWAY 1-19
B	TAXIWAY 1-19
C	RUNWAY 10-28
D	TAXIWAY 10-28
E	RUNWAY 5-23
X	CROSS TAXIWAYS
Y	CROSS TAXIWAYS
Z	CROSS TAXIWAY

d. TEST IDENTIFICATIONS

TEST	LOCATION	TIME	TEMP	DSM(W)
1-6	A000.5R15	2/0900/1	72.8	4840
2-6	A003.0L15	2/0910/1	76.8	5200
3-6	A005.5R15	2/0921/1	77.6	3640
4-6	A008.0L05	2/1044/2	85.3	3600
5-6	A008.0L15	2/1035/2	83.4	4560
6-6	A008.0L25	2/1024/2	78.9	4640
7-6	A008.0L35	2/1013/2	78.9	4240
8-6	A008.0L50	2/1004/2	79.8	4680
9-6	A008.0L70	2/0936/2	79.1	4240
10-4	A008.0L80	2/0945/2	80.0	0370
11-6	A010.5L15	2/1054/2	85.8	3060

e. Machine Data

NO.	RESPNS	AMPL	FREQ	RESPNS	AMPL	FREQ	RESPNS	AMPL	FREQ
1	000246	030028	006042	000405	030670	005542	000379	030327	005024
1	000438	029409	004517	000534	030207	004230	000400	029674	004026
1	000412	029274	003817	000413	029194	003637	000413	029338	003414
1	000400	029749	003224	000430	030088	003016	000455	029737	002809
1	000499	029194	002615	000504	029719	002413	000539	029625	002213
1	000571	029231	002006	000632	029567	001811	000702	029940	001605
1	000693	029307	001505	000764	029719	001403	000812	029944	001299
1	001024	030325	001202	001297	029968	001099	002012	030748	000999
1	001635	029791	000894	001388	030532	000797	001236	030503	000697
1	001637	030259	000592	001613	029745	000486			
2	000232	030613	006037	000285	029629	005560	000303	030570	005020
2	000296	029799	004525	000371	029752	004227	000367	029520	004013
2	000324	029574	003824	000345	029312	003632	000334	029740	003410
2	000324	029750	003216	000335	030098	003015	000393	030184	002809
2	000413	030139	002611	000412	030305	002420	000446	030078	002206
2	000587	029820	002013	000624	029878	001805	000566	029363	001606
2	000571	029559	001504	000582	029696	001405	000670	030264	001303
2	000622	031164	001302	000672	029590	001199	000964	030116	001100
2	001500	029774	001002	001207	029359	000902	000921	029870	000797
2	000890	029397	000699	001129	030107	000593	001172	029688	000502
3	000324	030290	006040	000426	029797	005539	000500	029640	005040
3	000462	030475	004527	000552	029373	004232	000643	029754	004032
3	000606	029294	003840	000607	029522	003623	000576	029984	003423
3	000559	030388	003212	000571	030417	003027	000615	030251	002812
3	000651	030036	002607	000664	030634	002410	000705	030474	002214
3	000771	030404	002007	000856	029872	001803	000828	029354	001604
3	000835	029254	001504	000852	029505	001400	000899	029825	001305
3	000972	030163	001200	001147	030651	001094	001956	029509	001000
3	001987	031199	000999	001953	029334	000902	001378	029494	000795
3	001335	030730	000700	001352	051607	000697	001552	029660	000595
3	001539	029548	000483						
4	000389	029590	006033	000552	029556	005553	000758	030320	005044
4	000671	029909	004543	000593	029949	004248	000727	030413	004022
4	000720	029333	003807	000679	029745	003635	000657	029754	003421
4	000645	029733	003222	000657	030380	003007	000689	030357	002824
4	000720	030106	002613	000729	030213	002409	000764	030454	002208
4	000799	030534	002012	000820	029951	001807	000807	029540	001604
4	000810	029708	001507	000816	029814	001402	000844	029681	001303
4	000909	030373	001203	001072	029440	001102	002012	030148	000995
4	002050	029838	000900	001529	029829	000799	001372	029664	000699
4	001497	029929	000598	001686	029424	000504			
5	000272	030094	006032	000362	029356	005562	000395	029499	005020
5	000376	029779	004521	000459	029600	004227	000533	029234	004017
5	000482	030070	003812	000453	029221	003637	000461	029314	003429
5	000448	030023	003228	000456	030215	003021	000497	030075	002812
5	000526	029734	002620	000533	030390	002411	000547	030603	002213
5	000573	030348	002013	000615	029610	001812	000620	029380	001604
5	000627	029217	001504	000660	030018	001400	000698	029294	001304
5	000802	030120	001205	000933	029454	001099	001686	029552	000995
5	001544	029930	000900	001160	029964	000793	001047	030002	000694
5	001232	029974	000597	001372	029617	000500			
6	000287	030241	006037	000412	030359	005549	000447	030443	005044
6	000386	029597	004517	000452	030413	004228	000534	029705	004023
6	000491	029374	003828	000497	029940	003620	000447	029942	003429

AD-A036 384 YANG STEVENS FABIAN ENGINEERS NEW YORK F/G 13/2
NONDESTRUCTIVE EVALUATION OF CIVIL AIRPORT PAVEMENTS.(U)
SEP 76 N C YANG DACW39-76-C-0010
UNCLASSIFIED FAA-RD-76-83 NL

2 OF 2
AD A036384

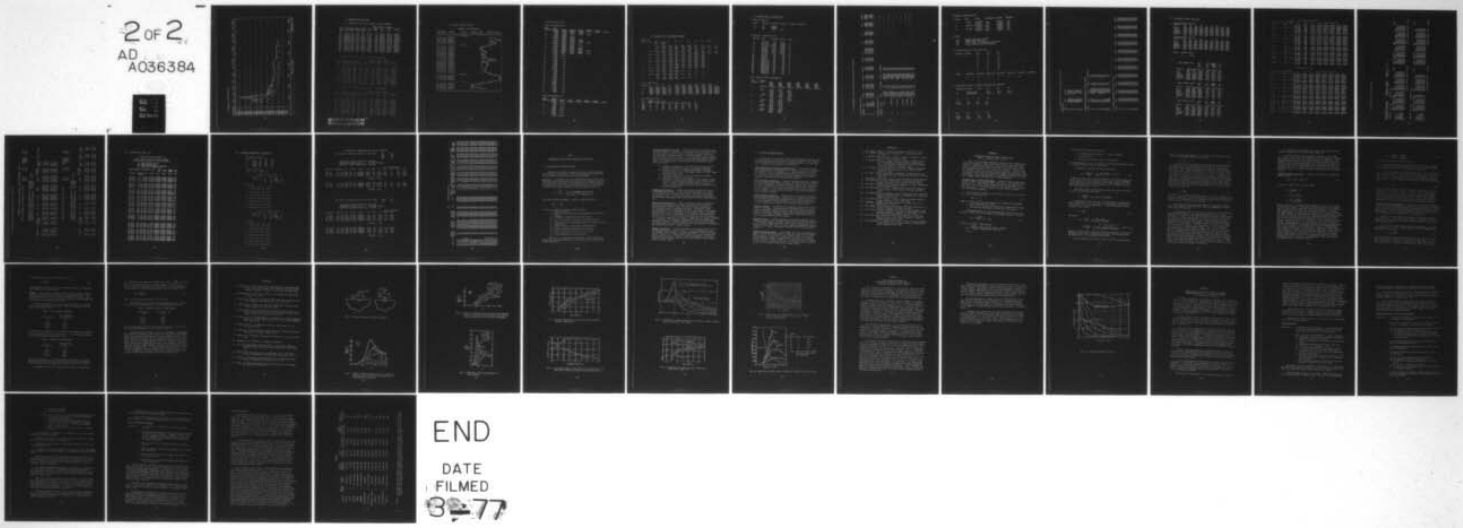

END

DATE FILMED
3-77

f. Graphic of Machine Data

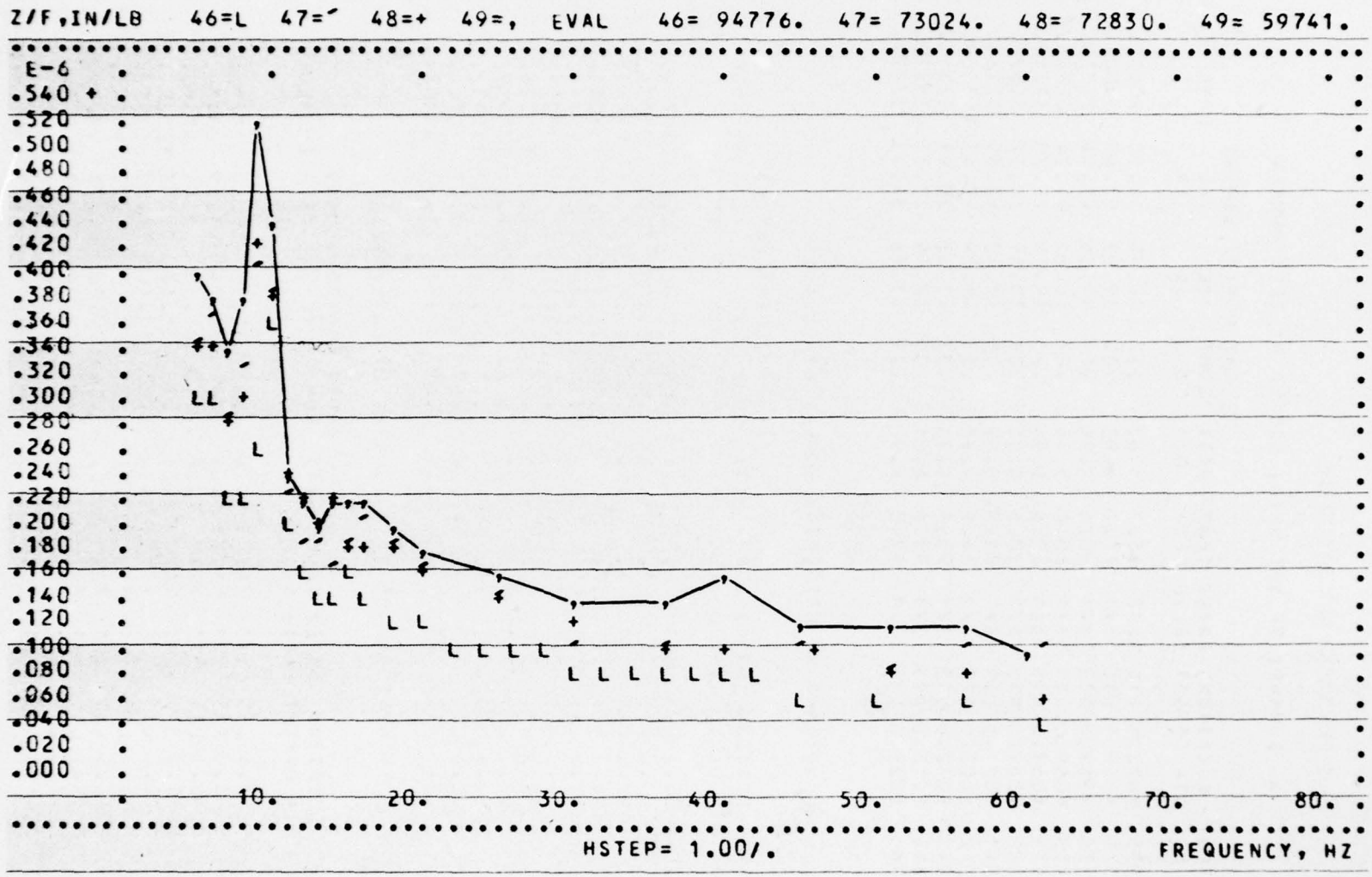

3.3 PROCESSED NDT DATA FILE

a. SUMMARY OF NDT DATA, SORTED BY TEST NUMBER

TEST NO.	LOCATION STA	OFFSET	DATE/ CALIB	TEMP DEGF	H(1) HZ	Z(N)/ SUMZ %	DSM(1) /E IN	DSM(W) /E IN	E-VALUE
135	Y022.5	R15	6/2	95.7	5.02	.17	40.95	16.10	20500.
136	Y049.5	L15	6/1	77.2	4.92	.20	39.01	53.40	55801.
137	Y069.0	R15	6/1	80.6	4.94	.19	39.36	45.04	27755.
138	Y069.0	R15	6/1	80.6	5.96	.22	36.93	41.94	29804.
139	Y069.0	R15	6/1	80.6	5.96	.23	39.19	38.20	32719.
140	Y069.0	R15	6/1	80.6	6.98	.28	36.89	34.37	36371.
141	Y091.5	L15	6/1	84.0	8.98	.58	31.42	42.35	62813.
142	E003.0	R15	3/1	84.9	4.98	.37	48.09	47.43	118069.
143	E012.0	L15	3/1	90.6	4.94	.23	42.32	30.91	32355.
144	E018.0	R15	3/1	91.6	6.01	.30	38.79	27.71	36810.
145	E024.0	L15	3/1	92.0	4.90	.19	41.96	38.71	37972.

b. SUMMARY OF NDT DATA, SORTED BY LOCATION

TEST NO.	LOCATION STA	OFFSET	DATE/ CALIB	TEMP DEGF	H(1) HZ	Z(N)/ SUMZ %	DSM(1) /E IN	DSM(W) /E IN	E-VALUE
2[illegible]	A [illegible]	R15	3/1	7[illegible]	[illegible].94	.69	32.[illegible]	46.[illegible]	67799.
[illegible]	A[illegible]	R15	3/1	[illegible]	9.[illegible]	.82	34.96	39.[illegible]	91536.
[illegible]	A[illegible]	L15	3/1	[illegible]	9.94	.93	33.47	38.66	87941.
[illegible]	A[illegible]	R15	3/1	[illegible]	9.04	.70	33.33	39.[illegible]	89016.
[illegible]	A[illegible]	L15	3/1	[illegible]	[illegible].03	1.10	32.10	39.34	[illegible]755.
[illegible]1	A[illegible]	L15	3/1	[illegible]	10.03	.71	31.10	39.10	[illegible]233.
[illegible]	A[illegible]	R15	3/1	[illegible]	[illegible].99	.96	31.02	41.13	169233.
[illegible]3	A[illegible]	L15	3/1	[illegible]	[illegible].01	.83	30.77	41.41	170989.
[illegible]4	A[illegible]	R15	3/1	91.[illegible]	10.03	.77	30.49	40.32	154932.
[illegible]	A[illegible]	L15	3/1	92.4	10.04	.69	30.41	39.62	75724.
[illegible]	A[illegible]	R15	3/1	[illegible]	[illegible].4	.61	30.71	[illegible].42	51767.

c. SUMMARY OF NDT DATA, SORTED BY DATE/CALIB

TEST NO.	LOCATION STA	OFFSET	DATE/ CALIB	TEMP DEGF	H(1) HZ	Z(N)/ SUMZ %	DSM(1) /E IN	DSM(W) /E IN	E-VALUE
1[illegible]	C[illegible]	L15	5/1	RAIN	9.[illegible]4	.69	33.10	39.83	[illegible]327.
104	C[illegible]	R15	5/1	RAIN	9.01	.64	29.74	43.19	32436.
10[illegible]	C[illegible]8.5	L15	5/1	RAIN	9.02	.60	30.10	39.41	41365.
10[illegible]	C[illegible]91.[illegible]	R15	5/1	RAIN	10.03	.80	31.67	31.92	102239.
1[illegible]	C[illegible]7[illegible].[illegible]	L15	5/1	RAIN	9.04	.67	30.[illegible]	39.61	52533.
11[illegible]	D[illegible]8.5	L15	6/1	74.[illegible]	9.[illegible]4	.55	29.49	38.79	99941.
11[illegible]	D[illegible]30.5	R15	6/1	72.[illegible]	10.03	.94	29.92	44.71	99474.
11[illegible]	D[illegible]39.5	L15	6/1	74.[illegible]	9.98	.67	30.04	39.49	104034.
1[illegible]	D[illegible]43.[illegible]	R15	6/1	74.[illegible]	9.99	.64	29.54	46.42	104259.
1[illegible]1	D[illegible]48.5	R15	6/1	75.[illegible]	9.95	.47	31.34	43.[illegible]	[illegible]6[illegible]4.

d. Graphic of NDT E-values

RUNWAY 1-19/PROFILE

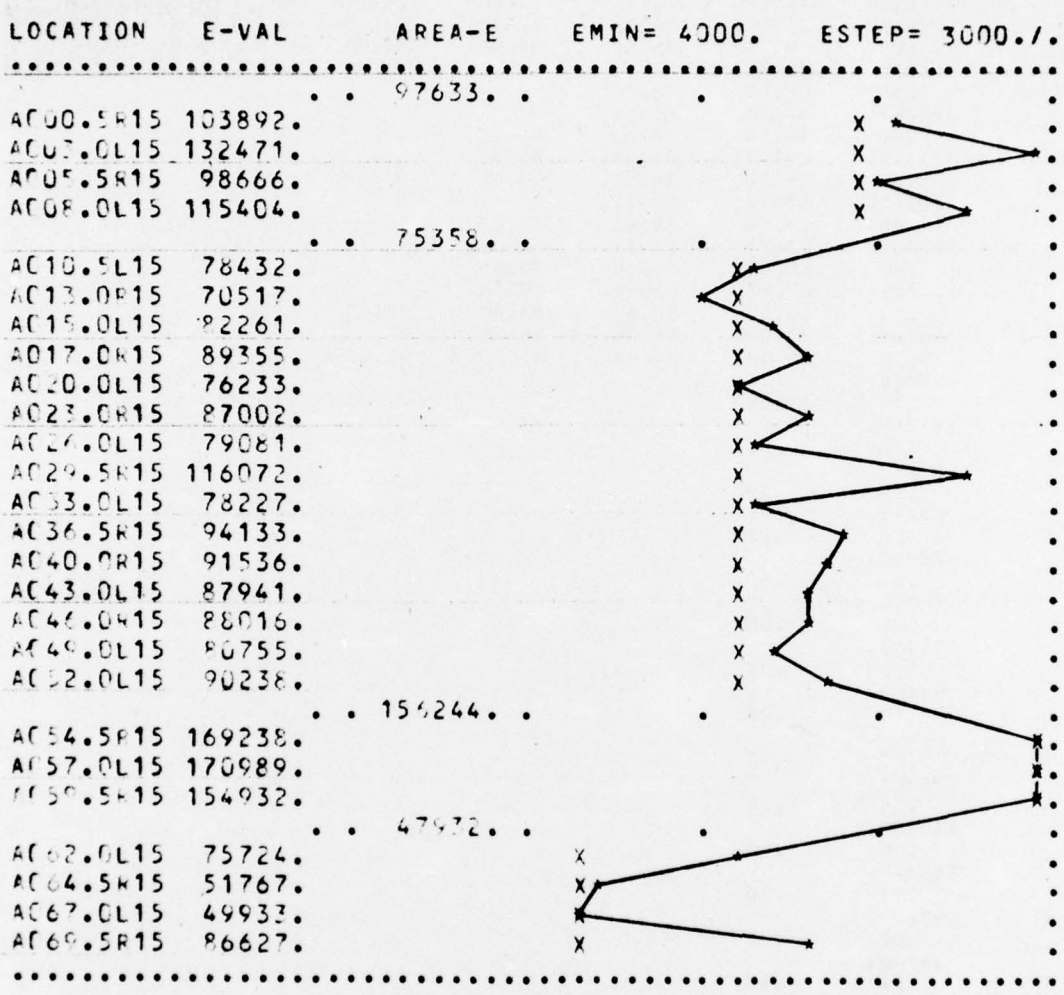

e. NDT Inventory Files

EPAV, NDT INVENTORY FILE

EPAV FACILITY	NDT EVALUE STATION	EVALUE STATION	EVALUE STATION	EVALUE STATION	EVALUE STATION	EVALUE STATION	STATION
1	97633.	75358.	156244.	47932.			
	.00	9.00	53.00	60.00	70.00		
2	68818.	35484.					
	5.50	66.00	92.00				
3	120761.	63643.	80411.				
	.00	14.00	34.00	70.00			
4	131114.	29227.	86994.	60586.			
	5.50	19.00	24.00	63.00	92.00		
5	120761.	63643.	80411.				
	.00	14.00	34.00	70.00			
6	120761.	63643.	80411.				
	.00	14.00	34.00	70.00			
7	131114.	29227.	86994.	60586.			
	5.50	19.00	24.00	63.00	92.00		
8	131114.	29227.	86994.	60586.			
	5.50	19.00	24.00	63.00	92.00		
9	29920.						
	.00	39.00					
10	171779.						
	.00	.00					
11	85613.						
	.00	.00					
12	62813.						
	.00	.00					
13	20500.						
	.00	.00					
14	126715.						
	.00	.00					
15	72933.						
	.00	.00					
16	99149.						
	.00	.00					
17	27498.						
	.00	.00					
18	179721.						
	.00	.00					
19	132283.						
	.00	.00					
20	148343.						
	.00	.00					
21	97629.						
	.00	.00					
22	20866.						
	.00	.00					

ESUB, NDT INVENTORY FILE

ESUB FACILITY	WETBAS EVALUE STATION	EVALUE STATION	EVALUE STATION	EVALUE STATION	EVALUE STATION	EVALUE STATION	STATION
1	5000.						
	.00	70.00					
2	5000.						
	5.50	92.00					
3	5000.						
	18.00	59.00					
4	5000.						
	21.50	83.00					
5	5000.						
	.00	18.00					

3.4 AIRCRAFT FILE AND DEMAND FORECAST

a. AIRCRAFT FILE

AIRCRAFT	CODE	MTOW WHEEL WHEEL	MLRW X-COORD Y-COORD	OEW	RANGE	MLG	WGT	PSI	FREQ	NWHEEL	
1	B747	710000.	564000.	353000.	LONG	.2336	.0584	185.0	1.2	16	
		.0	-44.0	.0	-44.0	106.0	150.0	106.0	150.0	-142.0	-186.0
		-142.0	-186.0	248.0	292.0	248.0	292.0				
		.0	.0	-58.0	-58.0	.0	.0	-58.0	-58.0	63.0	63.0
		121.0	121.0	63.0	63.0	121.0	121.0				
2	DC10/30	555000.	403000.	264000.	LONG	.3772	.0943	170.0	1.1	10	
		.0	-54.0	.0	-54.0	366.0	420.0	366.0	420.0	164.0	202.0
		.0	.0	64.0	64.0	.0	.0	64.0	64.0	2.0	2.0
3	DC10/10	430000.	364000.	235000.	LONG	.4700	.1175	170.0	1.1	8	
		.0	-54.0	.0	-54.0	366.0	420.0	366.0	420.0		
		.0	.0	64.0	64.0	.0	.0	64.0	64.0		
4	L1011	426000.	359000.	234000.	LONG	.4743	.1186	180.0	1.1	8	
		.0	-52.0	.0	-52.0	380.0	432.0	380.0	432.0		
		.0	.0	70.0	70.0	.0	.0	70.0	70.0		
5	DC8(B707)	355000.	258000.	159000.	LONG	.4808	.1202	185.0	1.4	8	
		.0	-32.0	.0	-32.0	218.0	250.0	218.0	250.0		
		.0	.0	55.0	55.0	.0	.0	55.0	55.0		
6	B720	210000.	168000.	128000.	MEDIUM	.4800	.1200	145.0	1.4	8	
		.0	-32.0	.0	-32.0	231.0	263.0	231.0	263.0		
		.0	.0	49.0	49.0	.0	.0	49.0	49.0		
7	B727-200	172000.	150000.	97000.	MEDIUM	.4618	.2309	170.0	1.6	4	
		.0	-34.0	191.0	225.0						
		.0	.0	.0	.0						
8	B727-100	150000.	132000.	95000.	MEDIUM	.4618	.2309	170.0	1.6	4	
		.0	-34.0	191.0	225.0						
		.0	.0	.0	.0						
9	DC9(B737)	100000.	86000.	65000.	SHORT	.4400	.2200	150.0	1.4	4	
		-26.0	.0	171.0	197.0						
		.0	.0	.0	.0						
10	F27	40000.	36000.	28000.	SHORT	.4200	.2100	110.0	1.5	4	
		.0	-17.5	265.5	283.0						
		.0	.0	.0	.0						

b. INPUT OF AIRCRAFT WEIGHTS

AIRCRAFT	TOW	LRW	TDW	XNZ	RADIUS TOW	RADIUS LRW	RADIUS TDW	FACTOR TOW	FACTOR LRW	FACTOR TDW	APY
1	615000.	507852.	761777.	44.0	7.8611	7.1435	8.7490	1.4713	1.4282	1.5248	.2289-02
2	515000.	383893.	575840.	54.0	9.5359	8.2331	10.0834	1.3215	1.2774	1.3401	.2638-02
4	400000.	341208.	511812.	52.0	9.1593	8.4594	10.3606	1.2516	1.2323	1.2847	.2711-02
5	300000.	230219.	345329.	32.0	7.8758	6.9002	8.4510	1.3246	1.2841	1.3484	.2211-02
7	170000.	148587.	222880.	34.0	8.5731	8.0150	9.8163	1.1686	1.1575	1.1935	.1284-02
9	106000.	89600.	134400.	26.0	7.0347	6.4676	7.9212	1.1750	1.1607	1.1975	.1036-02
10	40000.	36000.	54000.	17.5	4.9302	4.6772	5.7284	1.1603	1.1519	1.1869	.7895-03

c. ADM, AVERAGE DAILY MOVEMENT

ADM	ADMSUG NUMBER OF AIRCRAFT MOVEMENTS							
YEAR	B747	DC10/30	L1011	DC8(B707)	B727-200	DC9(B737)	F27	GA
1976	0.	0.	13.	19.	60.	55.	24.	37.
1977	0.	0.	18.	17.	64.	54.	24.	38.
1982	0.	1.	35.	17.	80.	49.	18.	44.
1987	1.	3.	51.	18.	98.	38.	10.	48.
1992	2.	4.	66.	18.	112.	25.	3.	50.
1997	4.	7.	83.	19.	117.	12.	0.	53.

3.5 AIRPORT TRAFFIC DISTRIBUTION

a. TYPE OF FACILITY

TYPE	FACILITY	FACILITY	FACILITY	FACILITY	FACILITY
1	RW	RUNWAY			
2	TW	TAXIWAY			
3	HP	APRON	GATE		

b. FACILITY, STATION AND TYPE

FACILITY	CODE	STA-FROM	STA-TO	TYPE
1	RW 1-19	.00	70.00	1
2	RW 10-28	5.50	92.00	1
3	TW 1-19	18.00	59.00	2
4	TW 10-28	21.50	83.00	2
5	HP/TW1	.00	18.00	3
6	HP/TW19	59.00	70.00	3
7	HP/TW28	5.50	21.50	3
8	HP/TW10	83.00	92.00	3
9	TW 5-23	.00	39.00	2
10	TW/X-HI	.00	.00	2
11	TW/X-LO	.00	.00	2
12	TW/Y-HI	.00	.00	2
13	TW/Y-LO	.00	.00	2
14	GATE/D-HI	.00	.00	3
15	GATE/D-LO	.00	.00	3
16	GATE/C-HI	.00	.00	3
17	GATE/C-LO	.00	.00	3
18	GATE/B-HI	.00	.00	3
19	GATE/B-LO	.00	.00	3
20	GATE/A-HI	.00	.00	3
21	GATE/A-LO	.00	.00	3
22	TW/GRID-Z	.00	.00	2

c. ATD, AIRPORT TRAFFIC DISTRIBUTION

ATD FACILITY	ATDSUG YEAR	TOW% LRW% TDW%	TOW% LRW% TDW%	TOW% LRW% TDW%	TOW% LRW% TDW%	TOW% LRW% TDW%	TOW% LRW% TDW%
	STATION	STATION	STATION	STATION	STATION	STATION	STATION
1	1976	40.0	80.0	40.0			
		20.0	20.0	20.0			
		10.0	.0	10.0			
	.00	25.00	45.00	70.00			
2	1976	18.0	20.0	2.0			
		80.0	80.0	80.0			
		5.0	.0	75.0			
	5.50	30.50	62.00	92.00			
3	1976	25.0	40.0				
		5.0	10.0				
	18.00	40.00	59.00				
4	1976	15.0	5.0				
		30.0	5.0				
	21.50	34.50	83.00				
5	1976	55.0	40.0				
		35.0	55.0				

3.6 MATERIAL FILE AND SYSTEM DEFAULT VALUES

a. SYSTEM DEFAULT VALUES

PAVEMENT	CODE	OVSFKL	OVSFSD	STRESS	FATIST	COVAR	A1	A2	D1	D2	COST-
1	LCF	1.0000	1.3333	.3800	.0920	.1500	10.0000	.0012	.6000	.6800	12.25
2	ASPHLT	1.1000	1.5000	.4000	.0860	.1200	8.0000	.0004	.4600	.6800	10.56
3	CONC	1.0000	1.3333	.4000	.0820	.1000	10.0000	.0014	.7800	.6800	7.29
4	LCFOV	1.0000	1.3333	.3800	.0920	.1500	10.0000	.0012	.6000	.6800	4.34
5	ASPHOV	1.1000	1.5000	.4000	.0860	.1200	8.0000	.0004	.4600	.6800	2.95
6	CONCOV	1.0000	1.3333	.4000	.0820	.1000	10.0000	.0014	.7800	.6800	1.56

b. DEFAULT SYSTEM FOR FAM

PAVEMENT	CODE	LAYER	THICKNESS	EVALUE	POISSON
1	1/LCF	1/ASTOP	3.0	300000.	.25
		2/LCFA	6.0	1000000.	.20
		3/LCFB	6.0	600000.	.20
		4/LCFC	9.0	400000.	.25
		5/SUB	INFI	7500.	.35
2	2/ASPHLT	1/ASTOP	4.0	300000.	.25
		11/ASBS	16.0	200000.	.25
		13/AGBS	6.0	20000.	.30
		5/SUB	INFI	7500.	.35
3	3/CONC	8/PCC	12.0	4000000.	.15
		10/CTB	6.0	200000.	.25
		14/SSBS	8.0	10000.	.35
		5/SUB	INFI	7500.	.35
4	4/LCFOV	1/ASTOP	3.0	300000.	.25
		2/LCFA	12.0	1000000.	.20
		6/PAV	INFI	40000.	.30
5	5/ASPHOV	1/ASTOP	2.0	300000.	.25
		11/ASBS	8.0	200000.	.25
		6/PAV	INFI	40000.	.30
6	6/CONCOV	7/PCCR	9.0	5000000.	.15
		1/ASTOP	1.0	300000.	.25
		6/PAV	INFI	40000.	.30

c. DEFAULT SYSTEM FOR PFL

PFLPAV	CODE	LAYER	THICKNESS	EVALUE	POISSON
1	1/LCF	15/PAVDF	4.0	100000.	.30
		6/PAV	INFI	40000.	.30
2	2/ASPHLT	15/PAVDF	4.0	100000.	.30
		6/PAV	INFI	40000.	.30
3	3/CONC	15/PAVDF	3.0	120000.	.30
		6/PAV	INFI	85000.	.30

d. PFLDI

.12	SMOOTH PAVEMENT SURFACE
.18	OPERATIONAL SURFACE
.25	UPPER LIMIT OF ROUGHNESS TOLERANCE
.30	MAJOR REHABILITATION REQUIRED

e. IDENTIFICATION OF KEEL AND SIDE

PAVEMENT NUMBER	KEEL	SIDE	SDFC
	4	4	.5
	5	5	.5
	6	6	.5
	1	5	.0
	3	5	.0
	1	1	.0
	2	2	.0
	3	3	.0

MWELP	PAVEMENT	PAVEMENT	PAVEMENT	PAVEMENT	PAVEMENT	PAVEMENT	PAVEMENT
	1	2	3	4	5	6	

f. NAVIGATION SYSTEM, DYNAMIC RESPONSE AND VELOCITY

BANDWIDTH	CODE1	CODE2	RW	TW	HP
1	NORM/VISUAL		40.0	16.0	16.0
2	LIGHTS/ILS		20.0	10.0	16.0

DI	RW	TW	HP
KEEL	.12	.12	.15
SIDE	.18	.18	.18

VEL	RW	TW	HP
KEEL	145.	50.	50.
SIDE	145.	50.	50.

3.7 COST FILE AND DEFAULT VALUES

a. COST FILE

COST	CODE	DOLLAR
1	PCBT	65.00
2	FIAGT	8.00
3	COAGT	9.50
4	ASCLT	70.00
5	HLBT	45.00
6	POZBT	15.00
7	SFST	3.50
8	RSWLB	1.00
9	LBBM	.25
10	CLHR	8.00
11	SLEHR	13.00

b. COMPONENT CHARACTERIZATION AND UNIT PRICE

LAYER	CODE	EVALUE	POISSON	UNIT-PRICE
1	ASTOP	300000.	.25	1.39
2	LCFA	1000000.	.20	.71
3	LCFB	600000.	.20	.58
4	LCFC	400000.	.25	.52
5	SUB	5000.	.35	.33
6	PAV	40000.	.30	.16
7	PCCR	5000000.	.15	2.52
8	PCC	4000000.	.15	1.68
9	RLC	2000000.	.15	1.22
10	CTB	200000.	.25	.71
11	ASBS	200000.	.25	1.29
12	ASTB	100000.	.30	.56
13	AGBS	20000.	.30	.78
14	SSBS	10000.	.35	.34
15	PAVDF	100000.	.30	.00

c. ICC PAVEMENT COMPONENTS AND DEFAULT VALUES

LAYER	PCBT	FIAGT	COAGT	ASCLT	HLBT	POZBT	SFST	RSWLB	LBBM	CLHR	SLEHR
1	.0000	.0235	.0500	.0051	.0000	.0000	.0000	.0000	.0000	.0112	.0217
2	.0007	.0000	.0200	.0000	.0020	.0067	.0374	.0000	.0000	.0027	.0102
3	.0006	.0000	.0064	.0000	.0016	.0074	.0460	.0000	.0000	.0027	.0088
4	.0005	.0000	.0000	.0000	.0013	.0073	.0516	.0000	.0000	.0027	.0088
5	.0000	.0000	.0000	.0000	.0000	.0000	.0000	.0000	.0000	.0048	.0222
6	.0000	.0000	.0000	.0000	.0000	.0000	.0000	.0000	.0000	.0024	.0111
7	.0102	.0181	.0433	.0000	.0000	.0000	.0000	.8440	.1430	.0321	.0127
8	.0102	.0181	.0433	.0000	.0000	.0000	.0000	.0000	.1430	.0321	.0127
9	.0051	.0181	.0433	.0000	.0000	.0000	.0000	.0000	.0000	.0139	.0171
10	.0051	.0000	.0000	.0000	.0000	.0000	.0596	.0000	.0000	.0036	.0110
11	.0000	.0235	.0500	.0037	.0000	.0000	.0000	.0000	.0000	.0112	.0217
12	.0000	.0000	.0000	.0025	.0000	.0000	.0593	.0000	.0000	.0042	.0110
13	.0000	.0000	.0704	.0000	.0000	.0000	.0000	.0000	.0000	.0016	.0074
14	.0000	.0000	.0000	.0000	.0000	.0000	.0651	.0000	.0000	.0016	.0074
15	.0000	.0000	.0000	.0000	.0000	.0000	.0000	.0000	.0000	.0000	.0000

3.8 EQUIVALENT AIRCRAFT OPERATION

a. APX FOR BANDWIDTH NORM/VISUAL

AIRCRAFT	RW			TW			HP		
	TOW	LRW	TDW	TOW	LRW	TDW	TOW	LRW	TDW
B747	.3781	.3436	.4208	.4329	.3934	.4818	.4329	.3934	.4818
DC10/30	.2730	.2357	.2887	.4655	.4019	.4923	.4655	.4019	.4923
L1011	.2362	.2182	.2672	.4557	.4208	.5154	.4557	.4208	.5154
DC8(B707)	.2281	.1998	.2448	.4696	.4114	.5039	.4696	.4114	.5039
B727-200	.1304	.1219	.1493	.2514	.2351	.2879	.2514	.2351	.2879
DC9(B737)	.1149	.1056	.1294	.2193	.2016	.2470	.2193	.2016	.2470
F27	.0691	.0655	.0803	.1616	.1533	.1878	.1616	.1533	.1878

APX FOR BANDWIDTH LIGHTS/ILS

AIRCRAFT	RW			TW			HP		
	TOW	LRW	TDW	TOW	LRW	TDW	TOW	LRW	TDW
B747	.3997	.3632	.4448	.5316	.4831	.5916	.4329	.3934	.4818
DC10/30	.4134	.3569	.4371	.5811	.5017	.6145	.4655	.4019	.4923
L1011	.4021	.3713	.4548	.5679	.5245	.6423	.4557	.4208	.5154
DC8(B707)	.3940	.3451	.4227	.6318	.5534	.6778	.4696	.4114	.5039
B727-200	.2121	.1983	.2429	.3335	.3118	.3819	.2514	.2351	.2879
DC9(B737)	.1818	.1671	.2047	.3088	.2839	.3477	.2193	.2016	.2470
F27	.1313	.1246	.1526	.2425	.2300	.2817	.1616	.1533	.1878

DESIGN	AIRCRAFT	WEIGHT
	7	170000.

MODEL PAVEMENT: CONC	PCC	12.0	4000000.	.15
	CTB	6.0	200000.	.25
	SSBS	8.0.	10000.	.35
	SUB	INFI	7500.	.35

AIRCRAFT	SURFACE DEFLECTION, WZ			STRESS AT LAYER: PCC		
	TOW	LRW	TDW	TOW	LRW	TDW
B747	.18243	.15130	.22493	397.2	335.2	479.8
DC10/30	.15235	.11461	.16985	437.7	339.8	481.4
L1011	.12653	.10857	.16067	415.2	362.3	511.4
DC8(B707)	.11627	.09008	.13318	395.8	313.3	448.1
B727-200	.07203	.06346	.09314	410.7	365.0	519.9
DC9(B737)	.04598	.03923	.05748	275.5	237.4	339.9
F27	.01580	.01419	.02123	117.0	106.7	152.2

MODEL PAVEMENT: ASPOV1	ASTOP	6.0	100000.	.30
	PAV	INFI	40000.	.30

AIRCRAFT	SURFACE DEFLECTION, WZ			STRESS AT LAYER: ASTOP		
	TOW	LRW	TDW	TOW	LRW	TDW
B747	.08028	.06908	.09494	47.5	50.8	41.7
DC10/30	.08153	.06555	.08851	34.8	43.1	30.7
L1011	.07699	.06865	.09210	40.2	44.8	30.9
DC8(B707)	.07069	.05795	.07862	47.5	51.7	43.9
B727-200	.06160	.05593	.07450	40.7	43.8	32.0
DC9(B737)	.04282	.03791	.05084	41.7	42.8	38.5
F27	.01988	.01837	.02473	30.1	29.2	31.7

MODEL PAVEMENT: ASPOV2	ASTOP	6.0	200000.	.30
	PAV	INFI	40000.	.30

AIRCRAFT	SURFACE DEFLECTION, WZ			STRESS AT LAYER: ASTOP		
	TOW	LRW	TDW	TOW	LRW	TDW
B747	.07178	.06099	.08605	135.6	133.4	135.1
DC10/30	.07323	.05771	.08010	125.6	127.5	123.2
L1011	.06837	.06024	.08314	135.3	136.0	130.4
DC8(B707)	.06228	.05004	.06998	136.3	132.4	136.5
B727-200	.05371	.04827	.06631	128.1	127.8	125.2
DC9(B737)	.03652	.03189	.04419	109.7	106.1	112.8
F27	.01616	.01480	.02064	66.6	63.4	75.1

c. ATM, AIRCRAFT TRAFFIC MOVEMENTS

FACILITY	SERVYR	FORECAST	STATION FROM-TO		B747	DC10/30	L1011	DC8(B707)	B727-200	DC9(B737)	F27	GA
RW 1-19	1	FAMSUG	0.- 25.	TOW:	.0000	.0000	.2263+04	.2628+04	.9052+04	.7957+04	.3504+04	.5475+04
				LRW:	.0000	.0000	.1131+04	.1314+04	.4526+04	.3978+04	.1752+04	.2737+04
				TDW:	.0000	.0000	.5657+03	.6570+03	.2263+04	.1989+04	.8760+03	.1369+04
RW 1-19	1	FAMSUG	25.- 45.	TOW:	.0000	.0000	.4526+04	.5256+04	.1810+05	.1591+05	.7008+04	.1095+05
				LRW:	.0000	.0000	.1131+04	.1314+04	.4526+04	.3978+04	.1752+04	.2737+04
				TDW:	.0000	.0000	.0000	.0000	.0000	.0000	.0000	.0000
RW 1-19	1	FAMSUG	45.- 70.	TOW:	.0000	.0000	.2263+04	.2628+04	.9052+04	.7957+04	.3504+04	.5475+04
				LRW:	.0000	.0000	.1131+04	.1314+04	.4526+04	.3978+04	.1752+04	.2737+04
				TDW:	.0000	.0000	.5657+03	.6570+03	.2263+04	.1989+04	.8760+03	.1369+04
RW 10-28	1	FAMSUG	5.- 30.	TOW:	.0000	.0000	.1018+04	.1183+04	.4073+04	.3581+04	.1577+04	.2464+04
				LRW:	.0000	.0000	.4526+04	.5256+04	.1810+05	.1591+05	.7008+04	.1095+05
				TDW:	.0000	.0000	.2829+03	.3285+03	.1131+04	.9946+03	.4380+03	.6844+03
RW 10-28	1	FAMSUG	30.- 62.	TOW:	.0000	.0000	.1131+04	.1314+04	.4526+04	.3978+04	.1752+04	.2737+04
				LRW:	.0000	.0000	.4526+04	.5256+04	.1810+05	.1591+05	.7008+04	.1095+05
				TDW:	.0000	.0000	.0000	.0000	.0000	.0000	.0000	.0000
RW 10-28	1	FAMSUG	62.- 92.	TOW:	.0000	.0000	.1131+03	.1314+03	.4526+03	.3978+03	.1752+03	.2737+03
				LRW:	.0000	.0000	.4526+04	.5256+04	.1810+05	.1591+05	.7008+04	.1095+05
				TDW:	.0000	.0000	.4243+04	.4927+04	.1697+05	.1492+05	.6570+04	.1027+05
TW 1-19	1	FAMSUG	18.- 40.	TOW:	.0000	.0000	.1414+04	.1642+04	.5657+04	.4973+04	.2190+04	.3422+04
				LRW:	.0000	.0000	.2829+03	.3285+03	.1131+04	.9946+03	.4380+03	.6844+03
TW 1-19	1	FAMSUG	40.- 59.	TOW:	.0000	.0000	.2263+04	.2628+04	.9052+04	.7957+04	.3504+04	.5475+04
				LRW:	.0000	.0000	.5657+03	.6570+03	.2263+04	.1989+04	.8760+03	.1369+04
TW 10-28	1	FAMSUG	21.- 34.	TOW:	.0000	.0000	.8486+03	.9855+03	.3394+04	.2984+04	.1314+04	.2053+04
				LRW:	.0000	.0000	.1697+04	.1971+04	.6789+04	.5968+04	.2628+04	.4106+04
TW 10-28	1	FAMSUG	34.- 83.	TOW:	.0000	.0000	.2829+03	.3285+03	.1131+04	.9946+03	.4380+03	.6844+03
				LRW:	.0000	.0000	.2829+03	.3285+03	.1131+04	.9946+03	.4380+03	.6844+03
HP/TW1	1	FAMSUG	0.- 12.	TOW:	.0000	.0000	.3112+04	.3613+04	.1245+05	.1094+05	.4818+04	.7528+04
				LRW:	.0000	.0000	.1980+04	.2299+04	.7920+04	.6962+04	.3066+04	.4791+04
HP/TW1	1	FAMSUG	12.- 18.	TOW:	.0000	.0000	.2263+04	.2628+04	.9052+04	.7957+04	.3504+04	.5475+04
				LRW:	.0000	.0000	.3112+04	.3613+04	.1245+05	.1094+05	.4818+04	.7528+04
HP/TW19	1	FAMSUG	59.- 70.	TOW:	.0000	.0000	.2263+04	.2628+04	.9052+04	.7957+04	.3504+04	.5475+04
				LRW:	.0000	.0000	.5657+03	.6570+03	.2263+04	.1989+04	.8760+03	.1369+04

d. Aircraft Movement - 20 Years

FACILITY	SERVYR	FORECAST	STATION FROM-TO		B747	DC10/30	L1011	DC8(B707)	B727-200	DC9(B737)	F27	GA
Rw 1-19	20	FAMSUG	0.- 25.	TOW:	.3650+04	.8395+04	.1478+06	.5183+05	.2778+06	.1058+06	.3139+05	.1369+06
				LRW:	.1825+04	.4197+04	.7391+05	.2591+05	.1389+06	.5292+05	.1569+05	.6844+05
				TDW:	.9125+03	.2099+04	.3696+05	.1296+05	.6944+05	.2646+05	.7847+04	.3422+05
Rw 1-19	20	FAMSUG	25.- 45.	TOW:	.7300+04	.1679+05	.2956+06	.1037+06	.5555+06	.2117+06	.6278+05	.2737+06
				LRW:	.1825+04	.4197+04	.7391+05	.2591+05	.1389+06	.5292+05	.1569+05	.6844+05
				TDW:	.0000	.0000	.0000	.0000	.0000	.0000	.0000	.0000
Rw 1-19	20	FAMSUG	45.- 70.	TOW:	.3650+04	.8395+04	.1478+06	.5183+05	.2778+06	.1058+06	.3139+05	.1369+06
				LRW:	.1825+04	.4197+04	.7391+05	.2591+05	.1389+06	.5292+05	.1569+05	.6844+05
				TDW:	.9125+03	.2099+04	.3696+05	.1296+05	.6944+05	.2646+05	.7847+04	.3422+05
Rw 10-28	20	FAMSUG	5.- 30.	TOW:	.1642+04	.3778+04	.6652+05	.2332+05	.1250+06	.4763+05	.1413+05	.6159+05
				LRW:	.7300+04	.1679+05	.2956+06	.1037+06	.5555+06	.2117+06	.6278+05	.2737+06
				TDW:	.4562+03	.1049+04	.1848+05	.6479+04	.3472+05	.1323+05	.3924+04	.1711+05
Rw 10-28	20	FAMSUG	30.- 62.	TOW:	.1825+04	.4197+04	.7391+05	.2591+05	.1389+06	.5292+05	.1569+05	.6844+05
				LRW:	.7300+04	.1679+05	.2956+06	.1037+06	.5555+06	.2117+06	.6278+05	.2737+06
				TDW:	.0000	.0000	.0000	.0000	.0000	.0000	.0000	.0000
Rw 10-28	20	FAMSUG	62.- 92.	TOW:	.1825+03	.4197+03	.7391+04	.2591+04	.1389+05	.5292+04	.1569+04	.6844+04
				LRW:	.7300+04	.1679+05	.2956+06	.1037+06	.5555+06	.2117+06	.6278+05	.2737+06
				TDW:	.6844+04	.1574+05	.2772+06	.9718+05	.5208+06	.1985+06	.5886+05	.2566+06
Tw 1-19	20	FAMSUG	18.- 40.	TOW:	.2281+04	.5247+04	.9239+05	.3239+05	.1736+06	.6616+05	.1962+05	.8555+05
				LRW:	.4562+03	.1049+04	.1848+05	.6479+04	.3472+05	.1323+05	.3924+04	.1711+05
Tw 1-19	20	FAMSUG	40.- 59.	TOW:	.3650+04	.8395+04	.1478+06	.5183+05	.2778+06	.1058+06	.3139+05	.1369+06
				LRW:	.9125+03	.2099+04	.3696+05	.1296+05	.6944+05	.2646+05	.7847+04	.3422+05
Tw 10-28	20	FAMSUG	21.- 34.	TOW:	.1369+04	.3148+04	.5543+05	.1944+05	.1042+06	.3969+05	.1177+05	.5133+05
				LRW:	.2737+04	.6296+04	.1109+06	.3887+05	.2083+06	.7939+05	.2354+05	.1027+06
Tw 10-28	20	FAMSUG	34.- 83.	TOW:	.4562+03	.1049+04	.1848+05	.6479+04	.3472+05	.1323+05	.3924+04	.1711+05
				LRW:	.4562+03	.1049+04	.1848+05	.6479+04	.3472+05	.1323+05	.3924+04	.1711+05
HP/TW1	20	FAMSUG	0.- 12.	TOW:	.5019+04	.1154+05	.2033+06	.7127+05	.3819+06	.1455+06	.4316+05	.1882+06
				LRW:	.3194+04	.7346+04	.1293+06	.4535+05	.2430+06	.9262+05	.2747+05	.1198+06
HP/TW1	20	FAMSUG	12.- 18.	TOW:	.3650+04	.8395+04	.1478+06	.5183+05	.2778+06	.1058+06	.3139+05	.1369+06
				LRW:	.5019+04	.1154+05	.2033+06	.7127+05	.3819+06	.1455+06	.4316+05	.1882+06
HP/TW19	20	FAMSUG	59.- 70.	TOW:	.3650+04	.8395+04	.1478+06	.5183+05	.2778+06	.1058+06	.3139+05	.1369+06
				LRW:	.9125+03	.2099+04	.3696+05	.1296+05	.6944+05	.2646+05	.7847+04	.3422+05

e. Equivalent Aircraft Operation

EQ. AIRCRAFT: B727-200 PAVEMENT: 5/ASPHOV FACILITY: RW 1-19
BANDWIDTH: NORM/VISUAL FORECAST: FAMSUG YEAR: 20

STATIONS 0. TO 25. LOCATION: KEEL

	DEFLECTION CRITERIA			AND			AAND	STRESS CRITERIA			ANS			AANS
	TOW	LRW	TDW	TOW	LRW	TDW		TOW	LRW	TDW	TOW	LRW	TDW	
B747	.257+01	.967+00	.465+01	.354+04	.606+03	.409+01		.361+00	.106+00	.129+01	.498+03	.662+02	.113+01	
DC10/30	.117+01	.212+00	.187+01	.267+04	.210+03	.298+01		.143+01	.285+00	.242+01	.329+04	.282+03	.387+01	
L1011	.596+00	.171+00	.321+01	.208+05	.275+04	.860+02		.287+01	.108+01	.106+02	.100+06	.175+05	.283+03	
DC8(B707)	.300+01	.532+00	.520+01	.355+05	.275+04	.365+02		.538+00	.882-01	.134+01	.636+04	.457+03	.938+01	
B727-200	.100+01	.365+00	.524+01	.362+05	.617+04	.698+02		.100+01	.409+00	.534+01	.362+05	.692+04	.711+02	
DC9(B737)	.109-01	.292-02	.137+00	.133+03	.163+02	.485+00		.237-01	.812-02	.110+00	.288+03	.454+02	.390+00	
F27	.459-06	.343-06	.184-03	.995-03	.353-03	.870-04		.871-04	.562-04	.348-03	.189+00	.578-01	.164-03	
				.989+05	.125+05	.200+03	.112+06				.147+06	.253+05	.369+03	.172+06

STATIONS 25. TO 45. LOCATION: KEEL

	DEFLECTION CRITERIA			AND			AAND	STRESS CRITERIA			ANS			AANS
	TOW	LRW	TDW	TOW	LRW	TDW		TOW	LRW	TDW	TOW	LRW	TDW	
B747	.281+01	.967+00	.000	.776+04	.606+03	.000		.361+00	.106+00	.129+01	.996+03	.662+02	.000	
DC10/30	.118+01	.212+00	.000	.542+04	.210+03	.000		.143+01	.285+00	.242+01	.657+04	.282+03	.000	
L1011	.576+00	.171+00	.000	.402+05	.275+04	.000		.287+01	.108+01	.106+02	.200+06	.175+05	.000	
DC8(B707)	.326+01	.532+00	.000	.771+05	.275+04	.000		.538+00	.882-01	.134+01	.127+05	.457+03	.000	
B727-200	.100+01	.365+00	.000	.724+05	.617+04	.000		.100+01	.409+00	.534+01	.724+05	.692+04	.000	
DC9(B737)	.783-02	.292-02	.000	.190+03	.163+02	.000		.237-01	.812-02	.110+00	.576+03	.454+02	.000	
F27	.123-06	.343-06	.000	.533-03	.353-03	.000		.871-04	.562-04	.348-03	.378+00	.578-01	.000	
				.203+06	.125+05	.000	.216+06				.294+06	.253+05	.000	.319+06

SUMMARY OF AIRCRAFT FORECAST AND FUNCTIONAL LIMITS

MODEL PAVEMENT FOR ANALYSIS: ASPOV2

ASTOP	6.0	200000.	.30
PAV	.0	40000.	.30
PAV	INFI	40000.	.30

EQUIVALENT AIRCRAFT OPERATION: B727-200
NAVIGATION: LIGHTS/ILS FORECAST: FAMSUG
LENGTH OF SERVICE PERFORMANCE: 20 YEARS

FACILITY	STATION FROM-TO	LOC	DI	VEL	E-SUP	AANS	AAND	DEFLECT. LIMIT	LAYER ASTOP STRESS LIMITS
RW 10-28	6.- 30.	KEEL	.12	145.	.688+05	.680+06	.117+06	.0420	77.1
RW 10-28	30.- 62.	KEEL	.12	145.	.688+05	.696+06	.123+06	.0419	76.9
RW 10-28	62.- 70.	KEEL	.12	145.	.688+05	.557+06	.675+05	.0434	78.2
RW 10-28	70.- 92.	KEEL	.12	145.	.355+05	.557+06	.675+05	.0536	78.2
RW 10-28	6.- 30.	SIDE	.18	145.	.688+05	.680+04	.122+04	.0776	134.2
RW 10-28	30.- 62.	SIDE	.18	145.	.688+05	.696+04	.129+04	.0772	134.0
RW 10-28	62.- 70.	SIDE	.18	145.	.688+05	.557+04	.705+03	.0819	135.6
RW 10-28	70.- 92.	SIDE	.18	145.	.355+05	.557+04	.705+03	.1012	135.6

MODEL PAVEMENT FOR ANALYSIS: CONC

PCC	12.0	4000000.	.15
CTB	6.0	200000.	.25
SSBS	8.0	10000.	.35
SUB	INFI	7500.	.35

EQUIVALENT AIRCRAFT OPERATION: B727-200
NAVIGATION: NORM/VISUAL FORECAST: FAMSUG
LENGTH OF SERVICE PERFORMANCE: 20 YEARS

FACILITY	STATION FROM-TO	LOC	DI	VEL	E-SUP	AANS	AAND	DEFLECT. LIMIT	LAYER STRESS LIMITS PCC	CTB	SSBS
TW 5-23	0.- 8.	KEEL	.12	50.	.500+04	.250+05	.282+06	.2036	411.0	91.9	20.6
TW 5-23	8.- 33.	KEEL	.12	50.	.500+04	.903+05	.147+07	.1872	381.6	85.3	19.1
TW 5-23	33.- 39.	KEEL	.12	50.	.500+04	.250+05	.282+06	.2036	411.0	91.9	20.6
TW 5-23	0.- 8.	SIDE	.18	50.	.500+04	.250+03	.342+04	.4117	653.6	146.1	32.7
TW 5-23	8.- 33.	SIDE	.18	50.	.500+04	.903+03	.181+05	.3628	616.4	137.8	30.8
TW 5-23	33.- 39.	SIDE	.18	50.	.500+04	.250+03	.342+04	.4117	653.6	146.1	32.7

3.10 PRESENT FUNCTIONAL LIFE

SUMMARY OF PRESENT FUNCTIONAL LIFE

DYNAMIC INCREMENT CAUSED BY AIRCRAFT MOVEMENT
OVER AND ABOVE PRESENT LEVEL OF SURFACE ROUGHNESS

.12 SMOOTH PAVEMENT SURFACE
.18 OPERATIONAL SURFACE
.25 UPPER LIMIT OF ROUGHNESS TOLERANCE
.30 MAJOR REHABILITATION REQUIRED

MODEL PAVEMENT FOR ANALYSIS: CONC PAVDF 3.0 120000. .30
PAV INFI 85000. .30

FACILITY	STATION FROM-TO	LOC	DI	VEL	E-SUP	AAND	ANDA	PFL
RW 1-19	0.- 9.	KEEL	.12	145.	.976+05	.435+04	.128+03	.03
RW 1-19	0.- 9.	KEEL	.18	145.	.976+05	.489+04	.151+05	3.++
RW 1-19	0.- 9.	KEEL	.25	145.	.976+05	.512+04	.280+07	3.++
RW 1-19	0.- 9.	KEEL	.30	145.	.976+05	.521+04	.101+09	3.++
RW 1-19	9.- 25.	KEEL	.12	145.	.754+05	.435+04	.710+02	.02
RW 1-19	9.- 25.	KEEL	.18	145.	.754+05	.489+04	.468+04	.96
RW 1-19	9.- 25.	KEEL	.25	145.	.754+05	.512+04	.461+06	3.++
RW 1-19	9.- 25.	KEEL	.30	145.	.754+05	.521+04	.107+08	3.++
RW 1-19	25.- 45.	KEEL	.12	145.	.754+05	.729+04	.710+02	.01
RW 1-19	25.- 45.	KEEL	.18	145.	.754+05	.825+04	.468+04	.57
RW 1-19	25.- 45.	KEEL	.25	145.	.754+05	.867+04	.461+06	3.++
RW 1-19	25.- 45.	KEEL	.30	145.	.754+05	.883+04	.107+08	3.++
RW 1-19	45.- 53.	KEEL	.12	145.	.754+05	.435+04	.710+02	.02
RW 1-19	45.- 53.	KEEL	.18	145.	.754+05	.489+04	.468+04	.96
RW 1-19	45.- 53.	KEEL	.25	145.	.754+05	.512+04	.461+06	3.++
RW 1-19	45.- 53.	KEEL	.30	145.	.754+05	.521+04	.107+08	3.++
RW 1-19	53.- 60.	KEEL	.12	145.	.156+06	.435+04	.463+03	.11
RW 1-19	53.- 60.	KEEL	.18	145.	.156+06	.489+04	.193+06	3.++
RW 1-19	53.- 60.	KEEL	.25	145.	.156+06	.512+04	.143+09	3.++
RW 1-19	53.- 60.	KEEL	.30	145.	.156+06	.521+04	.133+11	3.++
RW 1-19	60.- 70.	KEEL	.12	145.	.479+05	.435+04	.300+02	.01
RW 1-19	60.- 70.	KEEL	.18	145.	.479+05	.489+04	.846+03	.17
RW 1-19	60.- 70.	KEEL	.25	145.	.479+05	.512+04	.329+05	3.++
RW 1-19	60.- 70.	KEEL	.30	145.	.479+05	.521+04	.405+06	3.++
RW 10-28	5.- 30.	KEEL	.12	145.	.688+05	.787+04	.588+02	.01
RW 10-28	5.- 30.	KEEL	.18	145.	.688+05	.891+04	.322+04	.36
RW 10-28	5.- 30.	KEEL	.25	145.	.688+05	.935+04	.259+06	3.++
RW 10-28	5.- 30.	KEEL	.30	145.	.688+05	.953+04	.523+07	3.++
RW 10-28	30.- 62.	KEEL	.12	145.	.688+05	.801+04	.588+02	.01
RW 10-28	30.- 62.	KEEL	.18	145.	.688+05	.906+04	.322+04	.35
RW 10-28	30.- 62.	KEEL	.25	145.	.688+05	.952+04	.259+06	3.++
RW 10-28	30.- 62.	KEEL	.30	145.	.688+05	.970+04	.523+07	3.++
RW 10-28	62.- 66.	KEEL	.12	145.	.688+05	.677+04	.588+02	.01
RW 10-28	62.- 66.	KEEL	.18	145.	.688+05	.767+04	.322+04	.42
RW 10-28	62.- 66.	KEEL	.25	145.	.688+05	.807+04	.259+06	3.++
RW 10-28	62.- 66.	KEEL	.30	145.	.688+05	.822+04	.523+07	3.++
RW 10-28	66.- 92.	KEEL	.12	145.	.355+05	.677+04	.186+02	.00
RW 10-28	66.- 92.	KEEL	.18	145.	.355+05	.767+04	.330+03	.04
RW 10-28	66.- 92.	KEEL	.25	145.	.355+05	.807+04	.770+04	.96
RW 10-28	66.- 92.	KEEL	.30	145.	.355+05	.822+04	.668+05	3.++

3.11 THICKNESS DESIGN AND COST ANALYSIS

a. GRID SYSTEM FOR DESIGN CHARTS

PAVEMENT	LAYER	HMIN	HMAX	HSTEP
1	4/LCFC	4.0	22.0	3.0
2	2/ASBS	2.0	26.0	4.0
3	1/PCC	6.0	18.0	2.0
4	2/LCFA	4.0	16.0	3.0
5	2/ASBS	2.0	22.0	4.0
6	1/PCCR	6.0	14.0	2.0

NEW PAVEMENT ESUB GRID EVALUES

5000. 6000. 7500. 9000.

b. DESIGN CHART - STRESS CRITERIA

AIRCRAFT: B727-200 WEIGHT: 170000.

PAVEMENT: CONC

PCC	**	4000000.	.15
CTB	6.0	200000.	.25
SSBS	8.0	10000.	.35
SUB	INFI	**	.35

THICK./EVALUE

	5000.	6000.	7500.	9000.
6.0	.8877+03	.8596+03	.8265+03	.8006+03
8.0	.6948+03	.6734+03	.6484+03	.6288+03
10.0	.5480+03	.5309+03	.5111+03	.4959+03
12.0	.4423+03	.4275+03	.4107+03	.3980+03
14.0	.3660+03	.3527+03	.3378+03	.3266+03
16.0	.3098+03	.2977+03	.2840+03	.2739+03
18.0	.2672+03	.2561+03	.2436+03	.2342+03

c. DESIGN CHART - DEFLECTION CRITERIA

AIRCRAFT: B727-200 WEIGHT: 170000.

PAVEMENT: CONC

PCC	**	4000000.	.15
CTB	6.0	200000.	.25
SSBS	8.0	10000.	.35
SUB	INFI	**	.35

THICK./EVALUE

	5000.	6000.	7500.	9000.
6.0	.1390+00	.1212+00	.1027+00	.8997-01
8.0	.1211+00	.1051+00	.8868-01	.7738-01
10.0	.1068+00	.9406-01	.7895-01	.6861-01
12.0	.9968-01	.8807-01	.7203-01	.6239-01
14.0	.9236-01	.7980-01	.6675-01	.5774-01
16.0	.8597-01	.7446-01	.6239-01	.5400-01
18.0	.8016-01	.6964-01	.5855-01	.5077-01

d. SUMMARY OF PAVEMENT DESIGN AND COST ANALYSIS

UNIT PRICE OF PAVEMENT LAYERS, $/SY/IN: CONC

PCC	1.68
CTB	.71
SSBS	.34
SUB	.33

EQUIVALENT AIRCRAFT OPERATION: B727-200
NAVIGATION: NORM/VISUAL FORECAST: FAMSUG
LENGTH OF SERVICE PERFORMANCE: 20 YEARS

FACILITY	STATION	LOC	DI	VEL	E-SUP	ICC	AMC	PCV	LAYER THICKNESSES PCC	CTB	SSBS	SUB
TW 5-23	0.- 8.	KEEL	.12	50.	.500+04	28.79	.14	30.40	12.8	6.0	8.0	INFI
TW 5-23	8.- 33.	KEEL	.12	50.	.500+04	30.08	.14	31.72	13.6	6.0	8.0	INFI
TW 5-23	33.- 39.	KEEL	.12	50.	.500+04	28.79	.14	30.40	12.8	6.0	8.0	INFI
						AVERAGE		31.26				
TW 5-23	0.- 8.	SIDE	.18	50.	.500+04	21.65	.14	23.46	8.6	6.0	8.0	INFI
TW 5-23	8.- 33.	SIDE	.18	50.	.500+04	22.50	.15	24.53	9.1	6.0	8.0	INFI
TW 5-23	33.- 39.	SIDE	.18	50.	.500+04	21.65	.14	23.46	8.6	6.0	8.0	INFI
						AVERAGE		24.16				

UNIT PRICE OF PAVEMENT LAYERS, $/SY/IN: ASPOV2

ASTOP	1.39
PAV	.16

EQUIVALENT AIRCRAFT OPERATION: B727-200
NAVIGATION: LIGHTS/ILS FORECAST: FAMSUG
LENGTH OF SERVICE PERFORMANCE: 20 YEARS

FACILITY	STATION	LOC	DI	VEL	E-SUP	ICC	AMC	PCV	LAYER THICKNESSES ASTOP	PAV
RW 10-28	6.- 30.	KEEL	.12	145.	.688+05	3.54	.17	6.54	2.4	INFI
RW 10-28	30.- 62.	KEEL	.12	145.	.688+05	3.65	.17	6.64	2.5	INFI
RW 10-28	62.- 70.	KEEL	.12	145.	.688+05	2.39	.17	5.42	1.6	INFI
RW 10-28	70.- 92.	KEEL	.12	145.	.355+05	11.52	.17	14.22	8.2	INFI
						AVERAGE		8.44		
RW 10-28	6.- 30.	SIDE	.18	145.	.688+05	1.56	.19	5.10	1.0	INFI
RW 10-28	30.- 62.	SIDE	.18	145.	.688+05	1.56	.19	5.10	1.0	INFI
RW 10-28	62.- 70.	SIDE	.18	145.	.688+05	1.56	.19	5.07	1.0	INFI
RW 10-28	70.- 92.	SIDE	.18	145.	.355+05	1.56	.19	5.07	1.0	INFI
						AVERAGE		5.09		

FACILITY	DESIGN SERVICE YEARS	AIRPORT NAVIGATION SYSTEM	FORECAST AIRCRAFT MOVEMENT	EPAV	ESUB	PAVEMENT KEEL: SIDE:	WEIGHTED AVERAGE OF PRESENT CASH VALUE, $/SY LCFOV LCFOV	ASPHOV ASPHOV	CONCOV CONCOV	LCF ASPHOV	CONC ASPHOV	LCF LCF	ASPHLT ASPHLT	CONC CONC
Rw 1-19	20	NORM/VISUAL	FAMSUG	NDT	DRYBAS	:	11.75	9.11	24.18	13.23	19.77	16.54	37.06	27.31
Rw 1-19	20	NORM/VISUAL	FAMSUG	NDT	WETBAS	:	11.75	9.11	24.18	15.03	20.41	18.33	39.03	28.43
Rw 1-19	20	LIGHTS/ILS	FAMSUG	NDT	DRYBAS	:	11.80	9.16	24.31	12.16	17.05	16.33	34.50	26.85
Rw 1-19	20	LIGHTS/ILS	FAMSUG	NDT	WETBAS	:	11.80	9.16	24.31	13.69	17.54	17.86	37.83	27.93
Rw 10-28	20	NORM/VISUAL	FAMSUG	NDT	DRYBAS	:	12.77	10.80	25.37	13.04	19.36	16.35	36.73	26.64
Rw 10-28	20	NORM/VISUAL	FAMSUG	NDT	WETBAS	:	12.77	10.80	25.37	14.61	20.02	17.91	38.13	27.79
Rw 10-28	20	LIGHTS/ILS	FAMSUG	NDT	DRYBAS	:	12.84	10.75	25.46	11.99	16.75	16.17	34.03	26.21
Rw 10-28	20	LIGHTS/ILS	FAMSUG	NDT	WETBAS	:	12.84	10.75	25.46	13.33	17.22	17.50	36.54	27.29
Tw 1-19	20	NORM/VISUAL	FAMSUG	NDT	DRYBAS	:	12.46	8.24	25.23	15.04	24.04	17.09	32.14	28.77
Tw 10-28	20	NORM/VISUAL	FAMSUG	NDT	DRYBAS	:	11.70	8.66	23.66	14.48	22.96	16.50	30.60	27.30
HP/TW1	20	NORM/VISUAL	FAMSUG	NDT	DRYBAS	:	11.54	8.23	24.03	15.49	24.72	17.53	33.14	29.56
HP/TW19	20	NORM/VISUAL	FAMSUG	NDT	DRYBAS	:	12.36	8.20	25.35	15.31	24.49	17.35	32.70	29.27
HP/TW28	20	NORM/VISUAL	FAMSUG	NDT	DRYBAS	:	11.24	10.36	23.78	15.74	24.95	17.47	32.98	29.45
HP/TW10	20	NORM/VISUAL	FAMSUG	NDT	DRYBAS	:	12.42	8.06	24.85	14.41	22.94	16.50	30.60	27.30
Tw 5-23	20	NORM/VISUAL	FAMSUG	NDT	DRYBAS	:	15.14	19.94	29.34	16.12	24.81	16.73	31.20	27.88
Tw/X-HI	20	NORM/VISUAL	FAMSUG	NDT	DRYBAS	:	8.65	8.11	20.01	16.97	29.06	16.97	32.88	29.06
Tw/X-LO	20	NORM/VISUAL	FAMSUG	NDT	DRYBAS	:	11.48	8.11	23.08	16.97	29.06	16.97	32.88	29.06
Tw/Y-HI	20	NORM/VISUAL	FAMSUG	NDT	DRYBAS	:	13.76	8.20	27.35	17.96	30.93	17.96	34.84	30.93
Tw/Y-LO	20	NORM/VISUAL	FAMSUG	NDT	DRYBAS	:	17.96	26.00	33.67	17.96	30.93	17.96	34.84	30.93
GATE/D-HI	20	NORM/VISUAL	FAMSUG	NDT	DRYBAS	:	9.68	8.07	21.13	17.53	30.18	17.53	34.03	30.18
GATE/D-LO	20	NORM/VISUAL	FAMSUG	NDT	DRYBAS	:	12.69	8.07	25.37	17.53	30.18	17.53	34.03	30.18
GATE/C-HI	20	NORM/VISUAL	FAMSUG	NDT	DRYBAS	:	11.30	8.06	23.04	17.41	29.94	17.41	33.79	29.94
GATE/C-LO	20	NORM/VISUAL	FAMSUG	NDT	DRYBAS	:	15.98	22.12	31.13	17.41	29.94	17.41	33.79	29.94
GATE/B-HI	20	NORM/VISUAL	FAMSUG	NDT	DRYBAS	:	8.62	8.07	19.95	17.53	30.18	17.53	34.03	30.18
GATE/B-LO	20	NORM/VISUAL	FAMSUG	NDT	DRYBAS	:	9.20	8.07	20.68	17.53	30.18	17.53	34.03	30.18
GATE/A-HI	20	NORM/VISUAL	FAMSUG	NDT	DRYBAS	:	8.59	8.03	19.87	17.14	29.44	17.14	33.26	29.44
GATE/A-LO	20	NORM/VISUAL	FAMSUG	NDT	DRYBAS	:	11.10	8.03	22.62	17.14	29.44	17.14	33.26	29.44
Tw/GRID-Z	20	NORM/VISUAL	FAMSUG	NDT	DRYBAS	:	17.94	25.21	33.02	17.68	30.44	17.68	34.32	30.44

PART 4

RECOMMENDATION FOR FUTURE RESEARCH AND VALIDATION

4.1 MAJOR AREAS FOR FUTURE RESEARCH

Research into the NDT frequency sweep and functional pavement design methods is necessary to search for new approaches which are better and more reliable than those presently known.

NDT Theory The present data processing method assumes that multi-frequency spectral analysis can be applied to the response function whose damping characteristics are represented by a single degree of freedom system. A more exact mathematical model which can be used to express the dynamic response of a multi-frequency system is:

$$z_i = \Sigma \frac{c_n F_i}{k_n} \cdot \frac{1}{\sqrt{(1-(\omega_i/p_n)^2)^2 + (2\beta_n(\omega_i/p_n))^2}}$$

The combined spring constant k_o, under a static load will be:

$$\frac{1}{k_o} = \Sigma \cdot \frac{c_n}{k_n}$$

in which n = number of elastic layers in series,
i = NDT test counter,
c_n = coefficient of effective load distribution in the n-th layer,
p_n = fundamental frequency of the n-th layer,
β_n = structural damping coefficient of the n-th layer,
k_n = spring constant, reflecting E-value and thickness of the n-th layer,
k_o = spring constant of the entire layered system,
z_i = dynamic response measured at the i-th test,
F_i = double amplitude of force at the i-th test,
ω_i = forcing frequency at the i-th test.

There are 4 x n unknowns in this system. Valid solution will depend upon the number and quality of tests as well as the computer matrix operations.

Vibration-Smoothness Criteria Only one field test, conducted with the FAA's Convair 440 aircraft at JFK Airport, was used in this report for evaluating the transfer function between aircraft vibrations and longitudinal pavement waves. It would be desirable for the ATA, AIA, and airline pilots to cooperate in developing objective aircraft vibration criteria to be used for judging functional pavement performance. The following basic criteria should be considered in this research program:

(1) Dynamic acceleration of the flight deck and gear wheels should be monitored on separate instrument channels;
(2) Constant take-off or landing speeds should be managed during the test. Thus, the minimum length of a test runway should be 10,000 feet;
(3) B727-200 and DC-10/10 or L1011 are the most desirable commercial aircraft to be tested;
(4) The airport operator should measure three pavement surface profiles in the longitudinal wheel path at 25 foot intervals. A computer program developed by the contractor could be used to process the power spectral density of the surface configuration.

Progressive Deformation Actual field surveys should be conducted to determine the transfer function between longitudinal and transverse deformations. There are many factors involved in this transfer function, such as, regional conditions, construction practices, specification requirements, material variations, traffic distributions, etc.

Material Characterization When a refined and complex mathematical model such as the multi-wheel elastic layered system is used for pavement design analysis, rigid discipline should be exercised in the characterization of material properties. The default values are programmed for the convenience of early application of the complex design system. In the final stage of the design program, a standard material file should be established to characterize the physical properties by the: (1) linear stress-strain material ratio with respect to the tensile elongation, (2) tensile, compressive and fatigue strengths, (3) variability, (4) volumetric change and (5) time and temperature dependent properties. Reliable material characterization will assist the development of transfer functions between the progressive deformation and elastic deflection of pavement layers.

Computer Simulation The 1976 FAA study [17] confirms Article 2.3a's finding that the multi-layered system is a valid mathematical model for pavement design analysis. Further development of other basic mathematical models (i.e. finite element models) can be done through computer matrix operations. However, within the framework of the multi-layered system, simulation analysis can be performed to reduce dependence on default values.

4.2 VALIDATION PROGRAM OUTLINE

The concept of functional pavement design should reflect the user's requirements and the cost/benefits to airport management. The design procedure reported herein should be validated prior to its final adoption. Validation procedures are outlined below.

Implementation of the Computer Design Program The pavement design program developed by the contractor is on mag-tape and can be adopted to DOT computer center in Washington D.C., where program access would be restricted to AAP and ARD during the validation period. The center's graphic plotter would be utilized to supplement the pavement program by constructing the required design charts.

NDT and Pavement Evaluation Frequency sweep NDT have been conducted, or are in the planning stages at airports in many FAA regions except in the Rocky Mountains, New England and the northern Great Lake region It would be desirable to conduct validation tests at four airports in these regions. A well balanced geographic and climatic distribution of pavement evaluations would provide a diversified background for the research program.

Pavement Design Transition For successful transition from conventional pavement design and test methods to the functional design concept and frequency sweep NDT, special efforts should be devoted to (1) correlating NDT E-value and DSM(W) and (2) substituting computer oriented pavement design charts for the present design curves.

Technical Seminar The theoretical background and practical applications of the computer program should be disseminated at a series of technical seminars. Airport engineers, FAA staff, industry working groups, professional engineers, and academic researchers should be invited to participate in these seminars which would be held at airports conducting NDT validation studies.

Computer Process A group of seminar participants suggested by the contractor and approved by ARD/FAA should have a hand in the operation of the pavement computer program. They should be encouraged to (1) introduce actual input data, (2) reduce computer dependence on default values and (3) conduct independent research on NDT and the pavement concept.

Computer Operations Manual The ultimate goal of the validation program is the writing of an operation manual for users of the computer design program. It should be a simple booklet which will allow the average computer operator to appropriately input data. The manual should also assist airport engineers in formulating inputs according to their specific conditions, as well as in interpreting the computer outputs to be utilized in the final pavement design.

REFERENCES

1. N.C. Yang, "Design of Functional Pavements", McGraw Hill, 1972.
2. K. Terzaghi, "Theoretical Soil Mechanics", John Wiley, pp.447-454, 1947.
3. W. Heukelon and C.R. Foster, "Dynamic Testing of Pavements", Trans. ASCE, Vol.127, pp.425-457, 1962.
4. W. Heukelon and A.J.G. Klomp, "Dynamic Testing as a Means of Controlling Pavements during and after Construction", Proc., International Conference on Structural Design of Asphalt Pavement, pp.667-679, 1962.
5. L.W. Nijboer and c. van der Poel, "A Study of Vibration Phenomena in Asphalt Road Condition", Proc., AAPT, Vol.22, pp.197-331, 1953.
6. R. Jones, "A Vibration Method for Measuring the Thickness of Concrete Slabs in Situs", Concrete Research, Vol.7, No.20, p.97, 1955
7. Symposium on Vibration Testing of Roads and Runways, Amsterdam,1959.
8. J.L. Green and J.W. Hall, "Nondestructive Vibratory Testings of Airport Pavements", Vol.I, FAA RD-73-205-1, 1975.
9. R.A. Weiss, "Nondestructive Vibratory Testings of Airport Pavements", Vol.II, FAA RD-73-205-1, 1975.
10. J.R. Hall and F.E. Richard, "Dissipation of Elastic Wave Energy in Granular Soils", Jour., ASCE, Vol.89 SM6, pp.27-56, 1963.
11. V.J. McDonald and N.H. Newmark, "Aircraft Vibration Tests, LaGuardia Airport Runway Extension", unpublished Port of New York Authority report, 1964.
12. J.F. Shook and B.F. Kallas, "Factors Influencing Dynamic Modulus of Asphalt Concrete", Proc., AAPT, 1969.
13. FAA/NAFEC, "Pavement Evaluation Analysis", Atlantic City, N.J., Berger Assoc., 1971.
14. V.A. HoSang, "Field Survey and Analysis of Aircraft Distribution on Airport Pavements", FAA RD-74-36, 1975.
15. G.P. Vittas, "A User's Viewpoint on Airport Design Standards, Past, Present and Future", Symposium on Nondestructive Test, Waterways Experiment Station, pp.23-50, 1976.
16. A.S. Vesic and L. Domaschuk, "Theoretical Analysis of Structural Behavior of Road Test Flexible Pavements", NCHR 10, Highway Research Board, 1964.
17. J.E. Crawford, J.S. Hopkins and J. Smith, "Theoretical Relationships between Moduli for Soil Layers beneath Concrete Pavements", FAA-RD-75-140, 1976.

APPENDIX A

VIBRATION OF CIRCULAR PLATE ON ELASTIC SOIL

Daniele Veneziano, Prof., M.I.T.

Most of the available theoretical results are for circular footings on (homogeneous, linear) elastic half space, under stationary vibration. Extentions include the vibration of footings on a linear elastic stratum of finite depth, and a few results for footings on a multi-layered (typically, 2 or 3 layer) soil systems. A brief review of the basic results is given below, and a method is proposed for the estimation of the elastic soil moduli from nondestructive dynamic tests. Such method, which is based purely on the dynamic properties of plate-soil systems, might have some value in future research.

Circular Plate on Elastic Half Space Consider a body of mass m and circular contact area with an elastic half space. The problem considered here is to relate the stationary vertical displacement w(t) of the body to the intensity and frequency of the vertical periodic force P(t) applied to it. In the analysis, the half space is assumed to have zero material damping.

With reference to Figure 1, the equation of motion for the particles in the contact area is:

$$m\ddot{w} + Q = P \tag{1}$$

where $P = P(t) = P_o e^{i\omega t}$ is the applied force (positive if downward), a periodic function of time,
$Q = Q(t) = Q_o e^{i\omega t}$ is the force (positive if compressive) between the plate and the surface of the elastic half space.

Following Reissner [1] (who first developed the theory) or Quinlan [2], or Sung [3], the stationary relationship between ω and Q_o is:

$$\omega(t) = \frac{Q_o e^{i\omega t}}{Ga} (f_1 - if_2) \tag{2}$$

in which $G = \frac{E}{2(1-\mu)}$ = Shear modulus,
a = radius of the circular area of loading,
f_1, f_2 = "Reissner displacement functions",
$i^2 = -1$

f_1 and f_2 are complicated functions of:

- the dimensionless frequency $a_o = \omega R/C_s = \omega R\sqrt{\rho/G}$,
- Poisson's ratio, μ,
- the stress distribution over the loaded area.

In the expression for a_o, $C_s = \sqrt{\rho/G}$ is the shear wave velocity, and ρ is the mass density of the elastic medium.

Equivalently, Equation (2) can be written as:

$$\omega(t) = \frac{Q_o(1-\mu)}{4Ga} \cdot \left[\frac{4}{1-\mu}\sqrt{f_1^2 + f_2^2}\right] \cdot e^{(\omega t-\alpha)} \qquad (3)$$

in which the first term is the displacement of the elastic surface under the static load Q_o; the second term accounts for the dependence of the amplitude of the response on the forcing frequency; and the third term indicates that the displacement $\omega(t)$ "follows" the load $Q(t)$ with a phase lag $\alpha = f_1/f_2$.

For $\omega \to 0$ (static load) one finds $f_2 \to 0$ and $f_1 \to (1-\mu)/4$ so that in this case, Equation (3) yields:

$$\omega = \frac{Q_o(1-\mu)}{4Ga} = \text{the static displacement.}$$

If Equation (1) is solved for Q and the result is substituted into Equation (2) or (3), one finds the relationship between the external force P and the displacement ω. This relationship involves Reissner's "mass ratio":

$$b = \frac{m}{Pa^3} \qquad (4)$$

and reads:

$$\omega(t) = \frac{P(t)}{Ga} \cdot \frac{f_1 - if_2}{(1-a_o^2 bf_1) + ia_o^2 bf_2}$$

$$= \frac{P_o(1-\mu)}{4Ga} \cdot \frac{4}{1-\mu}\sqrt{\frac{f_1^2 + f_2^2}{(1-a_o^2 bf_1)^2 + (a_o^2 bf_2)^2}} \cdot e^{i(\omega t-\alpha)} \qquad (5)$$

Again, the three terms in Equation (5) have the meaning of static displacement (first term), dynamic amplification factor (second term), and phase lag (α) of the response (third term).

For the case when the vertical load $P = P_o e^{i\omega t}$ is provided by a

mass m_e (or two masses $m_1=m_e/2$, as in Figure 1) rotating with eccentricity e, the maximum force P_o is given by:

$$P_o = m_e \cdot e \cdot \omega^2 \tag{6}$$

The main problem in actually calculating the displacement $\omega(t)$ in Equation (5) is to find the functions f_1 and f_2. As indicated previously, these functions depend on the stress distribution over the loading area. Common approximations assume that the stress distribution on the circular contact zone is uniform, or parabolic (with the radius), or that it is the same as for a rigid base under static load conditions (Reissner [1], Barkan [4], Sung [3], Quinlan [2], Bycroft [5]). Different displacements are found under different stress distribution assumptions: for the case when b=5 and μ=1/4, the amplitude-frequency response curves at the center of the circular plate are shown in Figure 2 (after Richart and Whitman [6]). The effect of changing the stress distribution is due mainly to the change in the static spring constant:

$$k_v = \frac{kGa}{1-\mu} \tag{7}$$

in which k is a constant factor with values: 4 for the rigid-base stress distribution, π for uniform stress, and $3\pi/4$ for parabolic stress variation. The amplitude of the response increases with the assumed relative stress at the center of the plate.

The curves in Figure 3 show the effect of changing the Poisson ratio while keeping b constant (b=5), under the assumption of rigid-plate stress distribution.

An interesting aspect of the curves in Figure 2 is that they have the same general shape as the frequency-response curves of simple mechanical oscillators, a fact which has motivated using viscous elastic oscillators as dynamic equivalents of elastic half spaces (see below). The same curves show that even for zero material damping, there is enough geometrical (radiation) damping to make the response amplitude finite at all frequencies. The damping effect increases with decreasing b, as shown in Figure 4. For b=0 (no mass on the surface) there is no peak in the response amplification curve. The (normalized) peak displacement, ω_{max} is shown in Figure 5 as a function of b, for μ=1/4. In Figure 5, the results by Barkan [4], Sung [3], and Bycroft [5] are approximate (they correspond to different assumption about the stress distribution over the contact area), while those by Awojohi and Robertson were obtained by solving the exact problem with a rigid plate. The difference between the "exact" solutions is due to differences in the numerical methods used in evaluating the integrals. When compared with these solutions, the results from Sung's theory are found to be very accurate and slightly conservative.

All the theories (approximate and "exact") give values of the resonant frequency which are practically identical.

A different approach was followed by Lysmer [8], who divided the circular contact area into concentric rings and assumed a constant (but unknown) stress level at all the points of the same ring. The stresses in each ring were then found by Lysmer by imposing the condition that the average displacement of all the rings to be equal at any given time. This approach has allowed Lysmer to extend the calculation of f_1 and f_2 beyond the range of a_o ($a_o < 1.5$) over which it had been possible to calculate the same functions from earlier approximations.

Equivalent Simple Oscillators Equations (1) and (2) can be manipulated to give:

$$m\ddot{w} + c_v x_2 \dot{w} + k_v x_1 w = P \qquad (8)$$

in which $k_v = \frac{4Ga}{1-\mu}$ = static spring constant

$$c_v = \frac{4}{1-\mu}\sqrt{G\rho} \cdot a^2$$

$$x_1 = \frac{1-\mu}{4} \frac{f_1}{f_1^2 + f_2^2}$$

$$x_2 = \frac{1-\mu}{4} \frac{f_2/a_o}{f_1^2 + f_2^2}$$

While k_v and c_v do not depend on the frequency, x_1 and x_2 do, as shown by the plots in Figure 6 (for Lysmer's theory and $\mu=1/3$). The dependence of x_1 and x_2 on ω makes the "effective stiffness" and the "effective damping" of the elastic half space also depend on ω. However, when approximating the actual physical system by a one degree of freedom (ODOF) system, the parameters are fixed at appropriate values, which are then left constant over the entire spectrum of input frequencies. The cirteria for selecting the parameters of a ODOF system are not unique. In general, one tries to reproduce both the resonant frequency and the resonant amplitude. At the same time, one tries to produce accurate approximations in the high frequency range (this suggests taking m to be the mass of the vibrator) and in the low frequency range (this suggests taking $x_1=1$ in Equation 8). Then, only the damping ratio remains to be chosen and is generally impossible to match exactly both the resonant frequency and the resonant amplitude. Lysmer suggested taking $x_2=0.85$. From Figure 6 it is clear that this choice produces ODOF systems which give very good approximations for small frequencies (say, for $a_o < 1.0$). Corresponding to this choice of x_2 the damping ratio of the ODOF system is:

$$\beta_v = \frac{0.85\ c_v}{2\sqrt{k_v m}} = \frac{0.85}{\sqrt{b(1-\mu)}} \tag{9}$$

β_v is quite sensitive to the mass ratio b.

A comparison between the amplitudes of the half space response and the ODOF response (with mass m, stiffness k_v, and damping ratio β_v) is shown in Figure 7. The agreement is quite good.

One can also compare the resonant frequencies of the two systems. This is done in Figure 8, where Sung's theory with μ=1/4 is used for the elastic half space. The accuracy of the ODOF increases with the mass ratio, and in general, is quite good. The frequency normalization constant ω_v is the undamped natural frequency for the ODOF system, i.e.:

$$\omega_v = k_v/m \tag{10}$$

The discrepancy between the curves in Figure 8 comes primarily from assuming x_1=1 for the ODOF system. The choice of the mass and/or of the stiffness of the ODOF system in order to improve the agreement between the resonant frequencies has been discussed, among others, by Hseih [9]. However, for large b (this is the case with typical dynamic pavement tests) the parameter values given above provide approximations which are accurate enough for all practical purposes.

Estimation of the Shear Modulus G The theory of circular footings on elastic half space which was reviewed in the last two sections allows one to calculate the resonant frequency and resonant amplitude as functions of the parameters of the soil (shear modulus G, Poisson's ratio μ, mass density ρ), of the footing and machinery (mass m) and of the input (rotating mass m_e, eccentricity e, and frequency ω).

Actually, the soil properties on which the resonant amplitude ω_{max} depends are ρ and μ; i.e., ω_{max} does not depend on G. As a consequence, G cannot be found from the experimental value of the resonant amplitude alone.

On the contrary, the resonant frequency ω_n depends on all three soil parameters ρ, μ and G. Relationships between the dimensionless frequency a_o at resonance:

$$a_o = \omega_n\ a\sqrt{\rho/G} \tag{11}$$

and the mass ratio b are shown in Figure 9 for μ=0, 1/2, 1/4 (the results are for Sung's theory). From curves like these one can estimate G as follows. Given b for a specific experiment and given the Poisson ratio μ, one can find a_o from Figure 9. Then one calculates

G from a given ω_n and (solve Equation 11 for G):

$$G = \frac{\omega_n^2 a^2 \rho}{a_o} \tag{12}$$

This estimation procedure was used by Whitman [10] and is illustrated next through a numerical example.

Example The amplitude-frequency curves in Figure 10 were obtained by Fry [11] using circular footings on a homogeneous subsoil. The soil had a unit weight γ=117 pcf and a Poisson's ratio μ=0.35. The total weight of the footing and vibratory machine is 30,970 pounds and the radius of the footing is a=31 inches.

Each curve in Figure 10 is for a given eccentricity. Eccentricities and peak amplitude frequencies (from the smoothed curves) are given in the table below.

TABLE 1 MAX. AMPLITUDE FREQUENCY

Eccentricity in.	Max. amplitude frequency, f_R cps
0.105	21.7
0.209	20.2
0.314	19.2
0.418	18.5

The mass ratio, $b=\frac{m}{\rho a^3}$ = 15.35 corresponds to a dimensionless frequency a_o=0.67 (use plots in Figure 6 with μ=0.35). The following estimates of G are then obtained from Equation (12).

TABLE 2 ESTIMATE OF SHEAR MODULUS

Eccentricity in.	Estimate of G, from Eq. (12) psi
0.105	6980
0.209	6068
0.314	5464
0.418	5073

Note the nonlinearity in the force-deformation behavior of the soil, which reduces the modulus at higher strain levels (for the same site, the value G=5340 psi was suggested by Richart et al. [12], p. 354).

In pavement tests of the type conducted by Yang, the mass ratio

b, is generally very large and the ODOF model with $k_v = \frac{4Ga}{1-\mu}$, m = total mass of footing and vibrator, and small damping, is quite accurate. In this case, one might use ω_v in Equation (10) as an approximation to the frequency of maximum response amplitude and estimate G from:

$$G = \frac{\omega_v^2 m(1-\mu)}{4a} \tag{13}$$

where ω_v is the resonant frequency from the test.

Using Equation (13) in the previous example ($\omega_v = f_v \cdot 2\pi$ is given in Table 1), the following values of the shear modulus are found:

TABLE 3 ANOTHER ESTIMATE OF SHEAR MODULUS

Eccentricity in.	G, from Eq. (13) psi
0.105	7818
0.209	6776
0.314	61??
0.418	5682

Note the approximation by Fry [11] improves with large b values (e.g. with decreasing dimension of the vibrator footing).

The methods proposed above contain a few elements of uncertainty, which express the degree to which the elastic half space and the ODOF models are accurate in representing the actual physical system. The main sources of error are: (1) the "effective mass of the soil" which should be added to the mass of the vibrator and footing in the ODOF model, and (2) the material damping of the soil, which was neglected. Both approximations (neglecting the mass and the damping of the soil) make the measured resonant frequency smaller than the undamped natural frequency, Equation (10). In the approximation by Hsieh [14], it was assumed in addition, that the frequency ratio plotted in Figure 8 is 1. The nonlinearity of the force-deformation relationship have also effects of some importance (see Lorenz [13] and Alpan [14]).

REFERENCES

1. Reissner, E., "Stationare, axial symmetrishe durch eine shuttelude Masse erregte Schwingungen eines homogenen elastischen Halbraumes," Ingenieur - Archiv, 7, Pt. 6, pp. 381-396, 1936.

2. Quinlan, P.M., "The Elastic Theory of Soil Dynamics," ASTM STP No. 156, pp. 3-34, 1953.

3. Sung, T.Y., "Vibrations in Semi-Infinite Solids Due to Periodic Surface Loadings," ASTM STP No. 156, pp. 35-68, 1953.

4. Barkan, D.D., "Dynamics of Bases and Foundations", translated from Russian, McGraw-Hill, New York, 1962.

5. Bycroft, G.N., "Forced Vibrations of a Rigid Circular Plate on a Semi-Infinite Elastic Space and on an Elastic Stratum," Phil. Trans., Series A, 248, pp. 327-368, 1956.

6. Richart, F.E. Jr. and Whitman, R.V., "Comparison of Footing Vibration Tests with Theory," ASCE Journal, Vol. 93, No. SM 6, November 1967, pp. 143-168.

7. Richart, F.E. Jr., "Foundation Vibration," ASCE Trans. Vol. 127, pp. 863-898, 1962.

8. Lysmer, J., "Vertical Motion of Rigid Footings," a PhD dissertation, University of Michigan, August 1965.

9. Hsieh, T.K., "Foundation Vibrations," ICE Proc. Vol. 22, pp. 211-226, 1962.

10. Whitman, R.V., "Analysis of Foundation Vibrations"

11. Fry, Z.B., "Development and Evaluation of Soil Bearing Capacity, Foundations and Structures," WES Tech. Rep. No. 3-632, July 1963.

12. Richart, F.E. Jr., Hall, J.R. Jr., and Woods, R.D., "Vibrations of Soils and Foundations," Prentice-Hall, New Jersey, 1970.

13. Lorenz, H., "Elasticity and Damping Effects of Oscillating Bodies on Soil," ASTM STP No. 156, pp. 113-123, 1953.

14. Alpan, I., "Machine Foundations and Soil Resonance," Geotechnique, Vol. XI, pp. 95-113, 1961.

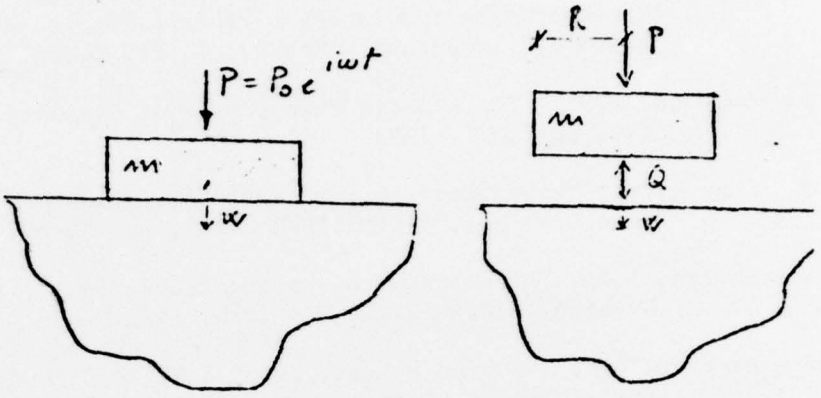

Fig. 1 Circular Footing on Elastic Half Space

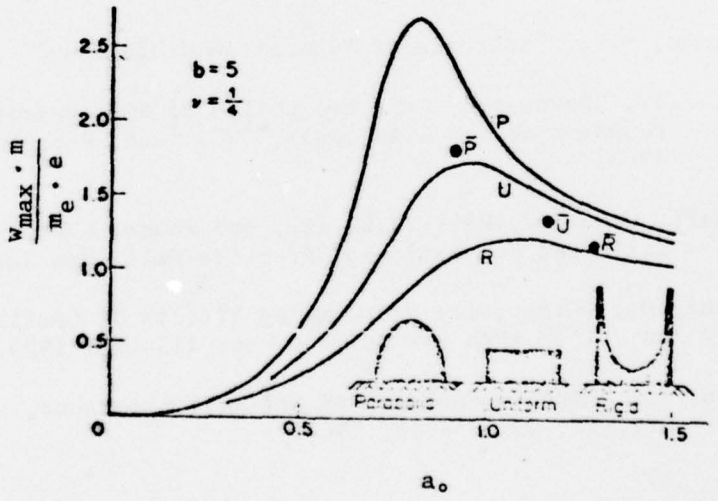

Fig. 2 Effect of Pressure Distribution on Theoretical Response Curves for Vertical Footing Motion, after Richart and Whitman

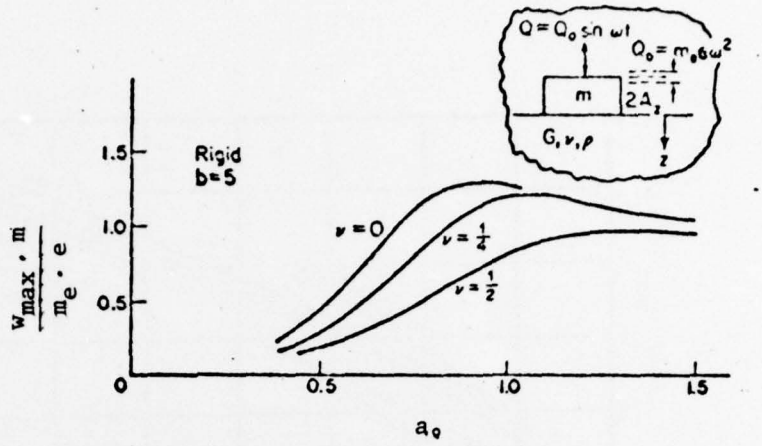

Fig. 3 Effect of Poisson's Ratio on Theoretical Response Curves for Vertical Footing Motion, Rigid Base St Stress Distribution, after Richart and Whitman

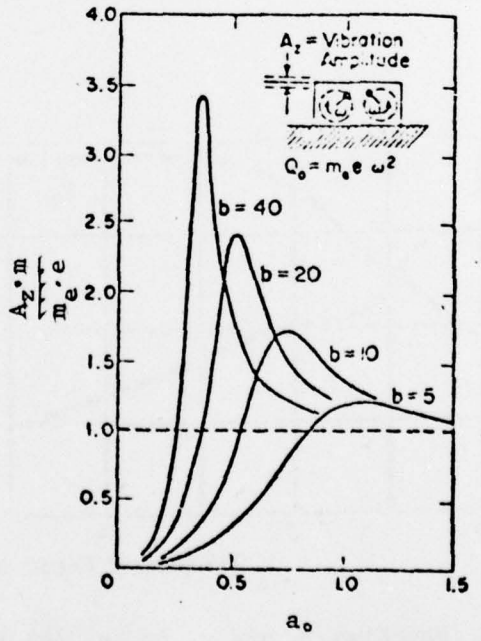

Fig. 4 Amplitude versus Frequency, $\mu = 1/4$ after Richart

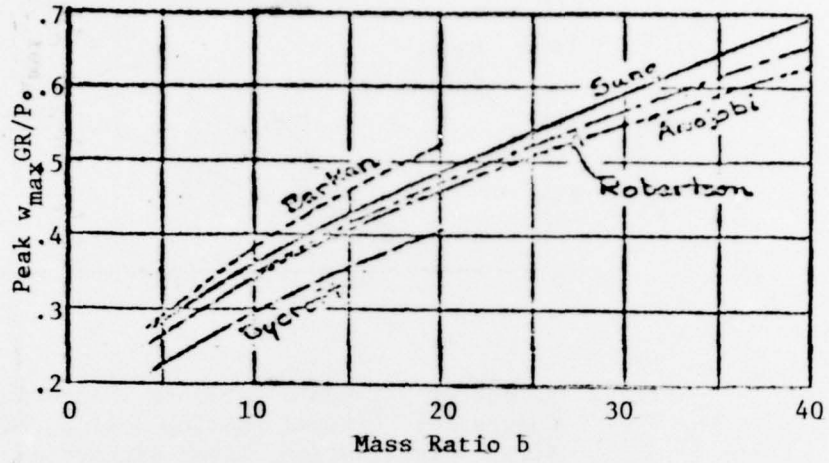

Fig. 5 Resonant Displacement by Several Theories, Whitman Personal Communication

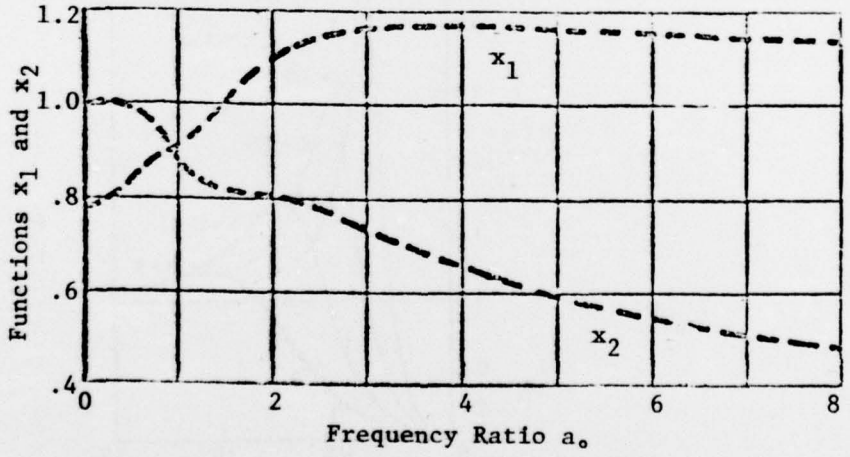

Fig. 6 Function x_1 and x_2 in Eq. (8) for Poisson's Ratio = 1/3 and Lysmer's Theory, Whitman Personal Communication

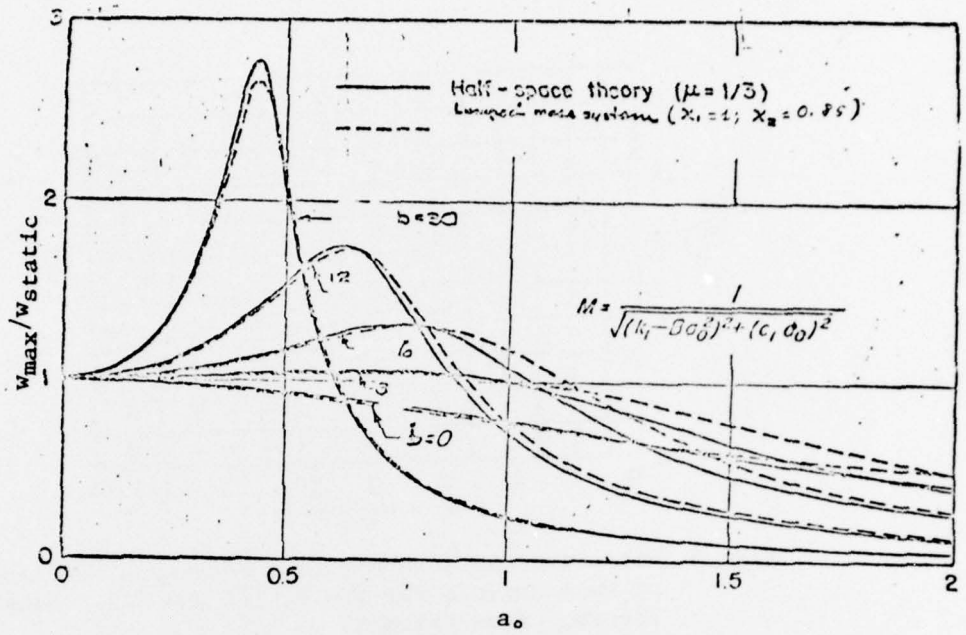

Fig. 7 Comparison of Response Curves for Half Space, Lysmer's Theory, and for Equivalent 1-dof System

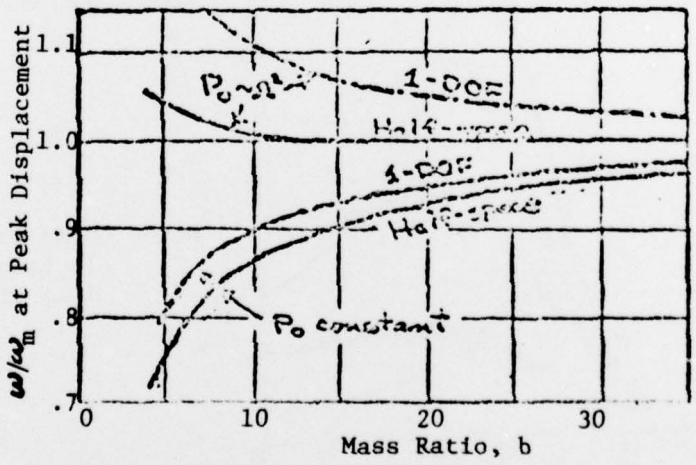

Fig. 8 Comparison of Damped Resonant Frequencies, Sung"s Theory, $\mu = 1/4$.

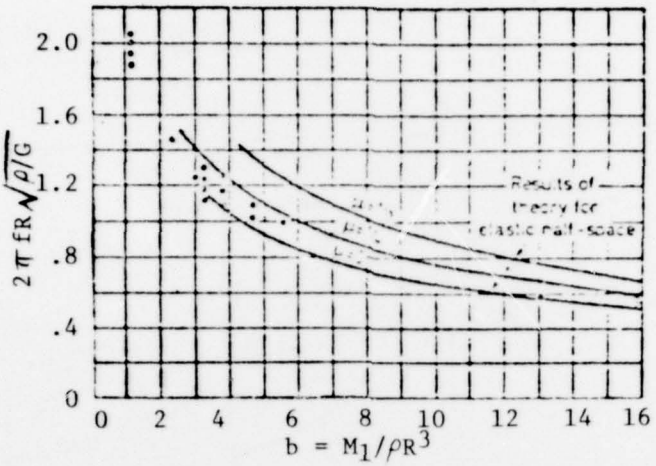

Fig. 9 Dimensionless Resonant Frequency as a Function of Mass Ratio b for $\mu = 0$, 1/4 and 1/2. Sung's Theory, after Whitman

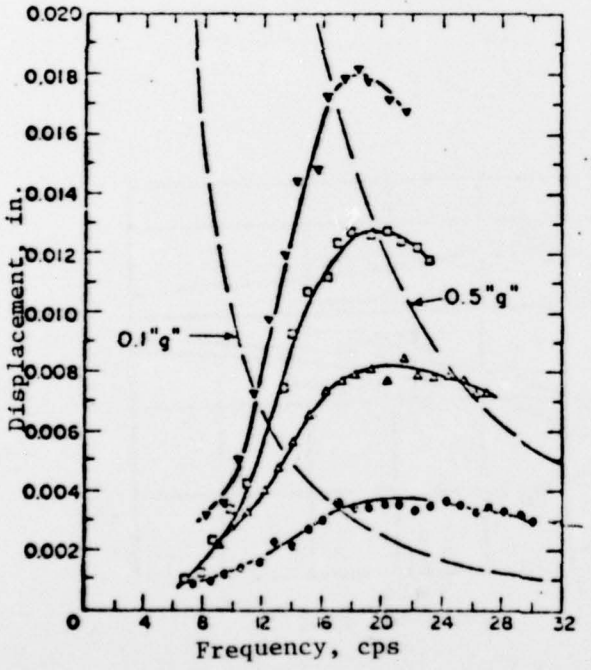

Legend

Symbol	Run No.	ECC Setting
●	6	.105"
△	7	.209"
□	8	.314"
▼	9	.418"

Note: 6655 lb ballast, 30970 lb total weight including vibrator.

Fig, 10 Amplitude-Frequency Curves from Tests on Model Footing after Fry.

APPENDIX B

A VIEW OF THE DEVELOPMENT OF THEORETICAL FRAMEWORK FOR NDT ANALYSIS

By William H. Walker, Prof., UICU.

The objective in this report is to set forth a view of the development of a theoretical framework for the analysis of NDT of forced vibration tests of airport pavements. Dynamic tests are faster, less disruptive to operation and less expensive than plate bearing tests, but to be useful they must be interpreted to yield information on stiffness of modulus which correlates well with plate bearing tests.

A dynamic test run at a single, unvaried frequency set without reference to the site conditions, the effect of geometry, layering, pavement thickness, subgrade properties, etc., i.e. the probable spectrum of response, would have problems unsolved. Although, once a spectrum of response has been established, then additional tests, say at various force levels could be run for a smaller number of selected frequencies. However, if a suitably automated testing apparatus is available to provide a sweep of test frequencies, then a more effective approach is to run a family of spectra at selected load levels. When tests are conducted with the spectrum approach, the task remains to reduce the data in a form which can be statistically correlated with the static properties of the pavement system.

The data processing equation 1.17, presented in the report is in essence a numerical method for weighing the displacement force relationship at the test frequencies. The contribution of the test data points varies inversely with the frequency. This reduction in the effect of the higher frequency components is consistent with the reduction in the terms in a Fourier representation of a function which is continuous to the second order, i.e., with terms of the form A/n where n is the frequency number.

The effect of the use of equation 1.17, which is based in equation 1.13, is to compare the shape or more exactly a measure of the shape of the spectrum within the range of the test frequencies with X(u). The correction equation 1.21, for the tail of the spectrum is probably not essential since the test data are also truncated. Also, it should be noted that the evaluation of the X(u)/u integral from u=1 to infinity is approximate for use in comparisons with measurements since the point u=1 is not known and must be deduced from the field results as the point of the apparent first peak in the response spectrum, i.e., it is more closely related to the quantity $u_{max} = (1-2\beta^2)^{\frac{1}{2}}$, the location of the peak in X(u). See attached Fig. B.1. The shift in location of the spectrum peak and also the change in the amplitude at u=1 become more important as the effective damping increases, both structural damping and damping associated with geometric dispersion. These comments all apply to a single-degree-of-freedom system model and do not reflect the important differences in shape of the more typical response spectrum including multiple peaks.

The approach of equation 1.17 is considered to be heuristic. Further studies are needed before a unified theoretical basis can be established. However, the present results of the application of equation 1.17 are encouraging, independent of the theoretical framework on which the method is based. Similar comparisons should be made to relate equation 1.17 to response spectra calculated for simple layered systems, the elastic half-space and selected multi-degree-of-freedom models.

The investigation of a simple two degree-of-freedom model with damping and a continuous shear beam model can be implemented readily. These studies will provide useful information on effective damping, the influence of multiple peaks in the spectrum, and a direct comparison of equation 1.17 and the theoretical static stiffness of the various models.

In summary, work on the NDT data reduction method could proceed along two lines: (1) Additional field tests for validation to broaden the statistical basis. This should be combined with continued studies of available data. (2) A parallel study to apply equation 1.17 to selected response spectra for simple models of the pavement system for which the static response is readily determined as a function of the parameters of the model.

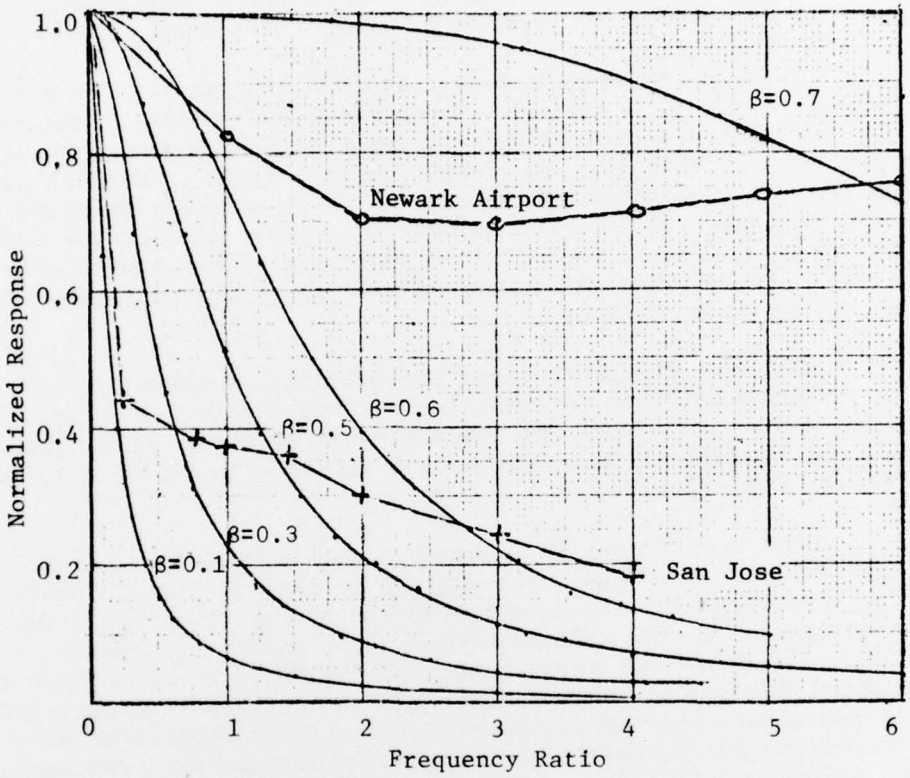

Fig. B.1 Normalized Response Function

APPENDIX C

ADMINISTRATIVE AND FISCAL POLICIES OF AIRPORT MANAGEMENT PERTAINING TO PAVEMENT MAINTENANCE

R.J. Sutherland, Consultant

Runways, taxiways and terminal aprons comprise the principal elements of airport pavements. The pavements composing these elements consist of either a mixture of bituminous materials and aggregates or portland cement concrete. The basic function of these airport pavements is to distribute aircraft wheel loads so that subgrade stresses do not exceed the capability of the underlying soils. At the same time airport pavements should be capable of providing a smooth comfortable riding surface for airline passengers as well as a safe operating environment for aircraft operations.

Airports represent large expenditures of funds and a major portion of such expenditures is spent for airport pavements. Statistics show that nearly 60% of all the federal funds allocated under the administration of Federal Airport Development Aid Program (ADAP) were for pavement construction.

This cost factor is expected to continue in the future and with this in mind it was felt appropriate to examine the administrative and fiscal policies of the managements and operators of the civil airports with respect to the maintenance of their airport pavements which represent such a large investment. It should be stressed that this study did not involve the technical methods or qualities of materials used in the maintenance of pavements but instead concentrated solely on the administrative policies governing the practices and programs relating to pavement maintenance. In other words it in effect examined the attitudes of the airport managements toward their investment in airport pavements.

For this study we arbitrarily selected some twelve airports located uniformly throughout the various regions of the United States. Included were some of the busiest airports in terms of enplaned passengers and aircraft operations as well as some with medium and smaller operational activity levels.

A list of questions was developed for discussion with the airport managements in an attempt to get uniformity of replies insofar as possible. The questions were divided into three groups. The first on general policy with respect to the selection of pavement type. The second on pavement maintenance policies and standards. The third on cost of pavement maintenance.

The reaction of the majority of the airport management represen-

tatives contacted to the questions was generally cooperative. In most cases they responded readily to the discussion type questions such as those in the first two groupings. When it came to the third group of questions on cost of pavement maintenance they all seemed to be much more reticent. Actual detailed cost records of pavement maintenance were not generally available except at a few airports. In no case did the annual O & M budget include a separate all-inclusive pavement maintenance item. By far the majority of airports covered pavement maintenance in a general overall airfield maintenance item which included such things as snow plowing, grass cutting, lighting and pavement marking as well as pavement maintenance operations. In some cases a much more business like approach was used involving separate items such as materials, equipment costs and manpower costs.

Table I lists the 12 airports included in the survey together with such items as number of runways, types of pavements, passenger and operational activities, pavement maintenance costs expressed in terms of cost per square yard and percentage of total O & M costs.

Based upon the overall results of the survey, the following general conclusions were reached.

General Policies

Questions:

1. Is pavement design considered to be an integral part of airport development planning, or does it follow along later as a detail item of development?

2. What is the basis for selection of type of pavement?
   a) Management decision based on personal preference;
   b) Operations committee preference;
   c) Personal preference of consultants designing pavement;
   d) Engineering decision based on site conditions;
   e) Is initial cost a dominant factor?
   f) Is expected maintenance cost a dominant factor?
   g) In pavement projects using ADAP funds does FAA design data play a dominant role on pavement type selection and design?
   h) With ADAP funding does personal preference of FAA representatives play a dominant role in pavement type selection?
   i) Are alternative designs of asphalt and concrete pavements generally put out for bids?

The design of airport pavements is considered to be a major part of airport developmental planning but is not part of the initial planning. It follows the overall master planning of airports.

Airport management seems to be playing a substantially smaller role in the selection of pavement type. They seem to be playing down

personal preferences and relying to a much greater extent on their consultant engineers decisions based generally on site conditions.

Initial construction costs are not a dominant factor in pavement design. Neither are expected maintenance costs a dominant factor in pavement design but the frequency of required pavement maintenance operations seems to be causing some concern.

Federal ADAP funding is almost always used in the original construction, reconstruction and rehabilitation of airport pavements. FAA pavement design standards are generally more favorably received than was evident a few years ago. The tendency seems to be to exceed such requirements. Alternate designs of both asphalt and concrete pavement are not prepared for bidding.

Pavement Maintenance Policies and Standards

Questions:

1. Is pavement maintenance considered to be a major responsibility of Management?

2. Is pavement maintenance included as a separate item in annual O & M budget? If not, how is it covered?

3. How is level of pavement maintenance funding determined?
   a) Percentage of original construction cost;
   b) An estimated amount based on previous experience;
   c) An estimated amount based on engineers determination of what maintenance requirements will be during the next year.

4. Are preventive maintenance procedures undertaken as a routinely established policy?

5. Is pavement maintenance based on need to preserve original investment?

6. Is pavement maintenance based on operational safety considerations?

7. How is need for pavement maintenance determined?
   a) Management or engineer's inspection?
   b) If so, is such inspection undertaken on a routine basis?
   c) If so, what is inspection schedule?
   d) Is need for pavement maintenance based on complaints by operating airlines?

8. If visual inspections indicate pavement deterioration, how are maintenance procedures to be undertaken determined?
   a) Airport staff

b) Consultant engineers
c) Combination of both

9. What is usual policy for undertaking maintenance action?
   a) Take runway or taxiway out of service regardless of operating restriction;
   b) During periods of minimum operational levels;
   c) Is maintenance routinely undertaken during night hours, i.e., 11:00 P.M. - 6:00 A.M. to minimize impact on operations?
   d) How is major reconstruction of a runway or taxiway scheduled?

The maintenance of pavements is considered to be a major responsibility of airport management.

Pavement maintenance costs are not usually covered under a separate item as such in annual O & M budgets.

Such costs are most usually covered under a general overall airfield maintenance item.

The level of pavement maintenance funding is most often determined by past experience and known problems to be undertaken during the coming year.

Maintenance procedures are generally based on the need to keep pavements in acceptable operating condition. Pavements are not usually let to deteriorate to the point where aircraft operational safety is involved. Pavement maintenance is not usually based on the need to preserve original investments.

The need for pavement maintenance is almost always initially detected by routine inspection of pavements by operations personnel. Such inspections are usually made from slow moving vehicles on a daily frequency basis. In some cases such inspections are made three times daily on a shift basis.

When visual inspection indicates such problems as surface cracking, joint spalling, extrusion of joint seals, surface rutting or uneven settlement, the maintenance procedures to be undertaken are generally determined by the airport staff itself or by representatives of municipal engineering departments. In some cases if the conditions look serious consulting engineers are called in.

Routine maintenance operations are usually conducted during periods of low operational activity. Where parallel or other multiple runways are available maintenance procedures do not usually result in serious operational delays.

Pavement maintenance is not usually undertaken during night time hours unless there is an unusual problem.

Airport staff members usually take care of all routine maintenance operations. For major problems contract work is generally used.

Cost of Pavement Maintenance

Questions:

1. Are detailed cost records kept of each maintenance project?

2. Are such records detailed to the point where the various cost items such as removal of existing pavement, compaction, aggregate, bituminous materials, steel reinforcing, portland cement and joint sealing materials are readily available?

3. What is annual cost of pavement maintenance at your airport?

4. What percentage of total annual operating cost is pavement maintenance?

5. What is the cost of asphalt pavement maintenance on a square yard basis?

6. What is the cost of concrete pavement maintenance on a square yard basis?

Detailed pavement maintenance cost records are not usually kept. Where they are kept they are not usually detailed to the point where itemized costs are readily available. As a matter of fact, very few of the airport management representatives contacted could provide readily available maintenance cost data. Most seemed to be providing such information from memory or after some discussion with other staff representatives provided data which they felt was more or less approximately correct. It is possible that the information provided may be suspect in some instances.

The annual cost of pavement maintenance varies widely, running from a low of 10¢ per square yard to a high of $1.62. Pavement maintenance costs as a percentage of annual airport O & M budgets varies from 2 to 12%.

In reviewing the maintenance cost figures, there appears to be some creditability of the figures afforded by the fact that Boston Logan and San Francisco International costs are the highest shown. These higher figures seem to be justified by the fact that both of these airports were constructed on unstable waterfront fill. The pavements at both airports are subject to more or less continuous uneven settlement thereby accounting for the higher maintenance costs.

General Conclusions

Airport managements as a whole seem to be much more interested in the performance of their pavements than was indicated just a few years ago. They seem to be well aware of the large investments represented by their pavements and of the need to keep them in good operating condition. As an indication, most of them are strengthening their staffs by adding people that have some background and previous experience in pavement maintenance. However, it is quite evident that maintenance and repair activities need much better coordination. Such coordination can be achieved only by continuous monitoring of traffic and the structural and functional conditions of the pavement and storage of such observations in a data base in order to update the original design strategies for use in planning future maintenance and repair activities.

It seems appropriate to point out the part the airlines are playing in the overall airport maintenance picture. At most locations, the airlines now generally guarantee that the airports will at least break even financially. They do this by agreeing to renegotiate the rates and charges they pay for the use of the airports on an annual basis so that the airport management will at a minimum recover all necessary costs. The airlines agree that such necessary costs should include all required pavement maintenance items and therefore there should be no reason why airport management should not be able to properly budget for adequate pavement maintenance programs. The airlines have come to understand that their ability to provide regularly scheduled airline service depends to a large extent on the continuous availability of properly maintained pavements and hence their willingness to fund justified pavement maintenance programs.

What is needed at this time is a more complete understanding of the overall airport pavement picture. As pointed out earlier, pavements represent a major portion of airport development funding. Is the industry really getting its moneys worth for these large investments in original pavement construction and continuing maintenance requirements? Are the pavement design methods currently in use entirely adequate insofar as structural soundness, availability of materials, ease of construction and minimized maintenance requirements are concerned? Who really has the responsibility to ensure that this more complete understanding of the pavement picture is available to the industry? Since the Government, represented by the FAA, has by law the overall responsibility for the administration of the Federal Aid Airport Program which finances most airport development and has adequate research capability, either through their own efforts or through the use of properly qualified outside consultants, it would appear that the Government must accept this responsibility. Aviation industry organizations, the Airport Operators Council International, the Air Transport Association, the Aircraft Industry Association and the professional engineering organizations must continue to urge the FAA to pursue all possible efforts to ensure that this more complete overall understanding of the airport pavement picture is available to the aviation industry.

TABLE I

Airport	Number Runways	Pavement Type	Annual Enplaned Passengers	Total Annual Operations	Air Carrier Operations	Annual Pavement Maintenance Cost/Sq. Yd.	Percent of Total O & M Costs
Boston	4	bituminous	4,824,000	288,076	190,000	$1.62	4%
Islip	4	bituminous	110,543	361,723	12,765	$0.12	6%
Atlanta	4	bit.&concrete	10,765,986	391,059	345,040	$0.12	2%
Tampa	3	bit.&concrete	4,803,149	196,756	102,171	$0.47	2½%
Buffalo	2	bit.&concrete	1,340,795	141,544	71,114	$0.10	3%
Indianapolis	2	concrete	1,248,326	201,539	84,125	$0.29	4½%
St. Louis	4	bit.&concrete	6,374,574	314,379	174,215	$0.36	3.3%
Dallas/Ft. Worth	3	concrete	7,341,142	341,418	282,229	**	**
Phoenix	2	bituminous	2,005,600	417,998	79,285	$0.14	8%
San Diego	1	concrete	2,230,000	185,700	70,700	$0.42	2½%
San Francisco	4	bituminous	8,598,546	351,000	279,000	$0.75	12%
Seattle	2	bit.&concrete	6,112,244	163,759	109,962	$0.49	4½%

** Note: The Dallas/Fort Worth Regional Airport is relatively new, being in operation for less than two years, therefore pavement maintenance costs have been minimal to date and are not representative when expressed in terms of costs/sq. yd. or % total O & M costs.

GPO 912-579